

STUDIES OF PHASE SEPARABLE SOLUBLE POLYMERS

A Dissertation

by

STEVEN MICHAEL FURYK

Submitted to the Office of Graduate Studies of
Texas A&M University
in partial fulfillment of the requirements for the degree of

DOCTOR OF PHILOSOPHY

May 2005

Major Subject: Chemistry

STUDIES OF PHASE SEPARABLE SOLUBLE POLYMERS

A Dissertation

by

STEVEN MICHAEL FURYK

Submitted to Texas A&M University
in partial fulfillment of the requirements
for the degree of

DOCTOR OF PHILOSOPHY

Approved as to style and content by:

David E. Bergbreiter
(Chair of Committee)

Michael A. Bevan
(Member)

Francois P. Gabbai
(Member)

Emile A. Schweikert
(Head of Department)

Daniel A Singleton
(Member)

May 2005

Major Subject: Chemistry

ABSTRACT

Studies of Phase Separable Soluble Polymers. (May 2005)

Steven Michael Furyk, B.S., Rider University

Chair of Advisory Committee: Dr. David E. Bergbreiter

The technique of phase labeling has the ability to greatly enhance synthetic protocol by simplifying purification and increasing efficiency. Traditional insoluble supports offer efficient and simple recovery of the “phase tagged” material but suffer from problems inherent to their heterogeneous nature. A solution to these problems has been to utilize phase separable soluble polymers in the design of “smart” responsive systems that offer the option of homogenous reaction conditions with heterogeneous separation conditions. The subject of this dissertation focuses on the application of soluble polymeric phase tags in systems where the miscibility between solid-liquid and liquid-liquid systems is thermally induced.

Low molecular weight poly(ethylene glycol) (PEG) oligomers were investigated as phase anchors for SCS palladacycle catalysts. The oligomeric PEG chains were sufficient to engender polar phase solubility in a heptane-DMA thermomorphic system. Microwave irradiation of these thermomorphic mixtures of palladium complexes and substrates was a viable scheme to recycle and significantly shorten reaction times for simple Heck reactions of aryl iodides.

Soluble polymeric supports possessing a lower critical solution temperature (LCST) were utilized in the sequestration of the S-triazine herbicide, atrazine, from contaminated water samples. The ability of poly(*N*-isopropylacrylamide) to sequester hydrophobic guests like atrazine was examined. A functionalized PNIPAM derivative containing secondary cyclic amines exhibited superior sequestration ability that was credited to the covalent binding of the atrazine.

In order to facilitate the design of tailored, thermally responsive, smart polymers, a high throughput temperature gradient microfluidic device was used to obtain LCST data in a fast, accurate manner. The specific ion effects of various alkali metal halide salts on the LCST of PNIPAM were investigated. The high precision in the measurements enabled more subtle effects such as changes in solvent isotope, polymer microstructure, molecular weight, and importance of end group effects on the LCST of poly(*N*-alkylacrylamide)s to be evaluated.

DEDICATION

To my parents, Baba, and Uncle Walter, may you all rest easier knowing that things turned out ok. And to Johnny and Michele for always pushing me to do better and looking out for me when times were tough. Finally to Dr. Sheats for showing me the way.

ACKNOWLEDGMENTS

I would like to thank Professor David Bergbreiter for direction and support during my graduate career. I would also like to thank Professor Paul Cremer for helping me to begin to see the beauty of thermodynamics, Professor Daniel Singleton for helping me to grow as a student and teacher, and Professor Eric Simanek for all of his help in the Atrazine club.

I would never have made it this far if it were not for the wonderful teachers who were like a family to me during my studies at Rider University; Professor John Sheats, Professor Richard Beach, Professor Feng Chen, and Professor Bruce Burnham.

Thank you Shayna for all of your help and for putting up with me while I was writing this.

I would also like to thank Dr. Philip Osburn for showing me the ropes and teaching me a great deal of chemistry both practical and theoretical; Dr. Andrew Kippenberger for not only being an excellent colleague but also a dear friend; Dr. Sergio Gonzalez, mi buen amigo, for an excellent collaboration ; and Eleanor Pate for providing me with a stimulating and enriching mentoring experience, it is truly amazing how much you can learn from teaching.

Finally I would also like to thank all of my friends and colleagues Dr. Yunshan Liu, Dr. Brian Walchuk, Dr. Jonathon Frels, Danielle Boran, Jared Hudson, Dr. Michael Szymanski, Dr. Jun Li, Dr. Loan Vo, Professor Antione Carty, Thomas Oliver, Patrick Hamilton, Denisse Ortiz-Acosta, Jeng-Shiung Jan, Dr. Yanjie Zhang, Dr. Izabela Owsik, Jianhua Tian, and Dr. Grunlan whose intellectual and philosophical discussions in both

the lab and the bar made my time here more tolerable. And finally Film for picking up where I left off.

TABLE OF CONTENTS

| | | Page |
|-------------------------|--|------|
| ABSTRACT | | iii |
| DEDICATION | | v |
| ACKNOWLEDGMENTS..... | | vi |
| TABLE OF CONTENTS | | viii |
| LIST OF FIGURES..... | | x |
| LIST OF TABLES | | xiii |
| CHAPTER | | |
| I | INTRODUCTION..... | 1 |
| | Thermodynamics of separations..... | 2 |
| | Separation strategies in synthesis..... | 10 |
| | Examples of phase planning in synthesis..... | 20 |
| II | OLIGO(ETHYLENE GLYCOL) SUPPORTED CATALYSIS..... | 42 |
| | Introduction..... | 42 |
| | Results and discussion..... | 45 |
| | Conclusions..... | 60 |
| III | LATENT SOLID-PHASE EXTRACTION USING THERMORESPONSIVE SOLUBLE POLYMERS | 62 |
| | Introduction..... | 62 |
| | Results and discussion..... | 65 |
| | Conclusions..... | 73 |

| Chapter | | Page |
|---------|--|------|
| IV | HIGH-THROUGHPUT STUDIES OF THE EFFECTS OF POLYMER STRUCTURE AND SOLUTION COMPONENTS ON THE PHASE SEPARATION OF THERMORESPONSIVE SOLUBLE POLYMERS..... | 75 |
| | Introduction..... | 75 |
| | Results and discussion..... | 78 |
| | Conclusions..... | 114 |
| V | EXPERIMENTAL..... | 115 |
| | REFERENCES..... | 141 |
| | VITA..... | 154 |

LIST OF FIGURES

| FIGURE | | Page |
|--------|---|------|
| 1 | The mixing of two gases at constant T and P..... | 4 |
| 2 | Closed system with component i moving from phase β to α | 8 |
| 3 | Stages of each step in a chemical synthesis | 11 |
| 4 | Two phase system containing phase label..... | 17 |
| 5 | Solvent precipitation to recycle a PEG _{5,000} SCS palladacycle Heck catalyst..... | 25 |
| 6 | pH induced precipitation to recycle a hydrogenation catalyst | 27 |
| 7 | Recovery of polyethylene-bound diphenylphosphine metal complexes using temperature dependant solubility | 28 |
| 8 | Thermodynamic argument for “normal” and “inverse” temperature dependant solubility of PNIPAM..... | 30 |
| 9 | Recovery of poly(<i>N</i> -isopropylacrylamide)-bound palladium catalyst via thermal precipitation | 31 |
| 10 | Ruh Chemie/ Rhône-Poulenc hydroformylation process | 33 |
| 11 | Fluoroacrylate-bound methyl red..... | 36 |
| 12 | Fluorous biphasic recycling of fluoroacrylate-bound hydrogenation catalyst..... | 37 |
| 13 | Recycling of a PNIPAM-bound palladacycle catalyst with the polar phase of a thermomorphic system..... | 39 |
| 14 | Recycling of a PNODAM-bound palladacycle catalyst with the nonpolar phase of a thermomorphic system..... | 41 |
| 15 | PNIPAM-bound triphenylphosphine Pd(0) Heck catalys | 43 |
| 16 | Pincer-type SCS-ligated Pd(II) Heck catalysts | 44 |
| 17 | Synthesis of oligo(ethylene glycol)-bound SCS palladacycle catalyst ... | 46 |

| FIGURE | Page |
|--------|---|
| 18 | ¹ H NMR spectra of complex 16 in CDCl ₃ showing dynamic changes in the peaks in the δ 3.8-4.6 region of the spectrum 48 |
| 19 | Representation of the two enantiomers of 21a (cis diastereomer) and 21b (trans diastereomer) that can interconvert through ring inversions (r.i.) or sulphur inversions (s.i.) 49 |
| 20 | Changes in concentration for iodobenzene (●) or methyl cinnamate (○) in a Heck reaction in DMF with conventional heating at 100 °C 50 |
| 21 | Thermomorphic recycling with 21 57 |
| 22 | Thermoresponsive polymeric sequestration agents (31 or 32), atrazine (33) and dye-labeled atrazine analogs (34 or 35) 66 |
| 23 | The protocols used for sequestration of monochlorotriazines..... 69 |
| 24 | TLC plate to corroborate the covalent sequestration of 34 73 |
| 25 | Schematic drawing of a temperature gradient device 83 |
| 26 | A typical clouding curve for PNIPAM 10 mg/mL in 0.4 M aqueous NaCl 85 |
| 27 | The effect of various sodium and potassium halide solutions on the LCST of PNIPAM..... 88 |
| 28 | The effect of alkali metal ion variation on the LCST of PNIPAM..... 90 |
| 29 | Solvent isotope effects on the LCST of PNIPAM measured using PNIPAM concentrations of 10 mg/mL in a series of solutions with Various mole fractions of D ₂ O contents..... 91 |
| 30 | The effect of NaClO ₄ at varying ionic strength on the LCST of PNIPAM in H ₂ O (●) and D ₂ O (○)..... 93 |
| 31 | The effect of NaI at varying ionic strength on the LCST of PNIPAM in H ₂ O (●) and D ₂ O (○)..... 93 |
| 32 | The effect of NaSCN at varying ionic strength on the LCST of PNIPAM in H ₂ O (●) and D ₂ O (○) 94 |

| FIGURE | Page |
|--------|---|
| 33 | The effect of the identity of the <i>N</i> -alkyl substituent on the LCSTs for isomeric poly(<i>N</i> -alkylacrylamide)s containing varying ratios of isopropyl/ <i>n</i> -propyl <i>N</i> -alkyl groups..... 95 |
| 34 | The variation of LCST with M_w of PNIPAM..... 101 |
| 35 | The effect of added monomer (<i>N</i> -isopropylacrylamide) on the LCST of PNIPAM ($M_w = 55,800$ (●) and 475,000(○))..... 103 |
| 36 | Synthesis of <i>N</i> -triphenylmethylhexaneamide..... 106 |
| 37 | Cleavage of triphenylmethyl group from <i>N</i> -triphenylmethylhexaneamide 106 |
| 38 | Synthesis of 4,4'-azobis(<i>N</i> -triphenylmethyl-4-cyanovaleramide) 107 |
| 39 | Synthesis of PNIPAM-CONH-Tr 107 |
| 40 | The variation of LCST with the M_w of PNIPAM-CONH-Tr (●) and PNIPAM-CONH ₂ (○)..... 109 |
| 41 | Conversion of PNIPAM-CONH-Tr to PNIPAM-CONH ₂ 110 |
| 42 | Synthesis of 80% isotactic PNIPAM 111 |
| 43 | Determination of PNIPAM tacticity by ¹ H NMR (DMSO- <i>d</i> ₆ , 130 °C) analysis..... 112 |

LIST OF TABLES

| FIGURE | | Page |
|--------|---|------|
| 1 | Comparison of conventional and microwave heating of Heck couplings employing 21 as a catalyst | 53 |
| 2 | Heck couplings of various organic-soluble aryl halides and alkenes promoted by microwave irradiation employing 21 as a catalyst..... | 56 |
| 3 | Recycling of 21 under thermomorphic conditions | 58 |
| 4 | Heck couplings of water-soluble aryl halides and alkenes promoted by microwave irradiation employing 21 as a catalyst..... | 60 |
| 5 | Common monochloro- <i>s</i> -triazine herbicides | 64 |
| 6 | Sequestration of atrazine (33) or atrazine analogs 34 or 35 from dilute aqueous solutions using thermally responsive polymers 31 and 32 | 71 |
| 7 | Repeated LCST measurements on two different samples of poly(<i>N</i> - <i>n</i> -propylacrylamide) (PNNPAM) prepared in two different solvents showing the precision of the LCST temperature analyses that use darkfield microscopy and the linear gradient temperature apparatus described here to measure LCSTs..... | 97 |
| 8 | LCST and M_w data for unfractionated (starting polymer) and fractionated PNIPAM samples..... | 100 |
| 9 | LCST and M_w data for unfractionated (starting polymer) and fractionated PNIPAM-CONH-Tr samples | 108 |
| 10 | Tacticity data for LCST polymers..... | 113 |

CHAPTER I

INTRODUCTION

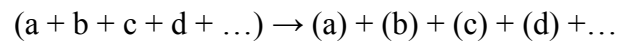
Man has been perfecting the art of separations since the dawn of civilization. Crude food processing operations such as milling, the isolation of sugars, and dairy separations can be traced back to antiquity. Textiles were produced from linen and cotton once their fibers were separated from the plants. The distillation of ethanol aided in the extraction of dyes, flavors, and natural medicines. The separation of elemental copper and then iron from its oxides and sulfides allowed man to make metallic tools and weapons. The dawn of the atomic era was dependent on the separation of U^{235} from U^{238} ; ironically, its survival seems dependant on the separation of its waste.^{1,2}

The chemistry involved in a given separation as well as the equipment required to carry out that separation can vary widely from application to application but the underlying theory of separation chemistry is the same for all methods. The explicit description of how materials are separated from one another will be followed by a discussion of how energy, entropy and the laws of thermodynamics apply to separations.

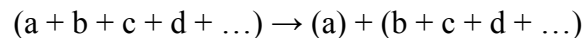
This dissertation follows the style of the *Journal of the American Chemical Society*.

Thermodynamics of separations

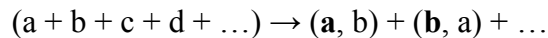
Separation can be defined as the process through which the mole fraction of a desired component in a mixture is increased in a specific macroscopic region via *selective* mass transport.³ The efficiency of a separation can range from the ideal case where n separate components are isolated from a mixture into n separate macroscopic regions



to partial separations where one component is separated from n-1 components



to an enrichment of one component relative to another in one or more regions.



This final description is the most accurate since no separation is perfect. The threshold for purity will vary depending on the application and the ability to detect impurities down to a given level.

Separations can be divided into two groups depending on the number of distinct phases involved⁴. Heterogeneous systems can be separated by mechanical means.

Homogeneous systems cannot be separated mechanically, these systems must first be separated at the molecular level into two or more distinct macroscopic phases.

Therefore for two completely miscible substances to be separated, their molecules must differ from one another in at least one physical-chemical property.

Equilibrium and separations

We have the ability to increase the effectiveness of a separation by understanding and controlling the two fundamental modes of displacement as precisely as possible. Homogeneous separations require an understanding of how components are moved through space on a molecular level and heterogeneous separations require the understanding of how components are moved through space on the macroscopic scale. Separation in both cases is governed by the same principle, that all isolated systems move by one path or another toward equilibrium. The application of a force allows one to shift the equilibrium to favor separative displacement. At the molecular level the spatial distribution of molecules is defined by chemical equilibrium. The spatial distribution of phases on the macroscopic scale is governed by mechanical equilibrium.

With macroscopic bodies it is unnecessary to worry about Brownian motion. Energy changes for the displacement in macroscopic systems are very large compared to those for molecules. The large energy terms associated with movement on the macroscopic scale completely dominate the small entropy terms. Without the entropy considerations equilibrium is governed by a minimization of the potential energy of the system. Macroscopic separations are achieved by applying the proper force in the correct orientation so that the system can achieve its lowest potential energy by separating n phases into n distinct regions in space. The common laboratory separation techniques mostly rely on gravity to supply this force. Separatory funnels to separate immiscible liquids and decantation to separate solids from liquids. Both cases involve separation by density along the gradient produced by gravity. Another example of force

to effect macroscopic separations is to use a magnetic field to separate magnetic from non-magnetic particles in a liquid-liquid, liquid-solid, or solid-solid mixture.

Entropy and separations

If we take the two glass bulbs connected by a stop-cock as depicted in Figure 1, each filled with a different gas at the same temperature and pressure and open the stop-cock the system will immediately begin to mix until there is a uniform composition of the two gases throughout the system.

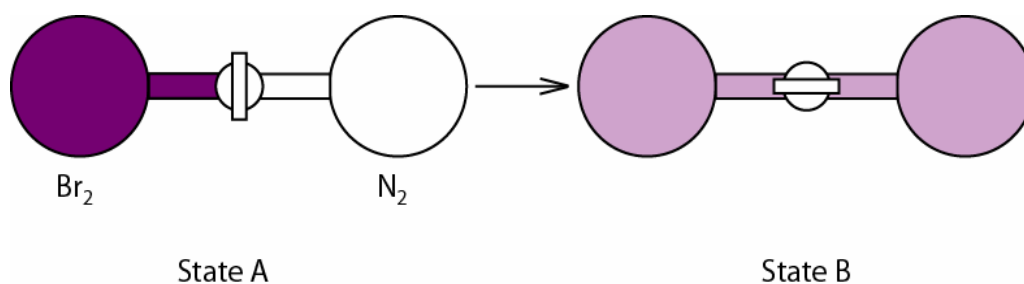


Figure 1. The mixing of two gases at constant T and P.

We know that this will happen every time we repeat the experiment and also know that the reverse process where the gasses separate into the two bulbs does not happen. We also know that there is no real enthalpic change for the system to go from state A to state B so the system is not moving toward a lower energy state because of bonding or molecule-molecule interactions. The driving force for this process is entropy.

From the second law of thermodynamics we have

$$\Delta S_{universe} \geq 0$$

where

$$\Delta S_{universe} = \Delta S_{system} + \Delta S_{surroundings}$$

This simple equation gives us the criterion to determine whether or not a process is spontaneous. Any process that decreases the entropy of the system must be coupled with a process that increases the entropy of the surroundings to an even greater degree in order for the net entropy change for the universe to be positive.

The process of mixing results in a less ordered system and therefore is entropically favorable. Separation, the opposite of that process, is therefore entropically unfavorable. The exact nature of the entropic barrier to separations is discussed below.

If we consider the two ideal solutions (a) and (b) being diluted at constant temperature and pressure

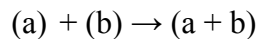
$$(a) \rightarrow (a)$$

$$(b) \rightarrow (b)$$

the change in entropy due to dilution for each solution is given by

$$\Delta S_{system} = nR \ln \left[V_{final} / V_{initial} \right]$$

If we now consider the solutions being mixed together at constant volume, temperature and pressure



the change in entropy due to mixing is given by

$$\Delta S_{system} = n_a R \ln[V_{final} / V_{a\,initial}] + n_b R \ln[V_{final} / V_{b\,initial}]$$

It is unimportant whether the components are diluted in pure solvent or in solvent with other components mixed in.^{3,5} There is no opposition to the separative transport of components from one another provided that they are not simultaneously concentrated. Of course any space through which transport can be used to structure the separation is also space through which dispersive or entropic transport can act to counter the separation. The objective to making a separation as efficient as possible is to try to maximize the amount of separative transport relative to the amount of dispersive transport.

Chemical potential and separations

Now that we have looked at the entropy of mixing and how it effects separations it is important to look at the chemical potential as a force that moves components from one phase to another.

If we consider that most simple laboratory separations are performed at constant temperature and pressure we can use the following state function to describe the spontaneity of a system.

$$\Delta G = \Delta H - T\Delta S$$

The lack of subscripts on each state function indicates all values are for the system. This equation simply relates ΔG which is $-\Delta S_{universe}$ at constant temperature and pressure to quantities from the system only. Therefore for a spontaneous process at constant temperature and pressure G of the system will decrease until it is at a minimum after which the system can no longer change. This minimum point for G is defined as the chemical equilibrium.

For any open system in which molecules are allowed to enter or exit the system the change in free energy is given by

$$dG = -SdT + Vdp$$

to account for the free energy gained or lost by the system from matter crossing its borders. If dn_i moles of a component i enter the system at constant temperature and pressure and no other components j cross in or out the change in free energy for the system is given by

$$dG = \left(\frac{\partial G}{\partial n_i}\right)_{T,p,n_j} dn_i$$

The magnitude of the change in free energy is proportional to the rate of change in free energy with respect to n_i . This quantity is defined as the chemical potential of the system and is given the symbol μ_i .

$$\mu_i = \left(\frac{\partial G}{\partial n_i}\right)_{T,p,n_j}$$

The chemical potential can be thought of as the amount of free energy brought into a system for each mole of component i added provided everything else was held constant.

Substitution of this quantity into our previous expression for dG gives us the simplified expression

$$dG = \mu_i dn_i$$

If we put the two open systems α and β together as is illustrated in Figure 2, components can only travel between the two phases and so the total system is closed.

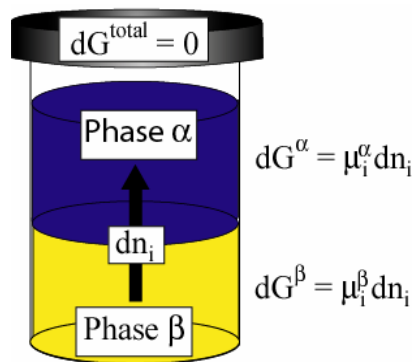


Figure 2. Closed system with component i moving from phase β to α .

So for the transfer of a small amount of component i from phase b to phase a we get

$$dG^{\text{total}} = dG^\beta + dG^\alpha = (\mu_i^\alpha - \mu_i^\beta) dn_i$$

and at equilibrium we have $dG^{\text{total}} = 0$ so

$$\mu_i^\alpha = \mu_i^\beta$$

which is intuitive since the phases are in equilibrium with each other.

We can take this model and account for the effects of concentration and the affinity that each solvent has for component i by adding the two terms below.³

$$\mu_i = \mu_i^0 + RT \ln c_i$$

where μ_i^0 is defined as the standard-state chemical potential, c_i is the concentration of solute i , and T and R are the temperature and gas constants respectively. The μ_i^0 term depends strongly on the energy of the solvent-solute interactions and is smallest when the solvent has a high affinity for the solute. The $RT \ln c_i$ term represents the entropic contributions to the chemical potential in the given phase due to dilution.

By substitution and rearranging we can generate an equation that relates the difference in affinity each solvent has for the component i relative to the concentration of i in each solvent.

$$\left(c_i^\alpha / c_i^\beta \right) = \exp(-\Delta\mu_i^0 / RT)$$

where $\Delta\mu_i^0 = \mu_i^{0\alpha} - \mu_i^{0\beta}$

The equilibrium ratio $\left(c_i^\alpha / c_i^\beta \right)$ of component i in phases α and β is the same as the partition coefficient and can be replaced yielding

$$K = \exp(-\Delta\mu_i^0 / RT)$$

So if phase α has a greater affinity than phase β for component i then $\mu_i^{0\alpha}$ is lower than $\mu_i^{0\beta}$ and $\Delta\mu_i^0$ is positive resulting in a higher concentration of component i in α relative to β . The magnitude of the affinity each solvent has for the solute along with the concentration difference between the solvents will determine the chemical potential between the phases.

Just as the difference in temperature is the driving force for the flow of heat from one phase to another, a difference in chemical potential is the driving force for the flow of chemical species i from one phase to another.

The distribution coefficient is at the heart of homogeneous liquid-liquid separations. The efficiency of these separations can vary widely depending upon the nature of the system as well as controlled variables such as temperature and pressure. We can consider the two limiting extremes to be the perfect separation where the concentration difference is very large resulting in all of the desired component in one phase and none of it in the other phase. The second extreme is when the concentration difference is very small and multiple extractions are required to carry out the separation.

Separation strategies in synthesis

While there are numerous strategies for carrying out a synthesis, the “work-up” typically involves the use of a standard set of purification techniques. It is not always clear in advance which one will work or how well a separation will work. In the area of synthesis, the separation process is often considered to be more of a technical problem than a scientific issue. Indeed, experimental sections of papers do not always fully describe the purification procedures used to isolate pure material. The many books devoted to the art of planning and executing synthetic strategies say little on the area of work-up and purification, focusing instead on strategies of bond connection/disconnection. However, this situation has begun to change. Such changes reflect issues in Green Chemistry, economic issues, and the practicalities of effecting simple but effective separations in high throughput and combinatorial chemistry.

The steps in a synthesis can be subdivided into three stages; reaction, purification and identification/analysis (Figure 3).⁶

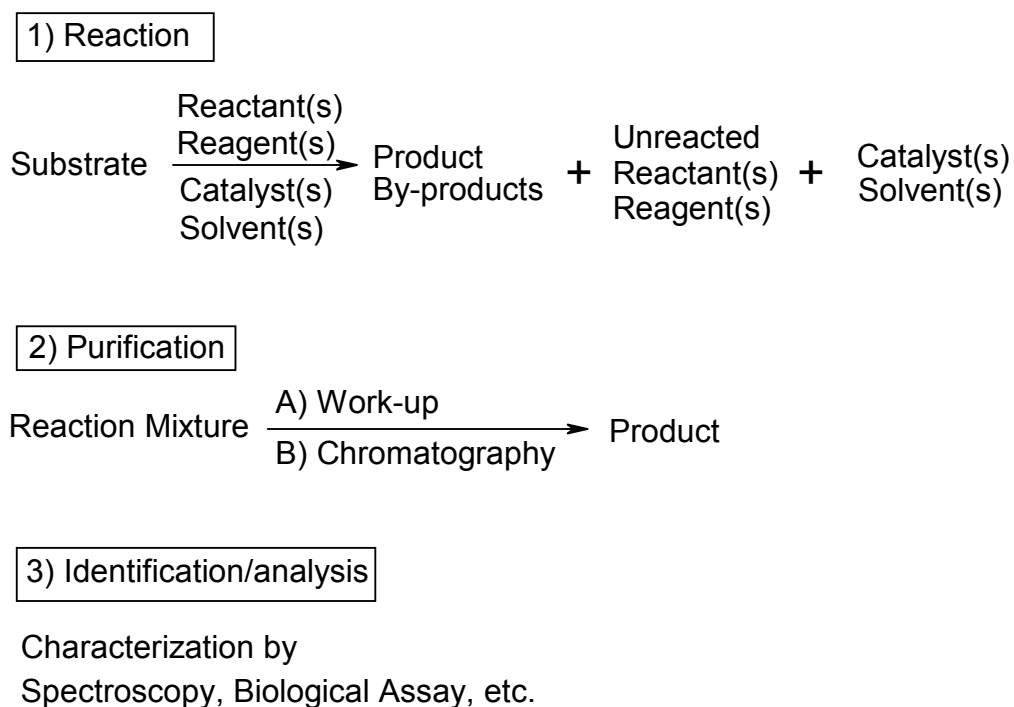
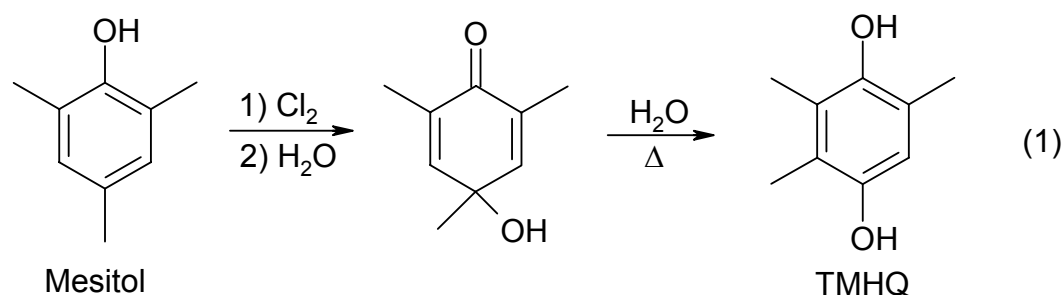


Figure 3. Stages of each step in a chemical synthesis.

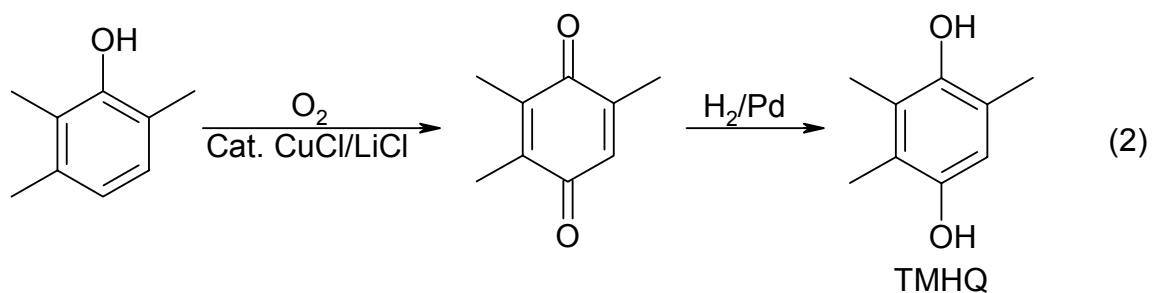
Most chemists prefer to use a collection of simple purification techniques. The use of chromatography is widespread as it affords a convenient albeit expensive way to isolate a single reaction product from a mixture of solvent, spent reagent or catalyst, and byproducts.

While the idea of running columns or using complicated multi-step purification procedures is feasible for academic chemists, practical separations for the industrial chemist are more restricting. Cost, safety, and environmental concerns associated with additional solvents/processes on the industrial scale weigh heavily into the planning of synthetic routes.⁷

The choice of manufacturing route that Rhône-Poulenc utilized in the production of the vitamin E intermediate trimethylhydroquinone (TMHQ) is an example of this.⁸⁻¹⁰ Rhône-Poulenc initially developed a scheme for TMHQ synthesis using some elegant chemistry and a cheap starting material (eq 1).



The work-up in this process produced a large volume of waste (50 kg per kg of product). Therefore, Rhône-Poulenc adopted the more complex process developed by the Mitsubishi Chemical Corporation involving two catalytic steps that generated less waste (2kg per kg of product) (eq 2).



In this second route, a more expensive starting material was required. However, the cost of work-up in the first case outweighed the disadvantages of the more expensive raw material in the second scheme.

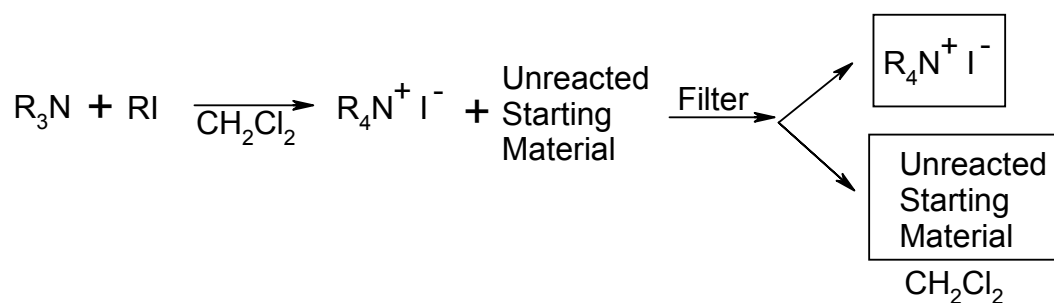
One might suppose that there exists an ideal purification in analogy to Wender's hypothetical "ideal synthesis."¹¹ In an ideal purification, the product would quantitatively and spontaneously separate into a different phase from everything else that is present in the reaction mixture. Simple mechanical separation could then be used to separate the phases allowing for the isolation of pure product in a single step.

Phase selective labels in synthesis

The idea of incorporating purification strategies into the design of a synthetic scheme has the advantage of allowing a researcher to combine an efficient separation strategy with the most efficient synthetic methodology.^{6, 12, 13} This process most commonly involves the use of a phase label to provide a convenient handle to manipulate one component of a system independently of other components. Merrifield's pioneering work on solid phase peptide synthesis is an example of the impact this

concept can have.¹⁴ This solid phase synthetic work received the Nobel Prize and is now recognized as the enabling chemistry for the biotechnology and combinatorial chemistry revolutions.

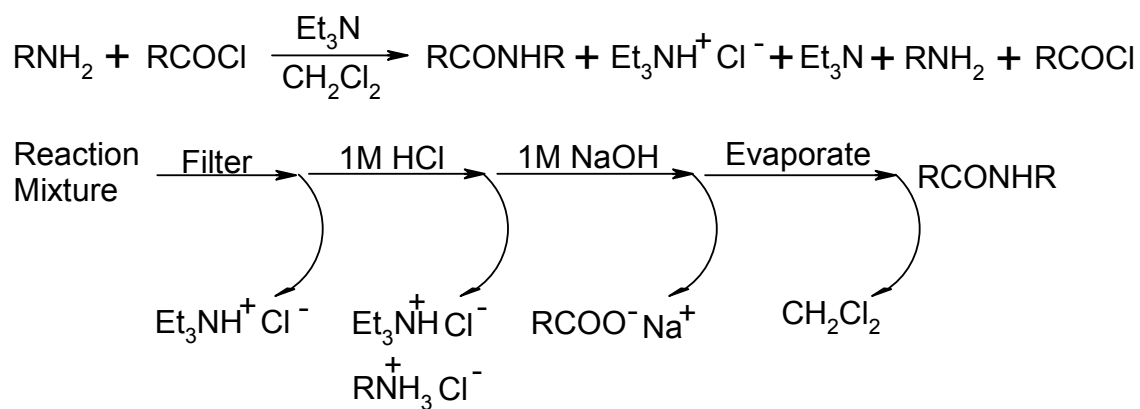
An analysis of how phase labels can be used in two standard synthetic schemes will illustrate these concepts. Scheme 1 illustrates the simplest system where all components are soluble at the start of the reaction and the product precipitates as it is formed. In this case polarity is the phase label and the pure product can be separated from the reaction mixture by simple filtration.



Scheme 1. Phase label forms as reaction proceeds.

Scheme 2 illustrates another example of separations involving phase labels. The starting materials are all organic soluble. As the reaction takes place the amine salts that form will precipitate and can be filtered away separating the polar salts from organic soluble components. Then acid extraction triggers a phase change preference for unreacted amine and the amine salts, which are now aqueous soluble and can be

removed from the organic soluble components. The extraction with base triggers another phase switch and now the salt of the organic acid is aqueous soluble and can be separated from the organic soluble components. Finally, heat is applied to separate volatile components from non-volatiles.



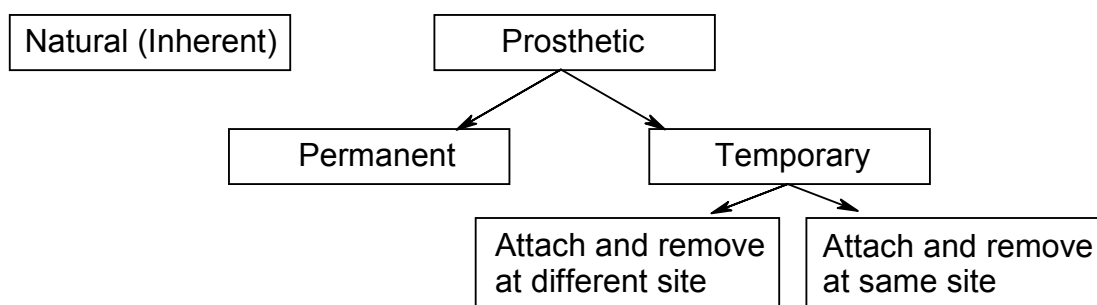
Scheme 2. Phase labels change as perturbants are added.

Classification of phase labels

Phase labels can be divided into groups based on the classification method in Scheme 3. First, there are two fundamentally different groups, the natural or inherent phase labels and the prosthetic phase labels. A natural phase label is simply the solubility profile that a molecule has due to its inherent functionality. The species discussed in Schemes 1 and 2 are examples. Prosthetic phase labels are labels that can bestow a solubility profile to a desired compound when it is attached to the label.

Examples of prosthetic phase labels are fluorous tags, insoluble polymer supports, and soluble polymer supports.

Types of Phase Labels



Scheme 3. Phase label classification system.

Prosthetic labels can be attached permanently or temporarily. Permanent labeling is useful when labeling a reagent that can be regenerated or catalyst that is to be recycled. Temporary linkers are useful when the desired product is attached to the label or if a particular scavenging agent is to be regenerated. The temporary linkers can be attached and removed in two ways. The first is to attach and cleave the compound at the same site. The second method involves a different site for attachment and cleavage.

The required efficiency of the phase label in partitioning between the phases will vary from application to application. In general, it is advantageous for the label to be as selective as possible for one phase over the other. When the phase label is used to facilitate recycling of a catalyst, the phase-selectivity must be large enough so that only a small amount if any is lost during each cycle.

We can describe the efficiency of a phase label by looking at the amount of material lost during each cycle in a recyclable system.¹⁵⁻¹⁷ Figure 4 depicts a system where a phase label is distributed between a two phase liquid-liquid system.

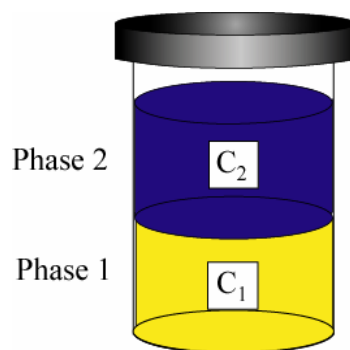


Figure 4. Two phase system containing phase label.

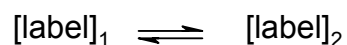
If we consider a system that consists of two equal phases where the label has a phase preference for phase 1 over phase 2 then we can describe the loss of catalyst from each cycle by the equation below.

$$\%Lost = 100/(1 + K)$$

Where C_1 = concentration of label in phase 1, C_2 = concentration of label in phase 2, and $K = C_1 / C_2$.

This equation tells us that for a system using a label with a selectivity of only 10 to 1 the loss is about 9% for each cycle. Selectivities of 100, 500, and 1,000 to 1 result in losses of 1, 0.2, and 0.1%, respectively.

The selectivity of a label for a given phase can be attributed to the chemical potential difference that the label has across the two phases. It is useful for this discussion to use the fact that chemical potential is ΔG_m in each phase. Therefore a label that is distributed between two phases 1 and 2 can be described as



and

$$K = \frac{[\text{label}]_2}{[\text{label}]_1}$$

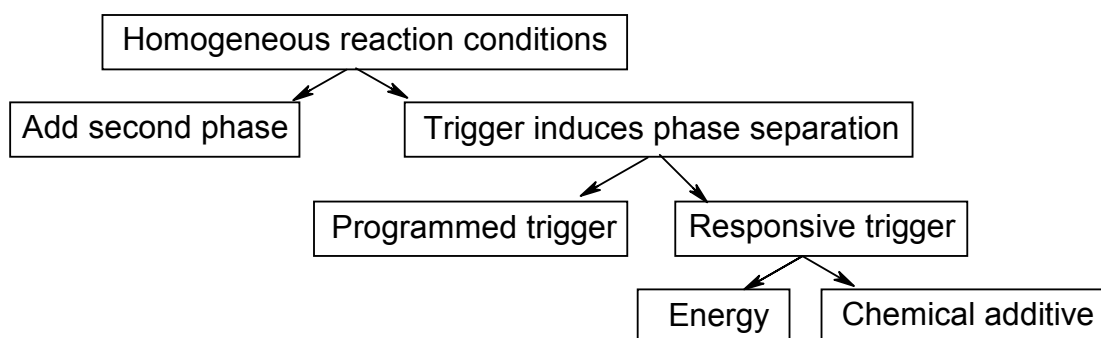
This equilibrium can be related to the change in free energy of the system by

$$\Delta G = -RT \ln K$$

This allows us to calculate what the difference in the change in free energies for a label must be in order to achieve a given selectivity. For example we can calculate the energy difference required in order to achieve the selectivities mentioned earlier. The corresponding free energy differences required for selectivities of 100, 500, and 1,000 to 1 at 25 °C are 11, 15, and 17 kJ/mol.

Generation of phases

The use of phase labels requires the formation of at least two separate phases in order for the separation to be carried out. One last important detail that needs to be discussed is whether the heterogeneity of the system is permanent. This is of particular interest during the course of a given reaction for reasons that will be discussed later. Examples of systems that employ permanent heterogeneity are reactions where insoluble cross-linked polymer supports are used and chemistry where two completely immiscible solvents (e.g. heptane and water) are used in liquid-liquid biphasic systems. Homogeneous systems too can be used but only if some event that will cause the system to become heterogeneous can occur. Several sorts of events or triggers can induce heterogeneity in an initially homogeneous system. These methods that induce heterogeneity into a homogeneous system are laid out in Scheme 4.



Scheme 4. Methods to separate homogeneous systems.

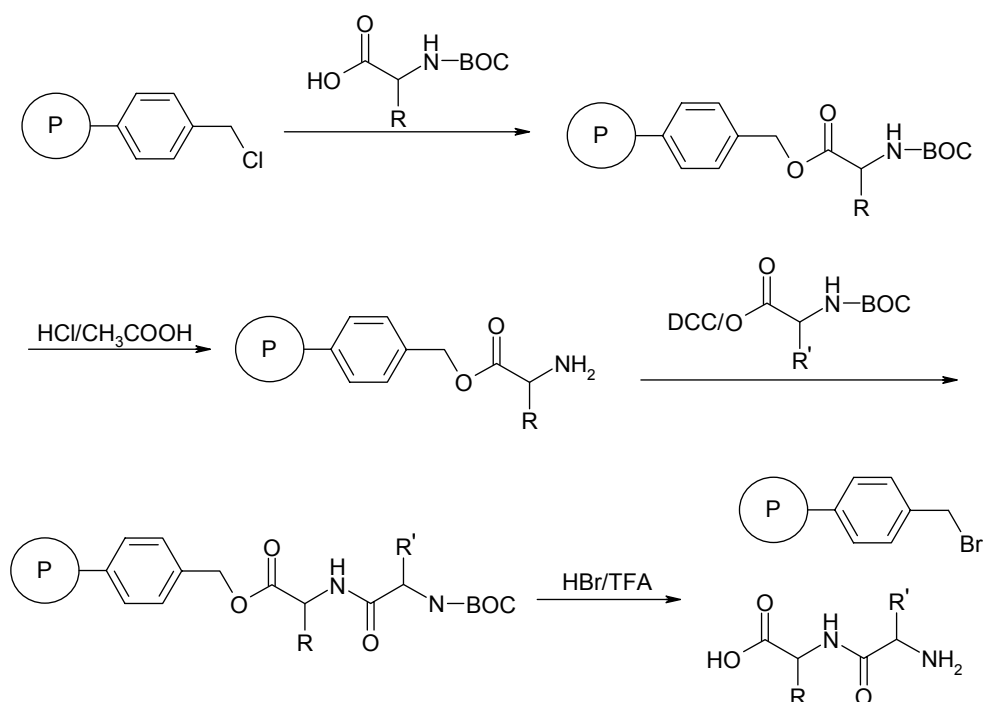
A homogeneous system can be turned heterogeneous by the addition of a second immiscible phase or by using some trigger to induce a phase separation within the homogeneous system itself. The trigger used to induce phase separation can be active or passive. The passive or “dumb” system utilizes some programmed event to trigger the phase segregation. An example of this is the formation of a precipitate in Scheme 3. The active or “smart” system requires some external stimulus to trigger the phase segregation.¹⁸ This induced phase separation can be permanent or reversible depending on the nature of the system. The perturbant can be a chemical additive (e.g. salt, small amount of solvent) or energy (e.g. heating, cooling, irradiating, exposure to an electric or magnetic field).

Examples of phase planning in synthesis

From the preceding section it should be apparent that there are many ways to phase label a reagent or catalyst. Due to their versatile nature, wide applicability, and ease with which their solubility can be tuned, polymers are an excellent choice for use as labels. In the case of liquid-liquid biphasic separations, varying the size or microstructure of a polymer allows the phase-selectivities of these materials to easily reach values of $>100,000:1$.¹⁷ The realization of this fact and its exposition in practical terms underlies the extensive background work of the Bergbreiter group using polymers as supports. For these reasons, the majority of the examples that follow will deal with polymeric labels.

Solid-liquid separations

It is appropriate to begin with Merrifield's work when reviewing phase labeling techniques since solid-phase synthesis was the first generally applicable method developed to bestow an orthogonal phase-selectivity to a synthetic component using a prosthetic phase label.^{14, 19} Although he was not the first to use polymer-supports in synthesis, Merrifield's work on solid-phase peptide synthesis is the most well known. It was for this work that he was awarded the 1984 Nobel Prize in Chemistry. The general features of this work are illustrated in Scheme 5.



Scheme 5. Merrifield's solid-phase peptide synthesis.

The great advantage of this technique stems from the simplified work-up procedure after each stage in the synthesis. The use of cross-linked insoluble supports such as divinylbenzene-cross-linked polystyrene allowed one to simply filter and wash the resin-bound product to purify it after each step. This greatly reduced the time required to synthesize a peptide when compared to conventional chemistry. The ability to use excess reagents was also important. While some effect of the polymer on the reactivity of the substrate is a drawback of this technique, excess reagent minimizes this problem. Diffusion limitations due to the heterogeneous nature of the support during reaction conditions sometimes resulted in lower rates and yields when compared to known solution phase chemistry. The chemo, regio, and enantioselectivities can also be affected by the heterogeneous resin's microenvironment. These effects can lead to lower selectivity when compared to conventional methods or enhanced selectivity can be seen. This often required reoptimization of reaction conditions when converting from traditional to supported synthesis.^{20,21} Other drawbacks to the use of insoluble supports stem from the inability to use conventional solution state spectroscopic techniques.²² The supports also prevent analysis by standard chromatographic methods.

The problems associated with heterogeneous supports seem to be magnified in catalysis.²³⁻²⁶ This has limited the use of insoluble polymer supports and solid-liquid separations in catalyst recovery in industrial scale synthesis.

In catalysis two sorts of species are used. Historically heterogeneous catalysts like Pd/C have been most used. While such chemistry can be very efficient, heterogeneous catalysis occurs at the interface of a mixed phase system. Starting

materials must first migrate to the interface where physisorption onto the catalyst's surface can occur.²⁷ Weak intermolecular forces bind the substrate near the surface until chemisorption occurs. Only the sites on the surface of the bulk catalyst are accessible greatly reducing the number of catalyst atoms that can actively participate in reactions. Limited spectroscopic information coupled with the extremely complex interactions at the liquid/solid and gaseous/solid interface make mechanistic information difficult to obtain.

Homogenous catalysis overcomes many of the limitations of heterogeneous catalysts.²⁸⁻³⁰ Catalyst solubility allows characterization of catalysts and intermediates using conventional spectroscopic methods (i.e. ^1H , ^{13}C , ^{31}P NMR, IR, etc). Spectroscopy is conducive to gaining mechanistic insight, especially as the complexity of a system increases. The use of ligands in the synthesis of homogeneous catalysts simplifies the tuning of a catalyst's activity to accomplish a specific goal. However catalyst recovery of soluble catalysts remains a problem. The added cost due to loss of precious metals or of ligands can be a major concern in industrial applications. Even in cases where catalysts have high turn over numbers (TON = mol of product/mol of catalyst), pharmaceutical applications demand ultra-high purity products. Trace contaminants and especially trace metals could lead to serious health hazards. In spite of these limitations, homogeneous catalysis accounts for most new processes in fine chemical synthesis. Though homogeneous catalysis accounts for only 20% of all industrial reactions, the importance of catalyst recovery and product purification has led

to ongoing efforts to design phase selective catalysts that combine the advantages of heterogeneous separations with homogeneous catalysts.³¹

One of the first attempts to combine the recovery of heterogeneous catalysts with the reactivity of homogeneous catalysts was to “heterogenize” a homogeneous catalyst by immobilizing it on an insoluble support.²³ This allowed for simple separation of the well defined homogeneous catalysts from products. However, the new “heterogenized” catalyst suffered from several of the problems associated with the heterogeneous nature of the support. Solid phase immobilization of homogeneous catalysts suffers from the balance for a strong covalent bond to hold the catalyst to the support and the degrees of freedom required for the catalyst to maintain optimal activity. The following section describes examples where soluble supports are used as a means to facilitate catalyst recycling without the drawbacks associated with insoluble supports.

The general idea is to have a polymer-bound catalyst that is completely soluble during a reaction but completely insoluble during separation.^{13, 28, 30} This way one can truly combine the advantages of homogeneous catalysis with heterogeneous separations. Solvent precipitation is the most common method used to precipitate polymers from solution. The basic scheme is to run the reaction in a medium that is a good solvent for the polymer support. Then after the reaction is complete the solution is added to a large amount (approximately 10 times the amount of good solvent) of a second non-solvent for the polymer which is miscible with the first solvent. The polymer then precipitates and, if the products are still in solution, simple filtration isolates the catalyst from

products. This method is one of the earliest approaches used to recover soluble polymer supported catalysts.

The example in Figure 5 involves solvent precipitation to separate a polymer-bound Heck catalyst from a homogeneous solution after a C-C coupling reaction has taken place.³² Air stable catalyst precursors like the pincer-type sulfur-carbon-sulfur (SCS)-ligated Pd(II) species **1** are advantageous in recycling systems since they simplify recycling protocol. Poly(ethylene glycol) (PEG) is used as the soluble support.

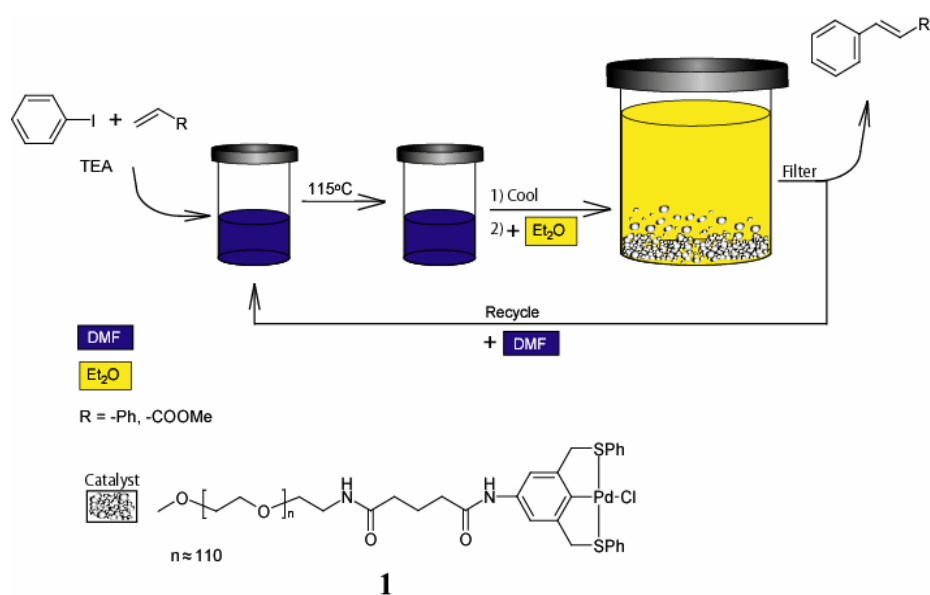


Figure 5. Solvent precipitation to recycle a PEG_{5,000}SCS palladacycle Heck catalyst.

Starting materials are then added to a solution of the PEG supported catalyst precursor in *N,N*-dimethylformamide (DMF) and the reaction occurs under homogeneous conditions.

The resulting product solution is then added to a 10 fold excess of ethyl ether causing the polymer to precipitate. The PEG-bound catalyst precursor can then be separated from the ether soluble products by a simple filtration. The catalyst in this system was recycled 3 times with no observable loss in activity. This example illustrates an important concept for recyclable catalysts; the effective turnover numbers are only limited by the number of cycles that can be run with a given catalyst.

The solvent precipitation method has the advantage that it is simple and generally applicable to a wide range of solvents and polymers. The major drawback of this method is the large amount of solvent required to precipitate the polymer. This is less of a problem in academic laboratories but negates the use of this method for large scale industrial processes.

Other methods to induce phase separation of the polymer once the reaction is complete include the use of stimuli to trigger the precipitation event. One such example of this is the use of pH change to precipitate polymers containing acid or basic residues. The recycling protocol in Figure 6 utilizes a catalyst bound to a copolymer containing amphoteric residues to carry out and recycle hydrogenation reactions in water.³³ Non-traditional reaction media such as water have begun to receive a great deal of attention in the area of Green Chemistry. The ligand was prepared by derivatizing the commercially poly(maleic anhydride)-*c*-poly(methyl vinyl ether) (Gantrez[®]) with amine terminated diphenylalkyl phosphine groups. The remaining anhydride residues are then hydrolyzed resulting in a terpolymer containing carboxylic acid residues. The resulting polymer-bound phosphine was then coordinated to a rhodium (I) species to generate the active

hydrogenation catalyst **2**. This polymer supported catalyst is soluble in water with a pH >7.5 and precipitates as a yellow solid when a small amount of acid ($\text{CF}_3\text{SO}_3\text{H}$) is added to the system.

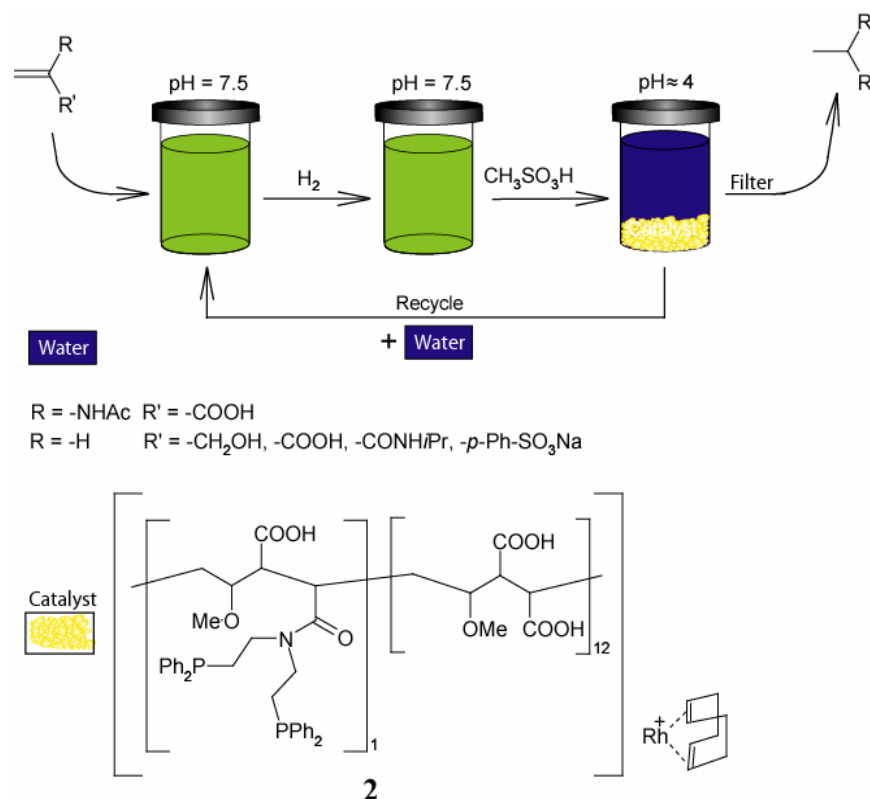


Figure 6. pH induced precipitation to recycle a hydrogenation catalyst.

This catalyst was used to hydrogenate several water soluble alkenes and was recycled by decreasing the pH of the solution, filtering the precipitated catalyst, and then adding the catalyst to fresh substrates in water. The activity of this polymer-bound homogeneous catalyst was only slightly lower when compared to a low molecular weight analog.

Heat has also been used as a trigger to make polymers go into or come out of solution. Early work in the Bergbreiter group utilized the temperature dependant solubility of polyethylene oligomers in organic solvents like toluene or xylenes to separate polyethylene-bound catalysts from solutions of products. Polyethylene oligomers with molecular weights in the range of 2,000 to 3,000 g/mol have strong temperature dependent solubility in non-polar solvents like toluene.³⁴ At 25 °C the polymer is completely insoluble (no detectable solubility) whereas solutions of polymer as concentrated as 1 g polymer/10 mL of solvent can be prepared at 100 °C. Figure 7 shows examples of how this type of system was used to recycle different transition metal catalysts prepared from diphenylphosphine terminated polyethylene oligomers **3a-d**.³⁵⁻³⁷

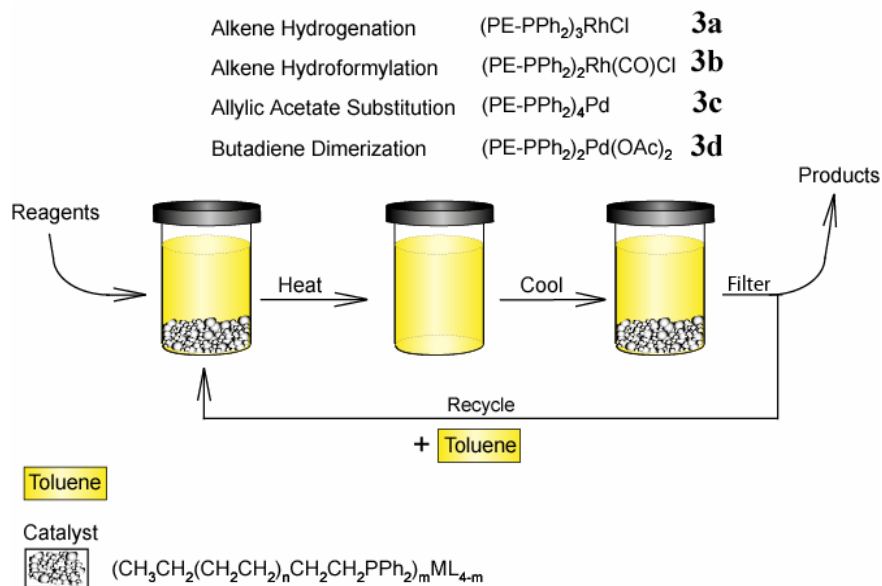
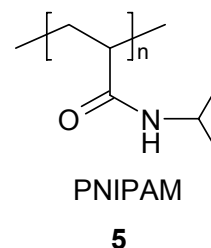
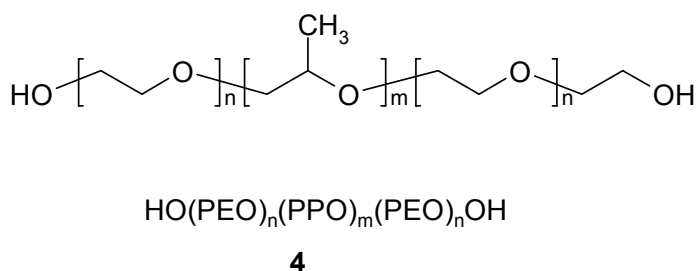


Figure 7. Recovery of polyethylene-bound diphenylphosphine metal complexes using temperature dependant solubility.

Other polymers have temperature dependant solubility that requires heating to precipitate the polymer. Polymers like triblock poly(ethylene oxide)-poly(propylene oxide)-poly(ethylene oxide) (Pluronics[®]) **4** and poly(*N*-isopropylacrylamide) (PNIPAM) **5** have a temperature dependant solubility in water that can also be used to separate catalysts or other materials bound to them.



These polymers are soluble in cold water and precipitate when the solution is heated above the polymer's Lower Critical Solution Temperature (LCST). The dependence of solubility with temperature in both cases can be explained by looking at the free energy of solvation for each case. If we assume that ΔH_{sol} and ΔS_{sol} remain constant in the temperature range just above and below the Critical Solution Temperature (CST) then we can use the two plots in Figure 8 to describe how the ΔG_{sol} will change in each case with changing temperature.

For the polyethylene/toluene system the solvation of the polymer has a favorable entropic term since the system is becoming more disordered. As the temperature

increases the $T\Delta S_{\text{sol}}$ term increases until it becomes larger than ΔH_{sol} . It is at this point that the ΔG_{sol} becomes negative and the process of solvation becomes spontaneous.

For the PNIPAM/water system the solvation of the polymer has an unfavorable entropic term. This is due to the increased order derived when water molecules organize themselves into cage-like structures around the hydrophobic components along the polymer.

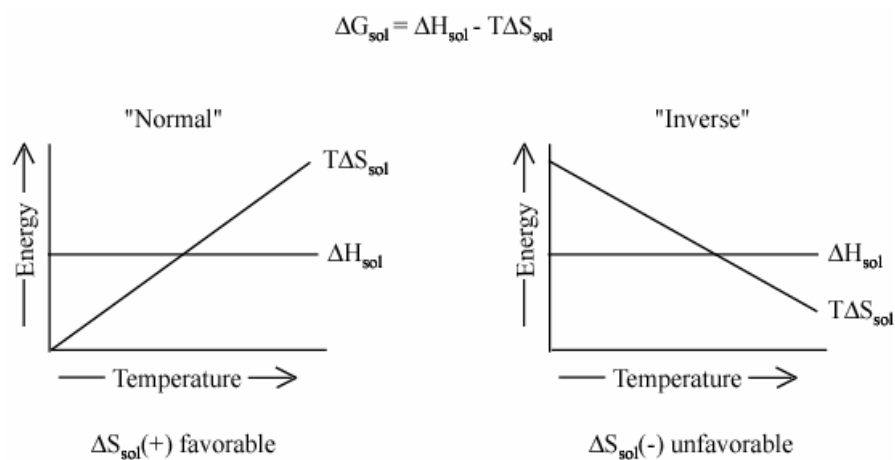


Figure 8. Thermodynamic argument for “normal” and “inverse” temperature dependant solubility of PNIPAM.

As the temperature increases the $T\Delta S_{\text{sol}}$ term decreases until it less than ΔH_{sol} . It is at this point that the ΔG_{sol} becomes positive and the process of solvation becomes unfavorable.

Figure 9 illustrates how the inverse temperature dependent solubility of PNIPAM can be used to separate a PNIPAM-bound catalyst from an aqueous solution of

products.³⁸ In this case a terpolymer containing diphenylphosphine groups was used to ligate palladium (0). The catalyst **6**, base, and water soluble Heck donors and acceptors were dissolved in cold water. The reactions were carried out at 8 °C (below the polymer's LCST), once the reaction was complete the solution was warmed to 25 °C (above the polymer's LCST) and the precipitated polymer can be separated from the reaction mixture by filtration. The polymer-bound catalyst was then dissolved in fresh water that could be used to carry out the next cycle. The catalyst remained active with only a moderate loss in activity after 15 cycles.

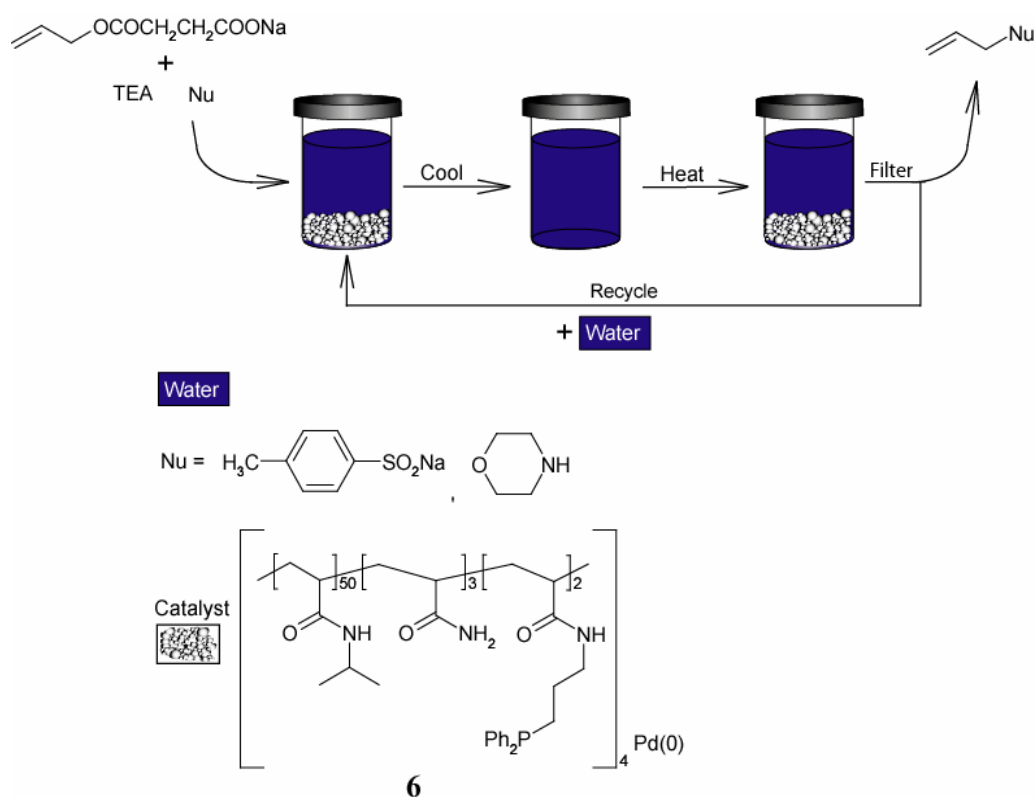


Figure 9. Recovery of poly(*N*-isopropylacrylamide)-bound palladium catalyst via thermal precipitation.

The next section will discuss the immobilization of phase selective catalysts in one phase of liquid-liquid biphasic systems.

Liquid-liquid separations

The Shell Higher Olefins Process (SHOP) developed in 1969 was the first industrial scale synthesis to utilize liquid-liquid biphasic catalysis in order to simplify recycling of a homogeneous catalyst.³⁹ The oligomerization of ethylene utilizing a nickel catalyst immobilized in 1,4-butanediol resulted in C₄ to C₂₀ α -olefins that form a second phase which allowed for simple separation of catalyst from product. This process is similar to the one outlined in Figure 10. The general principles of liquid-liquid biphasic catalysis involve the use of two immiscible liquid phases where one phase contains a homogeneous catalyst and the second contains products. Catalyst immobilization in this “liquid support” does not suffer from the limitations of insoluble solid supports.³¹ The next milestone in the area of liquid-liquid biphasic catalysis came in 1984 when Ruhrchemie/ Rhône-Poulenc began production of butyraldehyde using an aqueous biphasic hydroformylation process (Figure 10).^{39, 40} This process now produces 600,000 tons of butyraldehyde annually. One of the distinct advantages of this process is the use of water as an industrial solvent. Water has many features that make it an attractive solvent. The high polarity of water can often enhance rates by stabilizing the highly charged transition states of many organic reactions. The large difference in polarity and density of water when compared to most organics allow for the separation

of phases. Water is also very safe in that it is not explosive, flammable, or toxic. Finally water is cheap, abundant, and readily available.³¹

The Ruhrchemie/ Rhône-Poulenc hydroformylation process begins with the addition of propene and synthesis gas (CO/H₂) to a rhodium hydroformylation catalyst **7** immobilized in the aqueous phase. The reaction is then stirred to maximize the amount of surface area for mixing while the system is heated. Once the reaction is complete the mixture of isomers (95/5 *n/iso*) of butyraldehyde separates from the aqueous phase to allow for the simple isolation of product. Fresh reactants can then be added and the process repeated for additional cycles.

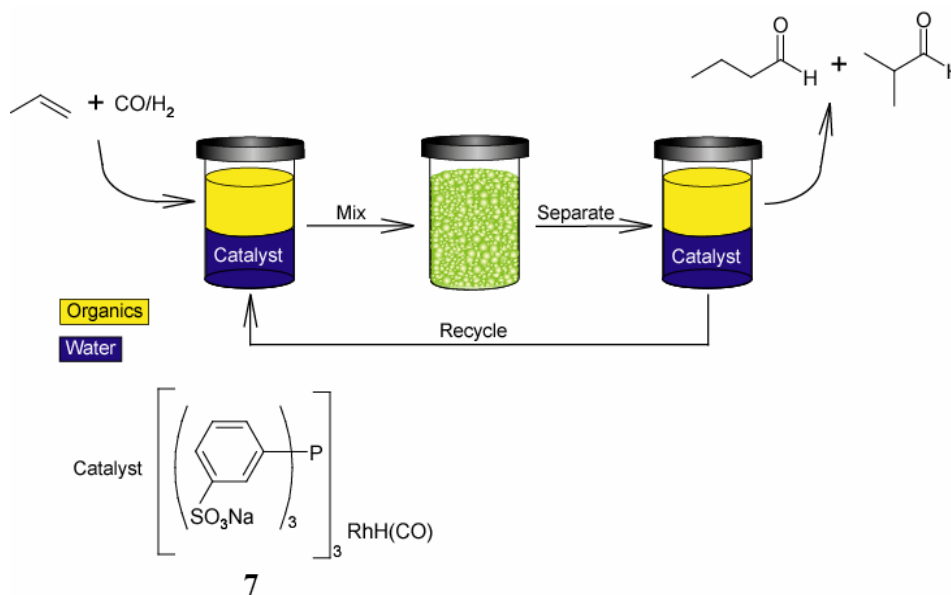


Figure 10. Ruhrchemie/ Rhône-Poulenc hydroformylation process.

Organic acids and their salts are the most common phase labels used to bestow aqueous solubility to the ligands of transition metal catalysts. Any type of phase label can be used provided that the activity of the catalyst is not diminished greatly and the phase selectivity of the label is sufficient to “hold” the catalyst in the aqueous phase. The extensive use of triphenylphosphine trisulfonate (TPPTS) stems from the good solubility of this ligand in water (1,100 g/L), the fact that it is insoluble in nearly all organics, and the fact that it behaves much like parent ligand triphenylphosphine.

The Shell Higher Olefins and Ruhrchemie/ Rhône-Poulenc hydroformylation processes rely on the fact that propene has some limited solubility in the catalyst containing polar phase. Both process’s success also depends on products that are sufficiently non-polar to ensure that there will be a separate organic phase to facilitate product isolation. These processes must balance the solubility of the starting materials during the reaction conditions with the post reaction insolubility of the bulk product phase. These processes are limited due to the fact that the starting materials must have some solubility in the polar phase in order for the desired transformation to be carried out in a reasonable time scale.⁴¹ An example of this can be seen when comparing the rate of the hydroformylation of higher alkenes such as 1-hexene via the Ruhrchemie/ Rhône-Poulenc hydroformylation process. The rates for hydroformylation of propene are much higher than for 1-hexene and higher α -olefins.^{41,42} Research in this area led to the utilization of fluorinated solvents to address some of these limitations. The application of a third “orthogonal” phase label greatly increases the diversity of this technology.

Horváth and Rabái took advantage of the unique tendency of fluorinated compounds to phase separate from aqueous and organic components and applied it to the area of biphasic catalysis.⁴³ They introduced the term fluorous to describe this third type of immiscible phase. This enabled researchers to think about running reactions that used combinations of hydrophilic, organophilic, and fluophilic components. Their initial work showed that you could increase the fluorophilicity of a catalyst by attaching sufficiently long fluorous pony tails to it.⁴⁴ The catalyst could then be immobilized in a fluorous solvent and reagents/products could be isolated from a second organic phase. This concept was applied to the hydroformylation of higher α -olefins such as 1-decene that could not be conducted with the traditional aqueous biphasic conditions.⁴⁵

The large amount of phasephilicity that is incorporated into a soluble polymer is advantageous in the area of biphasic catalysis. Work in the Bergbreiter group has shown that adding fluorous pendant groups along a polymer backbone results in a polymer that is highly fluorous soluble.⁴⁶ The UV active fluoroacrylate copolymer **8** (Figure 11) was prepared to quantitatively measure the selectivity of this fluorinated polymer for fluorous solvents vs aqueous and organic solvents.⁴⁷

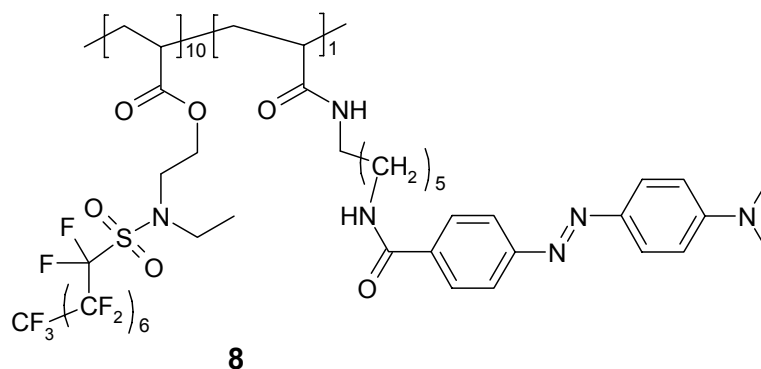


Figure 11. Fluoroacrylate-bound methyl red.

The polymer was dissolved in a fluorocarbon solvent (FC77, 3M Co., a fluorinated cyclic ether, C₈F₁₆O) and the solution was intimately mixed with tetrahydrofuran (THF) or water. No polymer could be detected in the aqueous or THF phase resulting in a loss of < 0.1% polymer from the fluorous phase. This number corresponds to a selectivity of > 1,000 to 1. The fluoroacrylate-bound hydrogenation catalyst **10** was used to hydrogenate several hydrophobic alkenes using fluorous biphasic conditions to recycle the catalyst and recover the products (Figure 12).⁴⁸

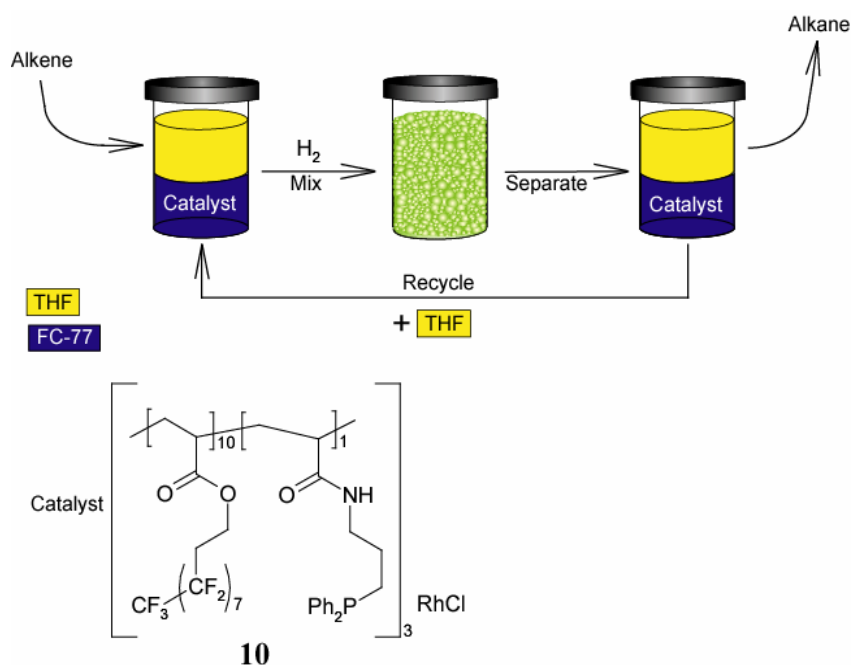


Figure 12. Fluorous biphasic recycling of fluoroacrylate-bound hydrogenation catalyst.

The catalyst was recycled 7 times without a loss in activity resulting in turnover numbers of 21,700.

In order to avoid the mass transfer issues associated with reactions carried out in binary systems it is advantageous to run reactions where all components are in one phase during the reaction and then separate afterwards. This type of system was actually discussed by Horváth and Rabái in their initial paper.⁴³ They reported that a biphasic mixture of perfluoromethylcyclohexane and *n*-hexane/toluene forms one phase when heated above 36.5 °C.

They used this system to extract a rhodium complex from a toluene solution using a fluorous phosphine. Knochel reported the first utilization of this homogeneous biphasic system to recycle a catalyst with a fluorous phase label.⁴⁹ They complexed nickel or rhodium with a perfluorinated 1,3-diketone that was then used to catalyze the oxidation of aldehydes and sulfides or form epoxides from olefins respectively.

The Bergbreiter group then explored the use of other solvent systems that had temperature induced miscibility and introduced the term thermomorphic to describe these types of systems.^{50, 51} These systems utilized two organic solvents with a significant difference in polarity such as DMF/heptane. The polarity of the system can be adjusted easily by adding a small amount of a modifier such as 10% water to the mixture. The example in Figure 13 involves the use of the polar polymer PNIPAM to phase label an SCS-palladacycle catalyst **11**.⁵¹

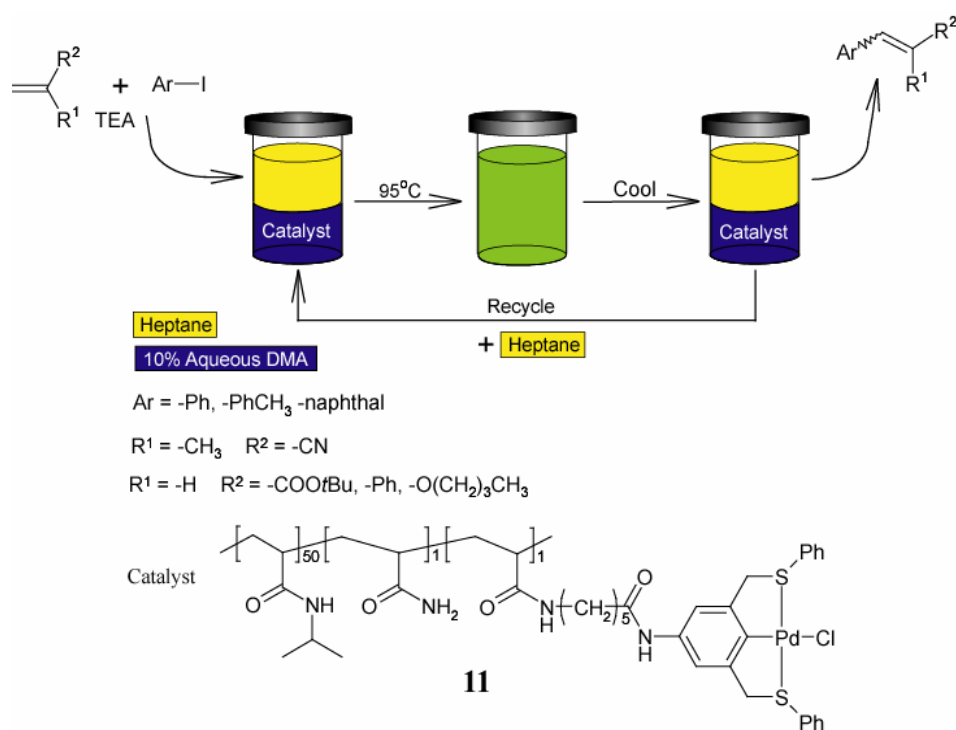


Figure 13. Recycling of a PNIPAM-bound palladacycle catalyst with the polar phase of a thermomorphic system.

This PNIPAM-bound catalyst is immobilized in the 90% aqueous *N,N*-dimethylacetamide (DMA) phase and reagents are added to the heptane phase. Once the mixture is heated above 70 °C the solution becomes completely monophasic and the reaction takes place with catalyst and reagents in one single homogeneous phase.

Upon completion of the reaction the reaction the solution is cooled to room temperature and the two phases separate allowing for facile separation of the catalyst phase from the product phase. Fresh reagents and heptane are then added to the catalyst containing 90% aqueous DMA phase and the process is repeated. This type of system is useful for reactions involving hydrophobic products since they will partition into the non-polar phase. However, if the desired products are relatively polar or if, as is the case in Figure 13, polar byproducts form that reduce the catalysts activity it is more useful to immobilize the catalyst in the non-polar phase. This type of system is illustrated in Figure 14.⁵²

In this case the same catalyst is now immobilized in the heptane phase by attaching it to the hydrophobic poly(*N*-octadecylacrylamide). The hydrophobic SCS-palladacycle catalyst **12** is sufficiently nonpolar to remain totally in the heptane phase. Combinations of polar Heck acceptors and donors were chosen to insure the coupling products would be sufficiently polar to partition into the DMA phase. This system has the advantage that salts formed in each cycle are removed from the catalyst phase.

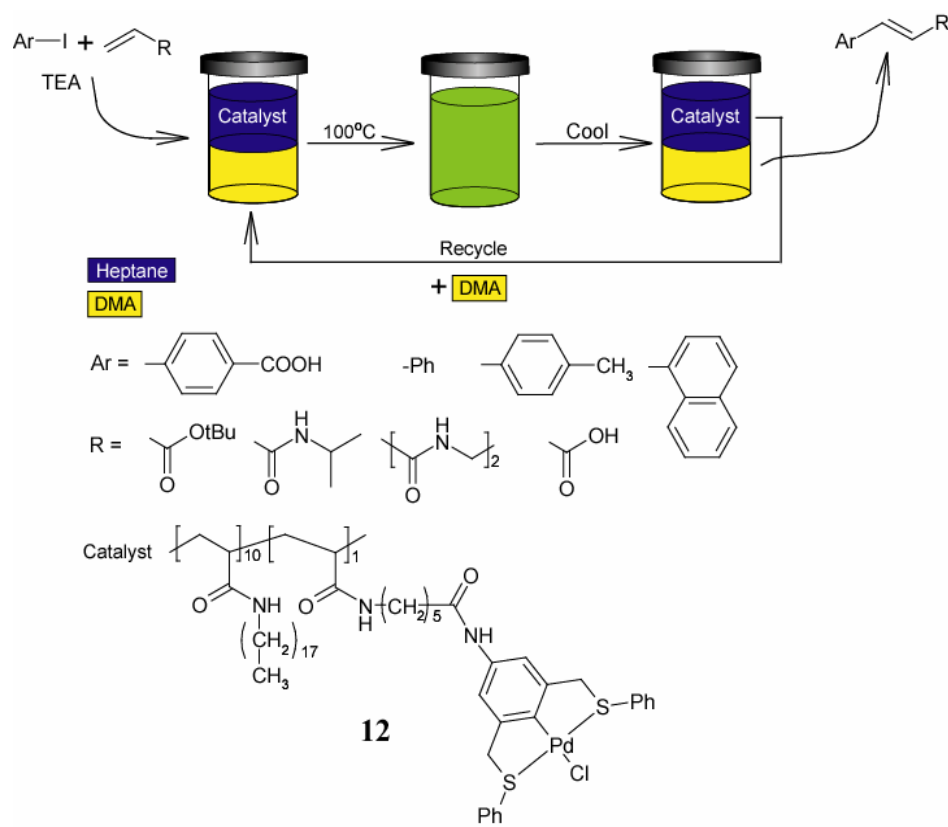


Figure 14. Recycling of a PNODAM-bound palladacycle catalyst with the nonpolar phase of a thermomorphic system.

CHAPTER II

OLIGO(ETHYLENE GLYCOL) SUPPORTED CATALYSIS

Introduction

The development of new ways to use and recycle catalysts as well as the investigation of alternative solvent systems to carry out catalytic reactions has allowed the Bergbreiter group to contribute to the area of Green Chemistry.⁵³ Catalytic reactions reduce the energy consumed during a process, require catalytic instead of stoichiometric amounts of a material, allow the use of less reactive/toxic reagents, and can decrease processing/work-up time and energy due to increased selectivity.^{54, 55} For these reasons catalysis has been called the “foundational pillar” of green chemistry.⁵⁵ Our research in the area of simplifying product/catalyst separation by allowing homogeneous catalysts to be separated in a heterogeneous manner is especially connected to the area of Green Chemistry. Previous work in the Bergbreiter group described the utility of transition metal complex catalysts or organic catalysts that can be attached to soluble polymer supports and used in fluoruous solvents, water, or monophasic/biphasic mixtures.¹³ The effectiveness of catalyst recycling in such cases depends on the efficiency of the separation technique as well as the stability of the catalyst. Robust, air-stable catalysts are ideal candidates for recycling since they eliminate the cumbersome procedures required to recycle the catalyst under inert atmosphere. Therefore the search for more stable catalysts has also been an area of interest in the Bergbreiter group.

Our work in the area of recyclable Heck catalysts began initially with polymer-bound analogues of traditional catalysts like the phosphine-ligated palladium(0) complexes **13** and **14** (Figure 15).^{56, 57}

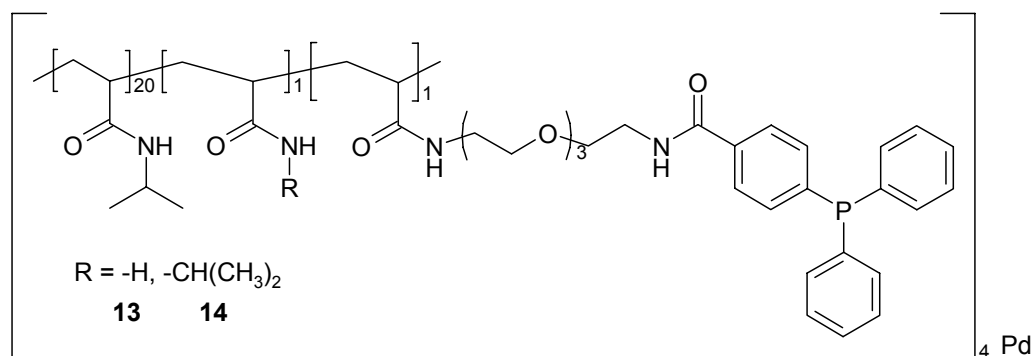


Figure 15. PNIPAM-bound triphenylphosphine Pd(0) Heck catalyst.

In 1997 Milstein and co-workers reported the use of cyclometallated palladium complexes containing pincer-type phosphorus-carbon-phosphorus (PCP)-ligated Pd(II) species to catalyze Heck couplings.⁵⁸ These PCP palladacycle catalysts were reported to show no signs of deactivation in air at temperatures as high as 180 °C. This led our group and others to the development of other XCX-type ligand systems as candidates for highly stable palladium catalysts. The new sulfur-carbon-sulfur (SCS)-ligated Pd(II) species **15**, **16**, and **17** (Figure 16) were found to be highly stable active Pd-sources for Heck catalysis.^{32, 56, 59-62}

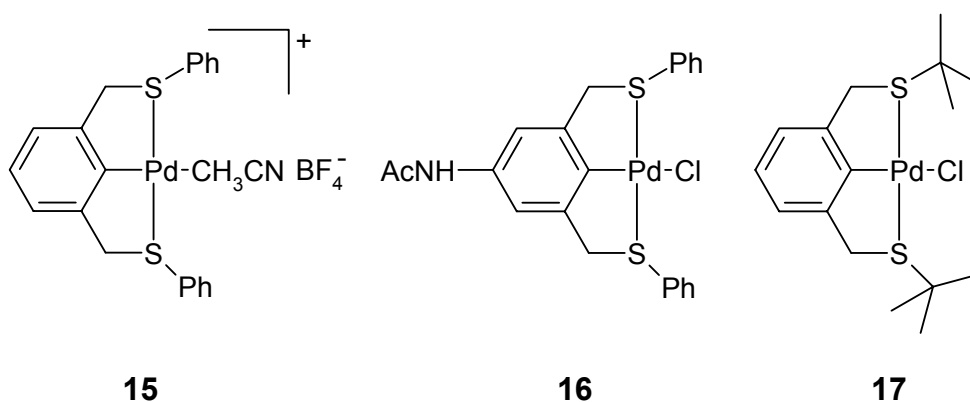


Figure 16. Pincer-type SCS-ligated Pd(II) Heck catalysts.

Moreover, previous results showed no Pd leaching in preparative scale Heck and Suzuki coupling reactions with polymer-bound **1** based on ICP analyses.^{32, 63}

Poly(ethylene glycol) is one of the most common soluble polymers used to support catalysts, reagents and substrates.^{64, 65} In addition to its ready recoverability by solvent precipitation, this polymer has the advantages of having a simple spectroscopic signature and compatibility with a variety of reagents. This polymer is soluble in water as well as many organic solvents. The relatively benign nature of this material is evidenced by its use as a drug conjugate. Thus, this polymer could also be considered a Green polymer support.^{66, 67} Since these PEG supports are end-functionalized, high molecular weight forms of this polymer have relatively low loading. However, branched or lower molecular weight PEG analogs can be prepared that have higher capacity.⁶⁸ PEG or other poly(alkene oxide) supports also have temperature regulated phase selective solubility.^{69, 70}

Smaller oligo(ethylene glycol) groups are also widely available. Such materials are commercially available with various end group functionality because of the widespread use of such oligomers and polymers in preparation of forming bioavailable drug conjugates.^{71,72} Such oligomers have water solubility that is similar to larger PEG analogs and these oligomers have the same chemistry as the larger PEG polymers. However, PEG oligomers are not easily recovered as solids as are their higher molecular weight analogs. Thus, to explore the utility of PEG-like polymers as solubility control elements for the design of recoverable, reusable SCS-Pd complexes, we have used these smaller oligomers to prepare oligo(ethylene glycol)-bound SCS complexes and used them both in aqueous and in mixed phase aqueous systems. These studies have shown that these polar Pd-complexes reactivity is conveniently accelerated by microwave irradiation and that these Pd-catalysts are recyclable when used in thermomorphic solvent mixtures.⁷³⁻⁷⁶

Results and discussion

The synthesis of the oligo(ethylene glycol)-bound SCS-Pd(II) complex **21** is shown in Figure 17.

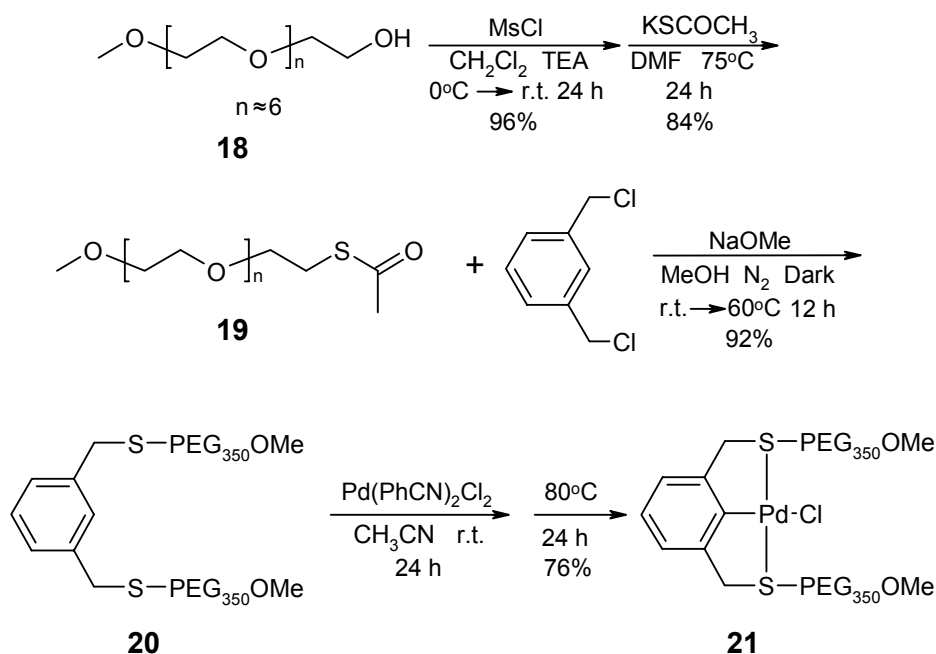
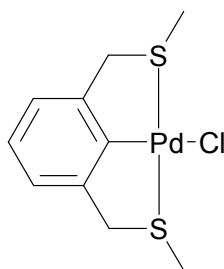


Figure 17. Synthesis of oligo(ethylene glycol)-bound SCS palladacycle catalyst.

The products of this synthesis were characterized by ^1H and ^{13}C NMR spectroscopy. There was no visual sign of decomposition of the final SCS-Pd(II) compound on heating this compound in sealed microwave tubes under an air atmosphere in either organic solvents or water to temperatures as high as 200 °C. This result is consistent with our prior reports and other TGA studies of other similar SCS-Pd(II) complexes.^{63, 77, 78}

While the synthesis of the SCS-Pd(II) complex **21** is straightforward and while **21** can be readily shown to have the structure shown, our studies showed that **21** exhibited interesting dynamic behaviour in ^1H NMR spectroscopy. Specifically, while the ^1H NMR spectrum of **21** had peaks at the expected chemical shifts (including the ipso carbon at δ 150 ppm in the ^{13}C NMR spectrum), the peak corresponding to the

benzylic protons in **21**'s ^1H NMR spectrum was broadened. We had noted this before in other SCS-Pd(II) complexes and interpreted this as being a result of the C_2 chirality of these complexes seen in crystal structures of low molecular weight SCS-Pd(II) complexes.³² While our explanation of dynamic behavior in the ^1H NMR spectrum in terms of dynamic chirality at sulfur was a plausible explanation for this spectroscopic observation, earlier work by Dupont where the similar complex **22** was studied had invoked a more complex explanation including *cis*- and *trans*-diastereomers of the pincer complex.⁷⁹

**22**

More extensive spectroscopic analysis of the dynamic behavior of **21** in CDCl_3 as studied by ^1H NMR spectroscopy agree with this more complex interpretation. Cooling a sample of **21** in CDCl_3 separated the high temperature singlet for the Ar- CH_2 -S- protons not into the doublet of doublets expected for a simple diastereotopic methylene group but rather into a pair of doublets of doublets as shown in the spectra in Figure 18.

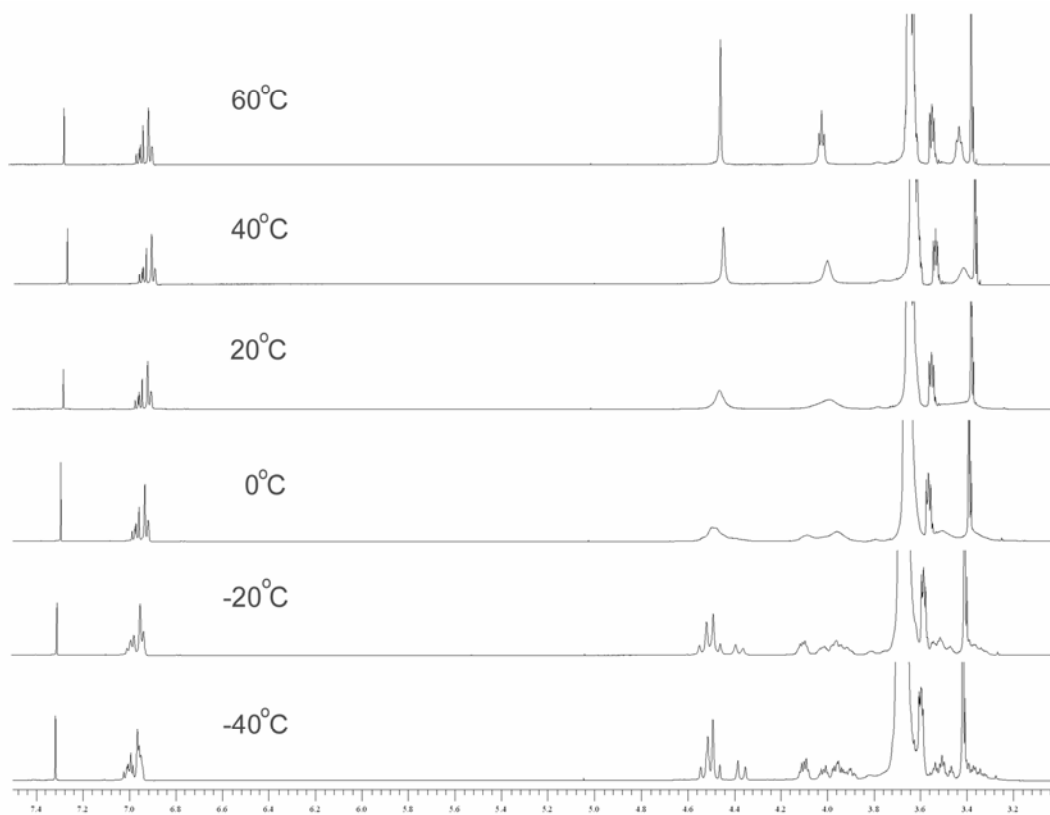


Figure 18. ^1H NMR spectra of complex **16** in CDCl_3 showing dynamic changes in the peaks in the δ 3.8-4.6 region of the spectrum. Smaller concomitant changes are seen in the δ 3.4-3.6 region.

This behavior is consistent with the oligo(ethylene glycol) groups interconverting between isomers **21a** (cis) and **21b** (trans) (Figure 19) through sulfur or ring inversions as described originally by Dupont.⁷⁹ Such behavior and the presence of multiple stereoisomers of these complexes may account for the inability of complexes like **21** to effect asymmetric catalysis.⁸⁰

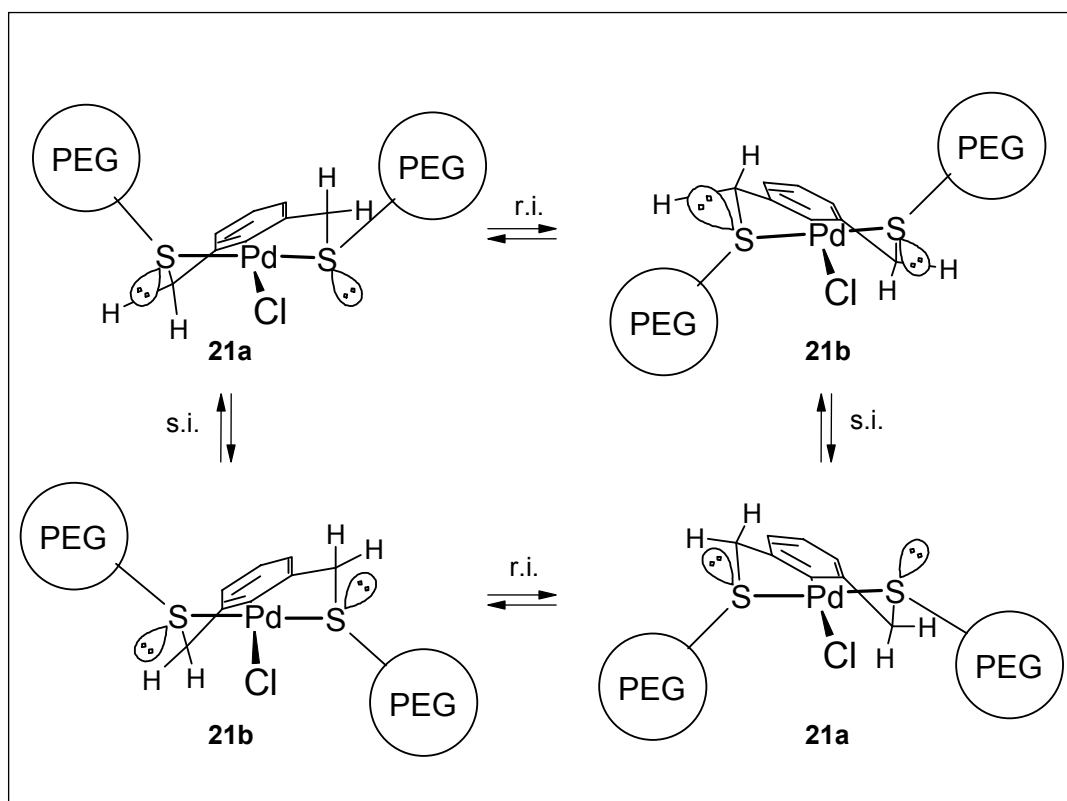
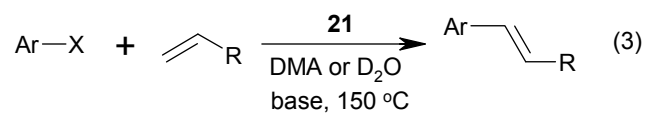


Figure 19. Representation of the two enantiomers of **21a** (cis diastereomer) and **21b** (trans diastereomer) that can interconvert through ring inversions (r.i.) or sulphur inversions (s.i.).

The catalytic activity of **21** in the Heck coupling of several aryl halides and alkene acceptors in a polar aprotic solvent like *N,N*-dimethylacetamide (DMA) or *N,N*-dimethylformamide (DMF) as well as water were investigated (eq. 3).



No special precautions such as purified reagents/solvents or inert atmosphere were necessary due to the stability of the SCS palladacycles. While no decomposition to Pd black was seen, the formation of undetectable amounts of a very active colloidal catalyst cannot be excluded.^{63, 81, 82} Indeed, some evidence that these SCS-Pd(II) complexes are precursors for an extremely active Pd-catalyst is the induction period observed in the plot in Figure 20.

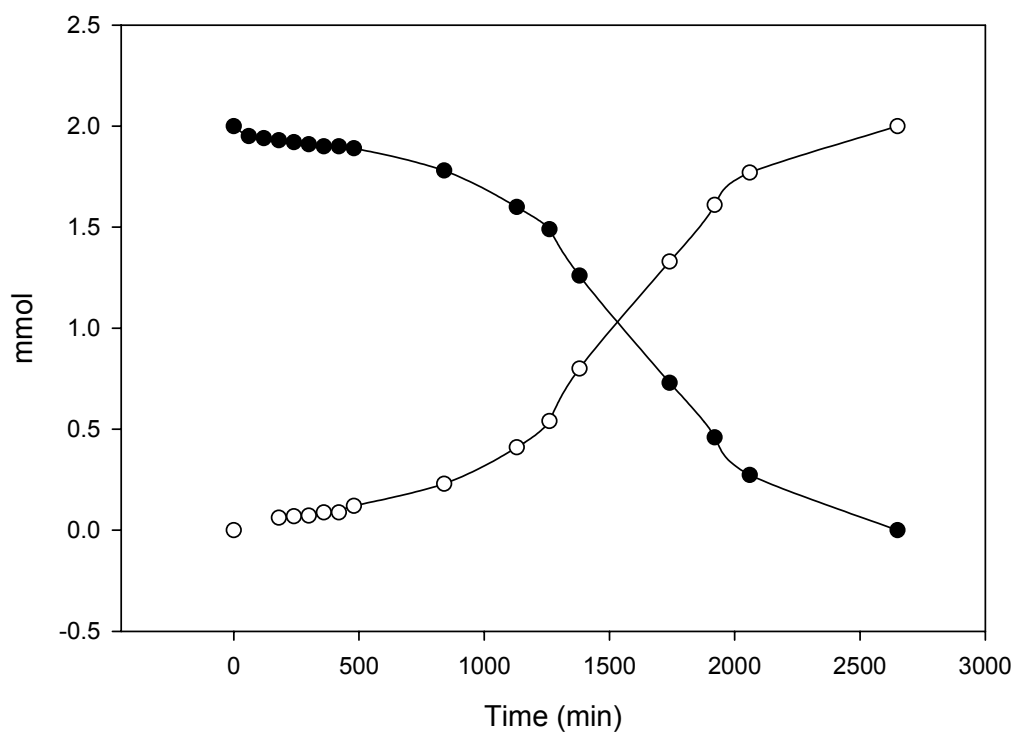


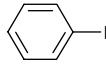
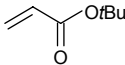
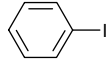
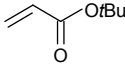
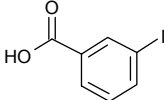
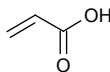
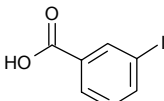
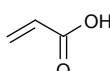
Figure 20. Changes in concentration for iodobenzene (●) or methyl cinnamate (○) in a Heck reaction in DMF with conventional heating at 100 °C. Pseudo first-order conditions were used with 0.05 mol% **21**, 2.0 mmol of PhI, and 20 mmol of both methyl acrylate and Et₃N in 10 mL of DMF.

Subsequent to our work with **21**, our group and Weck and co-workers carried out detailed studies to determine the nature of the active catalyst species for an SCS palladacycle complex in Heck coupling reactions.⁸³ These studies both noted the induction period during recycling experiments and poisoning of catalytic activity in experiments with Hg. Weck also noted poisoning with insoluble poly(4-vinylpyridine) (PVPy)(2% cross-linked) and carried out a three phase test with a silica bound catalyst and an iodobenzene derivative. All these results strongly suggest that the active form of the complex comes from leached/unsupported palladium that is in solution. Weck's studies suggest that palladium does not leach from their supported SCS palladacycle unless the base (TEA) *and* the aryl halide (PhI) *or* olefin (*n*-butylacrylate) is present. Weck speculated that the leaching with aryl halide and base is a result of oxidative addition of the aryl halide to the metal center but offered no suggestions for the leaching in the presence of the acrylate and base. Gladysz and Rocaboy also support this theory as they have used transmission electron microscopy (TEM) to directly observe the palladium colloids that formed when using similar palladacycle catalysts in Heck coupling reactions.⁸⁴ Similar work by Dupont and co-workers on other palladacycle catalysts also support the idea that these species serve as a "reservoir" of an active palladium species under the reaction conditions.⁸⁵ However studies by our group suggest that while SCS complexes themselves are not catalysts that leaching of Pd is virtually undetectable in well-designed experiments.

Specifically, < 50 ppb Pd leaching (the SCS-Pd reaction mixture contained 355 ppm Pd initially) was seen in recycling **21** (*vide infra*) and similarly low values for Pd leaching have been reported by others. I and others in the Bergbreiter group have often seen higher Pd leaching in the first cycle of Heck reactions that use SCS-Pd complexes as a Pd source. In some cases we have deduced that this initial leaching is due to decomposition of some S,S-Pd(II) complex (e.g. a complex of Pd(II) and **20** that did not carbometallate).

The use of microwave irradiation to enhance reaction rates and shorten process times is an area of growing interest.⁷³⁻⁷⁶ We thought that such effects might be particularly useful with these SCS-Pd complexes in Heck catalysis since microwave radiation should be effective whether these polar complexes themselves are catalysts or if unspecified so-called homeopathic colloids⁸¹ were the actual active species. The evaluation of microwave heating was carried out by running identical reactions in either an oil-bath or microwave reactor at 150 °C. The data in Table 1 clearly shows an enhancement in rate with microwave heating.

Table 1. Comparison of conventional and microwave heating of Heck couplings employing **21** as a catalyst.^a

| Entry | Aryl Iodide | Alkene | Heating Method ^d | Time (min) |
|----------------|---|---|-----------------------------|------------------|
| 1 ^b |  |  | C | 70 ^e |
| 2 ^b |  |  | M | 20 ^e |
| 3 ^c |  |  | C | 220 ^f |
| 4 ^c |  |  | M | 20 ^f |

^a These reactions used ArI (0.5 mmol), alkene (1.0 mmol) at 150 °C with varying amounts of base and catalyst. ^b Et₃N (2.0 mmol) and **21** (0.01 mol%) in DMA (2.5 mL) were used. ^c K₂CO₃ (1.5 mmol) and **21** (0.1 mol%) in D₂O (2.5 mL) were used. ^d Heating used a conventional oil bath (C) or microwave (M) reactor. ^e This is the time to reach 100% conversion based on PhI and cinnamate determined by GC using *n*-dodecane as internal standard. ^f This is the time to reach 100% conversion of ArX based on ¹H NMR spectroscopic analysis of the reaction mixture looking for peaks for the IC₆H₄CO₂H and product.

While this could reflect non-thermal “microwave effects”⁸⁶, it is premature to conclude that the microwave radiation itself is causing the rate acceleration since the active species in SCS-Pd(II) complex promoted reactions remains uncharacterized.

Recent reports by Leadbeater and Najera compared the effects of microwaves to conventional heating in palladium catalyzed coupling reactions and found no rate enhancement or “microwave effect”.^{87, 88} Curran has also reported enhanced rates when using microwave heating as compared to conventional heating in Heck couplings

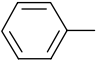
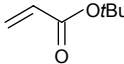
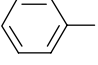
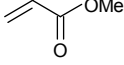
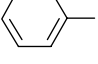
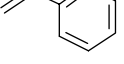
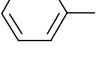
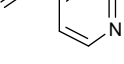
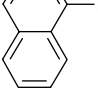
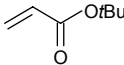
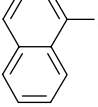
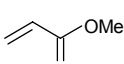
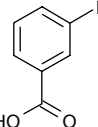
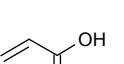
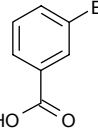
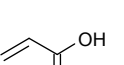
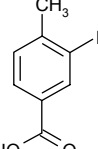
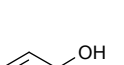
catalyzed by a pincer-type sulfur-carbon- sulfur (SCS)-ligated Pd(II) species similar to **21**, although he does not include the comparison data in his initial report.⁸⁹

I believe that some of the discrepancies between reports observing “non-thermal microwave effects” while others observe no effect may be due to the accuracy of the temperature measurements in the microwave reactor. The two major suppliers of single mode microwave reactors use the same method to measure the temperature inside the reaction vessel. An infra red probe is used to measure the temperature of the outside of the reaction vessel which is in turn converted to the inside temperature of the solution based on calibration data. Proper precise calibration of the instrument is essential for the comparison studies since even small temperature differences of only 5 to 10 °C result in drastic differences in reaction rate. First hand experience with both major manufacturers has led me to the conclusion that most users are not concerned with extremely precise temperature measurements and therefore both companies are not concerned with calibration tests, although both reactors can be calibrated to give highly accurate data. This may be the cause of observed “microwave effects” in some instances. One manufacturer produces an instrument that uses a one point calibration method that neither the technical staff nor the senior scientists could explain to me. The same company also promotes the use of cooling gas during reactions to “apply energy directly to the reactants while minimizing bulk heating”. This method will result in very drastic discrepancies between the reading temperature of the instrument and the actual temperature of the reaction solution for the reasons mentioned above. With that said, a properly tuned and calibrated system from either manufacturer that is checked regularly

should produce highly accurate, reproducible results. Even with well maintained accurate equipment several studies are still required to gain insight into this complex field. The complex issues of proving or disproving the sometimes controversial topic⁹⁰,⁹¹ of nonthermal “microwave effects” is apparent when reviewing the two recent reports by Larhed. In 2003 while studying Heck vinylations of aryl chlorides in ionic liquids, comparison studies showed a dramatic increase in rate for reactions promoted by microwave heating compared to conventional oil-bath heating.⁹² In 2004 they found no difference between microwave and conventional heating methods on reaction rates for the double arylation of olefinic vinyl ethers in 10% aqueous DMF.⁹³ It seems that effects of microwave heating vary not only for different reactions but can also vary on very similar reactions. It is hoped that my study as well as the aforementioned studies will stimulate further investigation into this field.

Catalytic reactions of **21** with several aryl halides and alkenes were carried out in DMA at 150 °C employing microwave irradiation (Table 2).

Table 2. Heck couplings of various organic-soluble aryl halides and alkenes promoted by microwave irradiation employing **21** as a catalyst.^a

| Entry | Aryl Halide | Alkene | Product | Time (min) | Yield ^c |
|-----------------|---|---|---------|------------|--------------------|
| 5 |  |  | 22 | 10 | 69% |
| 6 |  |  | 23 | 10 | 74% |
| 7 |  |  | 24 | 40 | 33% |
| 8 |  |  | 25 | 60 | 54% |
| 9 |  |  | 26 | 15 | 79% |
| 10 |  |  | 27 | 10 | 75% |
| 11 ^b |  |  | 28 | 10 | 63% |
| 12 ^b |  |  | 28 | 10 | 63% |
| 13 ^b |  |  | 29 | 10 | 97% |

^a These reactions used ArX (0.5 mmol), alkene (1.0 mmol), TEA (2.0 mmol), **21** (0.1 mol%) in DMA (2.5 mL) at 150 °C with microwave irradiation at 30 W. ^b K₂CO₃ (1.5 mmol) was used as the base. ^c This is an isolated yield. All the reactions' conversions of ArX were quantitative based on GC analysis *n*-dodecane as an internal standard to follow the disappearance of the ArX.

Since Heck chemistry using SCS-Pd complex is feasible in DMA and since DMA mixed with other solvents is an established thermomorphic system,⁵⁶ we decided to try recycling the catalyst using a thermomorphic solvent mixture consisting of equal volumes of 10% aqueous DMA and heptane (Figure 21). Results of these studies are summarized in Table 3 and show that catalyst recycling with thermomorphic solvent mixtures and microwave heating is an efficient and effective procedure.

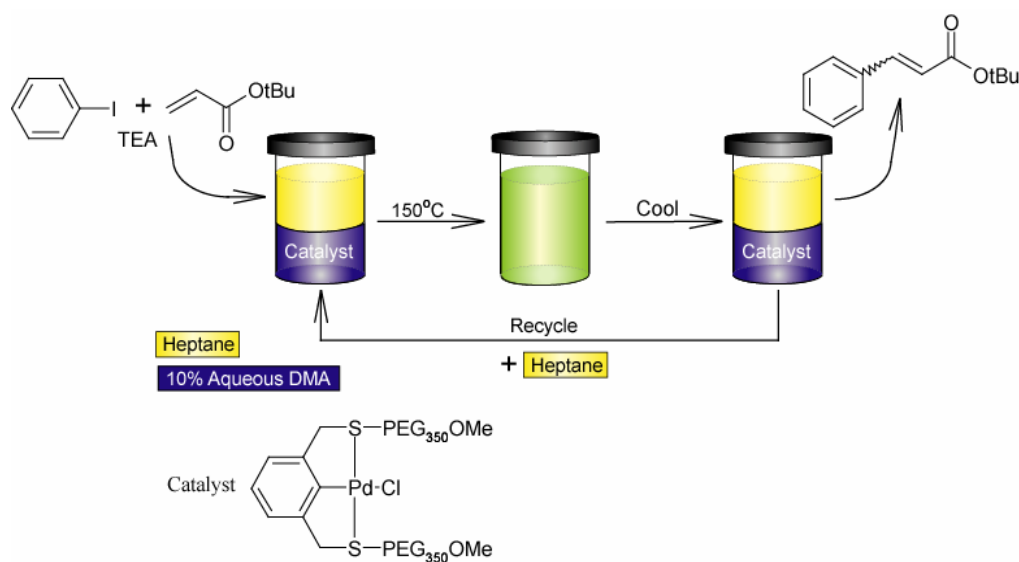
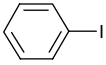
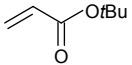


Figure 21. Thermomorphic recycling with **21**.

Table 3. Recycling of **21** under thermomorphic conditions.^a

| Entry | Aryl Iodide | Alkene | Product | 1 st Cycle | 2 nd Cycle | 3 rd Cycle | 4 th Cycle |
|-------|---|---|---------|-----------------------|-----------------------|-----------------------|-----------------------|
| 14 |  |  | 22 | 100(98) ^b | 100(98) ^b | 100(88) ^b | 100(78) ^b |

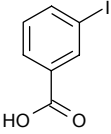
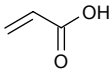
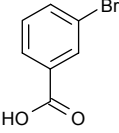
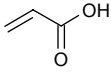
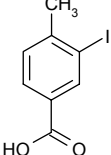
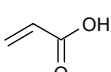
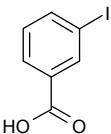
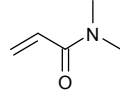
^a These reactions used ArI (0.50 mmol), alkene (0.60 mmol), TEA (0.75 mmol), **21** (0.2 mol%) in 1:2 (v/v) 90% aqueous DMA/heptane (3.0 mL) at 150 °C with microwave irradiation. The reactions were monitored by GC (following disappearance of ArI) and were complete within 20 min. ^b Yields are in parentheses for products isolated from the heptane phase. The small scale of the reactions accounts for the variable isolated yields for reactions that were quantitative based on ArI consumption.

No added solvent was required for product and catalyst isolation in such systems and catalyst recycling just required addition of a fresh substrate solution to the mixed aqueous solution of catalyst. Inductively coupled plasma emission-mass spectrometry (ICP-MS) was used to analyze the heptane phase for each cycle to investigate leaching of Pd from the polar phase. The amount of Pd detected in the heptane phase for cycles 1, 2, 3, and 4 were 133 ppb, 75 ppb, 80 ppb, and 64 ppb respectively. While there is certainly some Pd being leached into the non-polar phase, the amount of leached Pd may in fact be lower than these values since we are at the lower detection limit of the analysis. In fact, the amount of Pd detected in a blank sample containing no Pd was 21 ppb. The initial Pd concentration in this reaction was 355 ppm so the Pd leaching in cycles 2-4 of approximately 50 ppb is relatively low.

Water is an ideal solvent since it is cheap, abundant, and benign.^{31, 94} Water is also very polar making it highly microwave active so it is an attractive solvent for these types of transition-metal catalyzed coupling reactions as well.⁹⁵

Traditionally transition-metal catalysts have been made water soluble by trying to find a catalytically active metal salt or by making more traditional catalysts soluble with organic ligands that contain ionic or ionizable groups.³¹ However, transition metal salts are not always as soluble or active as desired. Modification of ligands can also have undesirable effects on the electronic nature of a ligand or can make catalysts acid or base sensitive. The oligo(ethylene glycol) ligands used here are less problematic in that regard since the Pd complex solubility is controlled by the nonionic oligomer which is relatively inert in all other chemistry. In a brief study, microwave irradiation was shown to be useful in promoting coupling reactions between several water-soluble aryl halides with water-soluble alkenes employing **21** as a Pd source (Table 4). These studies employed *meta*-substituted aryl halo acids as substrates because we could easily monitor reaction progress by ¹H NMR spectroscopy in D₂O.^{96, 97}

Table 4. Heck couplings of water-soluble aryl halides and alkenes promoted by microwave irradiation employing **21** as a catalyst.^a

| Entry | Aryl Halide | Alkene | Product | Time (min) | Yield ^c |
|-------|---|---|---------|------------|--------------------|
| 15 |  |  | 28 | 20 | 42% |
| 16 |  |  | 28 | 30 | 42% |
| 17 |  |  | 29 | 30 | 58% |
| 18 |  |  | 30 | 20 | 82% |

^a Reaction conditions: ArX (0.5 mmol), alkene (1.0 mmol), K₂CO₃ (1.5 mmol), **21** (0.1 mol%) in D₂O (2.5 mL) at 150 °C with microwave irradiation at 30 W. ^b K₂CO₃ (0.5 mmol) was used as the base. ^c This is an isolated yield. All reactions had a quantitative conversion of the aryl halide to product based on ¹H NMR spectroscopic analysis of the reaction mixture and the disappearance of peaks for the ArX and the appearance of product peaks.

Conclusions

In summary, oligo(ethylene glycol) ligands can engender water or polar phase solubility into Pd-sources for Heck reaction catalysis. Catalytic reactions using such complexes exhibit no visual evidence for complex decomposition and the speed of the catalytic reactions is significantly increased with microwave radiation. Although recent evidence shows that the SCS palladacycles act as precatalysts that provide a slow and steady source of palladium (0) nanoparticles, leaching of the Pd is insignificant in our

studies. Water is a viable solvent for these types of coupling reactions provided that the substrates are water soluble. Recycling of the precatalyst using a thermomorphic system was possible even with small oligo(ethylene glycol) groups and microwave irradiation of these thermomorphic mixtures of palladium complexes and substrates is a viable scheme to significantly shorten reaction times for simple Heck reactions of aryl iodides.

CHAPTER III

LATENT SOLID-PHASE EXTRACTION USING THERMORESPONSIVE SOLUBLE POLYMERS

Introduction

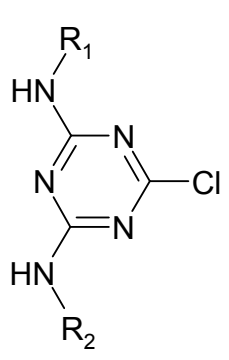
Over the past 200 years we have seen unprecedented advances in science and technology. The prosperity that our civilization has enjoyed is a result of this technological progress. Unfortunately our rapid industrial progress has had some deleterious side effects on our environment. Environmental remediation of anthropogenic contaminants is becoming more important as we expand the scale of our environmental footprint. The ever increasing complexity and magnitude of environmental contamination results in the need for new and improved remediation technologies.^{98,99} Separation science is the key element to remediation technologies. For example while incineration of a hydrocarbon contaminant is feasible as a 10 wt% aqueous sludge, a 100 ppb aqueous solution cannot be similarly treated unless the hydrocarbon is separated from water.

The separations needed for handling dilute waste can be carried out in numerous ways depending on the nature of the bulk phase and the contaminant. Separations of aqueous solutions of metal ion contaminants have been accomplished by methods as simple as precipitation with salts. While simple and effective this method suffers from lack the specificity and requires large amounts of precipitating agents and is not so effective with very low concentrations of contaminants. A more elaborate method of

removing contaminants from a solution is the use of a separable sequestration agent that will bind the contaminants. Commonly this method involves the use of solubilizing ligands followed by extraction into organic solvents. Insoluble polymeric sequestration agents like cross-linked ion exchange resins are also commonly used.¹⁰⁰⁻¹⁰² Soluble polymers have been used as well though their use is less common.^{103, 104} These soluble sequestration agents are advantageous in that they avoid the diffusion limitations associated with their insoluble counterparts. Previous work in the Bergbreiter group involved the use of poly(*N*-isopropylacrylamide) (PNIPAM) bound chelating ligands to act as a latent solid phase for the sequestration of metal contaminants from aqueous solution.¹⁰⁵ This concept is similar to that used by Hoffman and co-workers to prepare a thermally induced precipitation immunoassay.¹⁰⁶ A latent solid phase separation strategy offers the advantages of separation of insoluble supports coupled with the efficiency of soluble reagents. Our current research efforts in this area involve the use of PNIPAM as a latent solid phase for the sequestration of the s-triazine herbicide atrazine from aqueous solutions in a collaborative effort with professor Simanek's group.

Atrazine is the most important member of the family of herbicides based on monochlorotriazines (Table 5). As a selective herbicide, atrazine inhibits photosynthesis in certain plants.¹⁰⁷ Atrazine is primarily used on corn for the selective control of broadleaf weeds, such as pigweed, cocklebur, and velvetleaf, as well as certain grass weeds. Annual sales for atrazine average between 80-90 million pounds per year. According to recent water quality studies, atrazine is found 10 to 20 times more frequently than the next most detected pesticide.¹⁰⁸

Table 5. Common monochloro-*s*-triazine herbicides.

| | Herbicide | R₁ | R₂ |
|---|------------------|---|------------------------------------|
|  | Atrazine | —CH(CH ₃) ₂ | —CH ₂ CH ₃ |
| | Simazine | —CH ₂ CH ₃ | —CH ₂ CH ₃ |
| | Cyanazine | —CH $\begin{matrix} \text{CH}_2 \\ \\ \text{CH}_2 \end{matrix}$ | —CH ₂ CH ₃ |
| | Terbutylazine | —C(CH ₃) ₃ | —CH ₂ CH ₃ |
| | Eglinazine | —CH ₂ COOH | —CH ₂ CH ₃ |
| | Proglinazine | —CH ₂ COOH | —CH(CH ₃) ₂ |
| | Propazine | —CH(CH ₃) ₂ | —CH(CH ₃) ₂ |

High dose animal oral exposure has been shown to adversely affect the lungs, liver, kidney, spleen, adrenal glands, and brain of test subjects. The Environmental Protection Agency (EPA) has officially classified atrazine as a possible human carcinogen (class C). In recent changes to the Safe Drinking Water Act, the “safe” concentration of atrazine has been set to 3 ppb, although atrazine concentrations in the Midwest are often as high as 33 ppb.¹⁰⁹ The best available technology for removal of herbicides is “granulated activated carbon” (GAC). Studies have shown that high doses of GAC are needed when atrazine concentrations exceed 15 ppb.¹⁰⁸ This treatment technology is effective when atrazine concentrations are low, but the equipment needed for this treatment is expensive. Other techniques like ozone, advanced oxidation, reverse

osmosis, photocatalytic reactions,¹¹⁰ and synthetic resins such as molecularly imprinted polymers show promise, but require additional study.¹¹¹ The necessity of an efficient system for the removal of atrazine from water is an on-going problem.

Results and discussion

Here, we describe how PNIPAM and PNIPAM derivatives can be used as latent solid phase supports for the physical sequestration or reactive scavenging of low concentrations of hydrophobic contaminants from aqueous solutions. PNIPAM is a thermoresponsive polymer that is soluble in water at low temperature, but it has the feature that it quantitatively precipitates from solution above a lower critical solution temperature (LCST).¹¹² This behavior has been exploited in the design of “smart” materials for catalysis,^{56, 113} in the design of thermally responsive coatings,¹¹⁴ in preparation of soluble polymeric ligands,¹⁰⁵ in the development of supports for heavy-metal scavenging,¹¹⁵ and in forming temperature or pH-sensitive materials for drug delivery applications.¹¹⁶ More recently, PNIPAM has been conjugated with a variety of biologically-relevant molecules for separation and recovery.¹¹⁷ Here we expand the use of such thermoresponsive supports for the physical sequestration and/or the reactive scavenging of hydrophobic monochlorotriazines from aqueous solutions.

The polymers and guests used in this study are shown in Figure 22. Poly(*N*-isopropylacrylamide), **31**, was chosen as an unreactive thermally-responsive polymer. This polymer has an LCST of 30.2 °C.¹¹⁸ A reactive piperidine-functionalized copolymer, **32**, containing a 95:5 mol:mol mixture of *N*-isopropylacrylamide and 4-(acrylamidomethyl)piperidine groups was also prepared.

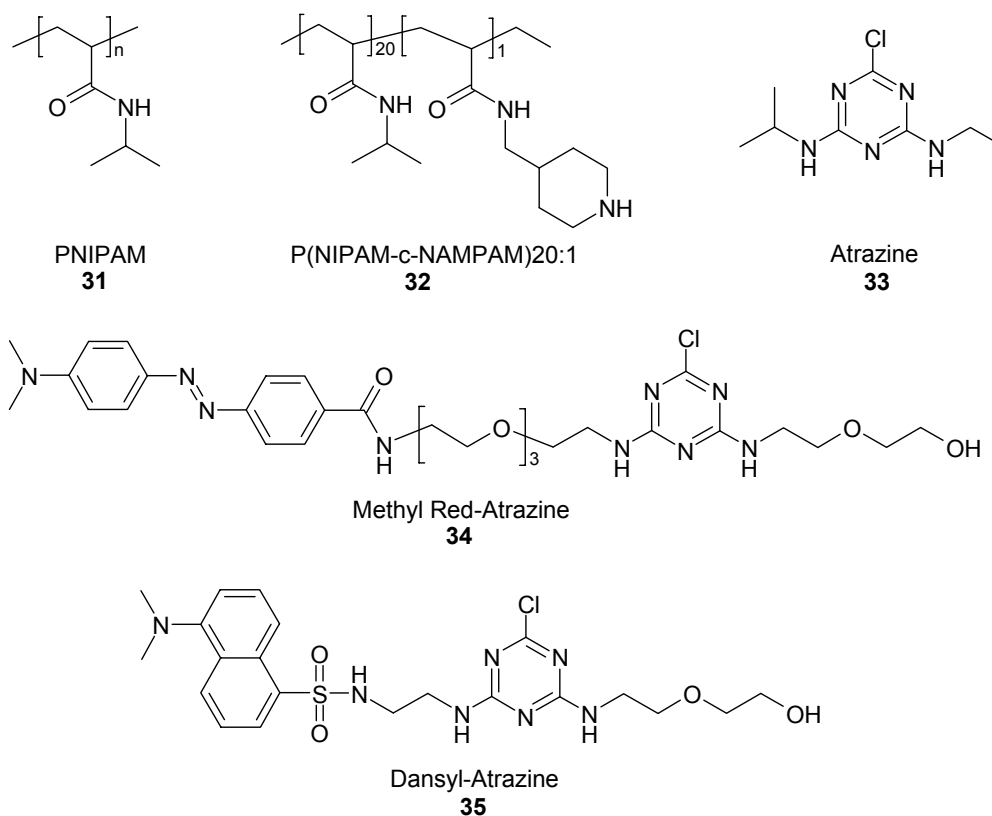


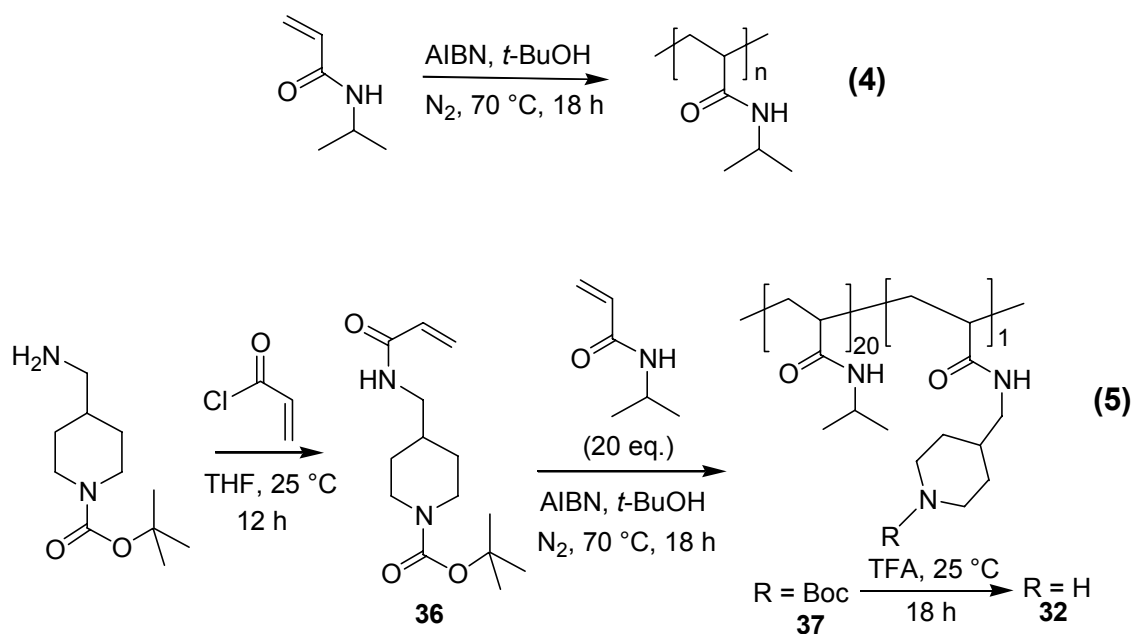
Figure 22. Thermoresponsive polymeric sequestration agents (**31** or **32**), atrazine (**33**) and dye-labeled atrazine analogs (**34** or **35**).

This latter polymer had an LCST of 40 °C. In both cases, solutions of these polymers precipitated above their LCST temperature to form a solid hydrogel phase.^{112, 118} As shown below, this hydrogel phase can physically absorb a significant amount of a nonpolar monochlorotriazine from a dilute aqueous solution. Incorporation of a nucleophilic secondary amine covalent scavenger produces an even more efficient reactive scavenger. This modified thermally responsive polymer leads to recovery of > 98% of the same monochlorotriazines that were only partially sequestered by **31**. Such

sequestration and covalent scavenging, coupled with the ability to effect nearly quantitative removal of the precipitated polymer by filtration or centrifugation makes these and related polymers potential candidates for applications in remediation and scavenging technology.

Atrazine, **33**, was chosen as a substrate because it is an example of an environmental contaminant of current concern. Two more dye-labeled analogs of atrazine examined in this study included the monochlorotriazines **34** and **35**. One of these atrazine analogs was designed to contain a dansyl group for fluorescence analysis (**35**). In the second case, an atrazine analog was labeled with a methyl red group to facilitate visual and spectrophotometric analysis (**34**). Atrazine (**33**) concentrations were measured by liquid chromatography-mass spectrometry (LC-MS).

The thermoresponsive polymers **31** and **32** were prepared to compare physical and chemical scavenging of monochlorotriazines by a latent solid phase extractant. Polymer **31** is a homopolymer of *N*-isopropylacrylamide, and was prepared accordingly to equation 4. It was not expected to chemically react with **33**, **34**, or **35**. Polymer **32** is a copolymer of *N*-isopropylacrylamide and **36**, and was prepared as shown in equation 5. The secondary amine groups in polymer **32** were expected to react in a covalent manner with a monochlorotriazine based on earlier studies performed in the Simanek research group.¹¹⁹⁻¹²¹



A general representation of our sequestration procedure is shown in Figure 23. In these experiments, an initial homogenous solution of analyte (**33-35**) in water was first prepared. Then, polymer **31** or **32** was added as a solution (in the fast precipitation protocol) or as a solid (in the slow precipitation protocol). The resulting solutions were heated to precipitate the polymer sequestrant or scavenger (15 min for fast precipitation protocol, and 8 h for slow precipitation protocol). Salt was added to facilitate separation of the polymeric precipitate.¹²² Separation of the supernatant containing residual monochlorotriazine from the polymer **31** or **32**, and any sequestered monochlorotriazine was then accomplished by centrifugation at temperatures above the LCST of **31** or **32**.

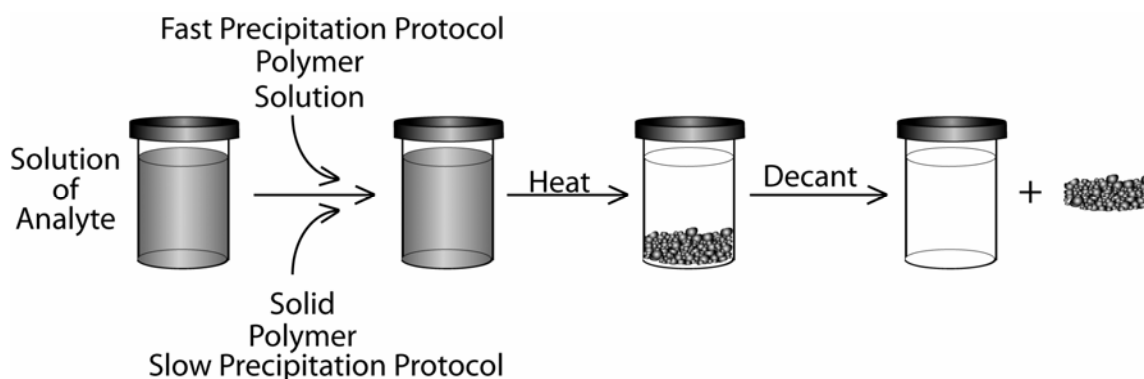


Figure 23. The protocols used for sequestration of monochlorotriazines.

The sequestration of analytes **33-35** was monitored over a concentration range that varied depending on the analyte. In the case of **33**, relatively low concentrations of approximately 100 ppb were used. This level of **33** was studied because the “safe” concentration of atrazine (**33**) in water is 3 ppb, and typical atrazine concentrations in runoff can be as high as 120 ppb.^{123, 124} Higher concentrations of 5-10 ppm were used for the dansyl- and methyl red labeled monochlorotriazines. Substrates **34** and **35** provided a spectroscopic labeled analog for atrazine **33** or other chlorotriazine herbicides. In the cases where the reactive polymer **32** was used, the concentration of reactive groups on the polymer was approximately 10^{-3} N, which amounted to a >100-fold excess over the concentration of any of the analytes.

Analysis of the effectiveness of polymers **31** or **32** to effect sequestration of monochlorotriazines derivatives were carried out using several techniques. For a low 100 ppb concentration of **33**, LC-MS was used to measure the concentration of analyte in solution. For **35**, fluorescence spectroscopy was used. For the UV-visible dye labeled

atrazine analogue **34**, quantitative analysis was carried out by UV-visible spectroscopy, although qualitative visual analyses were also possible. For example, non-covalent sequestration of **34** by **31** was visually evident since both the supernatant and precipitated polymer were visually yellow in color. The solution was nearly colorless when **34** was sequestered by the reactive polymer **32**.

The results of the sequestration experiments are listed in Table 6. In general, non-covalent sequestration occurs with all analytes, but a significant amount of the analyte remains in solution regardless of whether a “fast” or “slow” precipitation protocol was used. Quantitative sequestration was achieved using the “slow” precipitation protocol for polymer **32** with all the monochlorotriazine substrates **33–35**. However, polymer **32** was not as effective in the “fast” protocol for the most relevant triazine substrate **33**. While the reason for this difference was not examined in detail, we presume it reflects kinetic problems associated with the bimolecular reaction of low concentrations of a substrate like **33**, even in the presence of an excess of amine groups. The rates for complete reaction of a very low concentration of monochlorotriazine with the soluble polymer-bound secondary amine **32** were comparable to the rates seen with insoluble polymer-bound secondary amines which also required extended reaction times to reduce concentrations of **33** to < 1 ppb. There is a notable difference between the effectiveness of polymers **31** and **32**. We attribute the efficiency of **32** to be due to the reactivity of the pendant piperidine groups. These groups can undergo nucleophilic aromatic substitution with monochlorotriazines derivatives.

Table 6. Sequestration of atrazine (**33**) or atrazine analogs **34** or **35** from dilute aqueous solutions using thermally responsive polymers **31** and **32**.

| Fast Precipitation Protocol | | | | Slow Precipitation Protocol | | |
|-----------------------------|-----------|-------------------|----------------------------|-----------------------------|-------------------|----------------------------|
| Polymer | Analyte | Initial [Analyte] | % Sequestered ^a | Analyte | Initial [Analyte] | % Sequestered ^a |
| 31 | 33 | 96 ppb | 46 | 33 | 100 ppb | 56 |
| | 34 | 6.4 ppm | 78 | 34 | 8 ppm | 83 |
| | 35 | 8 ppm | 60 | 35 | 10 ppm | 71 |
| 32 | 33 | 96 ppb | 72 | 33 | 100 ppb | > 99 ^b |
| | 34 | 6.4 ppm | 97 | 34 | 8 ppm | 98 |
| | 35 | 8 ppm | 96 | 35 | 10 ppm | 98 |

^aThe values for the % sequestered are based on the average of two experiments in each case. ^bThe concentration of atrazine remaining in the solution was below the detection limit (1 ppb) of the LC-MS analysis.

Distinguishing between non-covalent sequestration and covalent sequestration was possible using a simple thin layer chromatography experiment. When the precipitated polymer from a sequestration experiment involving **32** with **34** or of **31** with **34** using either the “slow” or “fast” protocol was redissolved, a qualitative analysis of the solution indicated that most of the dye was back in solution. This result superficially corresponds to earlier results, where most of the atrazine sequestered by an insoluble reactive polymer could be released from the polymer by an acid digestion. However, the

qualitative reappearance of color in a solution of redissolved polymer does not distinguish between non-covalent and covalent sequestration of **34** by the polymer. TLC experiments were successful in making this distinction. When the precipitated polymer **32** that had essentially quantitatively sequestered **34** was spotted on a TLC plate and developed with CH₂Cl₂-MeOH (10:1), the only dye species detectable was a species at the origin. Under the same conditions, **34** had an R_f of approximately 0.35 (Figure 24). In a similar experiment, TLC of a solution prepared from a precipitate of **34** and **31** (a precipitate that was presumed to be a physical mixture of **31** and **34**) had a spot with an R_f of approximately 0.35 coincident with the R_f of free **34**. TLC experiments using the products from the coprecipitation of **31** and **35**, or of **32** and **35**, had similar results. In the latter case, no free **35** was detected by TLC when the precipitate of **32** and **35** was redissolved. In the former case with physical entrapment, a fluorescent spot for free **35** was detectable by TLC when the precipitate of **31** and **35** was redissolved.

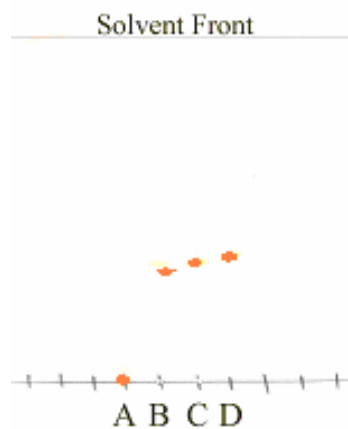


Figure 24. TLC plate to corroborate the covalent sequestration of **34**. TLC spots of polymer **32** (**A**) and polymer **31** (**B**) after sequestration of **34**. Co-spot of **34** added to polymer **31** after non-covalent sequestration of methyl red atrazine (**C**). Spot for methyl red atrazine **34** (**D**).

Conclusions

Two new atrazine derivatives with spectroscopic tags have been synthesized. The methyl red derivative (**34**) provides an instant visual indication of the efficiency of a particular sequestering agent. Simple UV-VIS analysis provides a convenient, quantitative method to determine the amount of **34** that has been removed from solution by a sequestration agent. The increased sensitivity of fluorescence spectroscopy allows us to measure the amount of the labeled analyte more precisely. These tagged molecules provide a fast and convenient way to evaluate the efficiency with which different materials can sequester s-triazine herbicides. LC-MS can then be used to measure this efficiency more precisely on the actual herbicide.

The ability of the thermoreponsive polymer PNIPAM to sequester hydrophobic guest molecules has been evaluated. The PNIPAM homopolymer itself can sequester 56% of the atrazine from a 100 ppb solution. The functionalized PNIPAM copolymer (**32**) containing cyclic, secondary amines was able to remove >99% of the atrazine contained in a 100 ppb solution. The experiments above show that soluble polymers that precipitate under mild heating can serve both as physical and chemical sequestrants. In the case of monochlorotriazines, chemical sequestration using a functional polymer containing a secondary amine is significantly more successful at sequestering monochlorotriazines. The increased ability of **32** to remove atrazine from water is attributed to the ability of the secondary, cyclic amine pendant groups along the backbone to undergo nucleophilic aromatic substitution with the triazine ring. The nature of the binding of atrazine to the polymers were investigated and the experimental evidence supports nonreversible binding of the hydrophobic guests. This covalent binding leads to higher sequestration of the reactive guests from solution.

CHAPTER IV

HIGH-THROUGHPUT STUDIES OF THE EFFECTS OF POLYMER STRUCTURE AND SOLUTION COMPONENTS ON THE PHASE SEPARATION OF THERMORESPONSIVE POLYMERS

Introduction

Thermoresponsive polymers such as the poly(*N*-alkylacrylamide)s undergo folding that results in a dramatic decrease in their solubility above a lower critical solution temperature (LCST).^{112, 125} The phenomena seen with these synthetic polymers mirror the cold denaturation processes of peptides and proteins.^{126, 127} Although there exists a level of uncertainty about the exact mechanism of polymer folding both in the synthetic and biological cases,^{128, 129} the release of hydrophobic hydration water is believed to play a crucial role in the process. At low temperature, water molecules bind to hydrophobic residues of the polymer in a low entropy configuration. At temperatures above the LCST, the ordered water molecules are released into the bulk solution, increasing the system's entropy and, thereby allowing the endothermic desorption of the water to be coupled into a net exergonic process.

Current methods for studying LCST phenomena in thermoresponsive polymers include light scattering, UV-vis absorption measurements, differential scanning calorimetry, and infrared spectroscopy.¹³⁰⁻¹³⁵ Most of these techniques, however, are low throughput, slow procedures and require relatively large amounts of polymer for analysis. These factors limit the ability to probe the myriad of subtle solvent and

polymer structure effects that presumably would have to be part of any complete study designed to elucidate the molecular details of the folding mechanism. This is unfortunate, because such information obtained for structurally diverse synthetic polymers like poly(*N*-alkylacrylamide) copolymers might be broadly applicable to the understanding of related processes such as the cold denaturation of proteins. To help remedy this situation, we have enlisted the expertise of the Cremer group in a collaborative effort to utilize a novel linear temperature gradient device to obtain all temperature readings in an LCST measurement simultaneously as a function of position rather than sequentially as a function of time.¹³⁶ The process works by exploiting the fact that when a thermoresponsive polymer folds and aggregates above its LCST, the solution becomes cloudy, leading to a readout of the phase transition temperature by the position on the temperature gradient of the abrupt change in the amount of light scattered. The need for no more than 2 μ L of total solution in order to make a measurement is an especially advantageous feature of this method. Moreover, as shown below, we can couple the use of this new device with pool-split syntheses of libraries of poly(*N*-alkylacrylamide)s.¹⁶ Using such syntheses, we can compare poly(*N*-alkylacrylamide) copolymers whose *N*-alkyl substituents are varied but whose degree of polymerization and polydispersity are identical. Such syntheses provide us with a way to probe very similar polymers without facing ambiguities due to synthesis variabilities inherent in typical radical addition polymerizations.

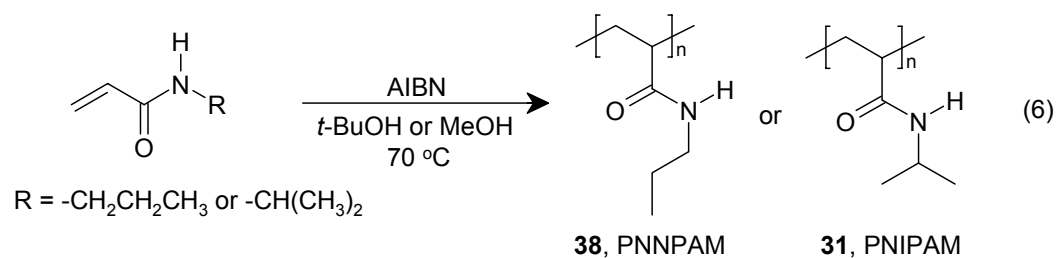
Herein the effects of solvent components and polymer structure variance on the folding of PNIPAM and related polymers are explored using our newly developed

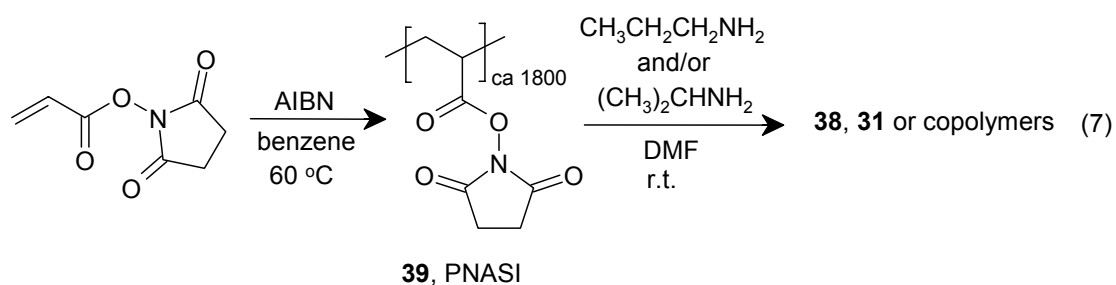
techniques. First, the effect of halide and alkali ions on the LCST of PNIPAM was systematically studied and the results are compared with the known Hofmeister series data for PNIPAM and proteins. Second, solution isotopic effects on the LCST were measured with various mole ratios of D₂O: H₂O. The results indicate a linear relationship between the mole fraction of D₂O and the LCST of a poly(*N*-alkylacrylamide).¹³⁷ The precision of this technique for LCST determination was evaluated using repetitive analyses of the same polymer sample and of separately prepared but otherwise identical polymers. We then used a series of isomeric poly(*N*-alkylacrylamide)s to show the subtle effects of polymer structures on the macromolecular folding processes. These studies used LCST measurements of a series of poly(*N*-*n*-propylacrylamide-co-*N*-isopropylacrylamide) samples of identical molecular weight that were isomeric by virtue of having 1-propyl or 2-propyl substituents on the amide nitrogens of the polymer. A linear relationship between the mole fraction of the more hydrophobic poly(*N*-*n*-propylacrylamide) and the LCST temperature was found with the more hydrophilic poly(*N*-isopropylacrylamide) having a 5.4°C higher LCST. Finally, the effects of M_w on poly(*N*-isopropylacrylamide)'s LCST were investigated. The change in LCST with the lower M_w samples combined with the leveling off of LCST at higher M_w led us to investigate the importance of end group effects. The effects of the hydrophobic/hydrophilic nature of the end groups on PNIPAM were found to significantly alter the LCST as the chain length of the samples decreased.

Results and Discussion

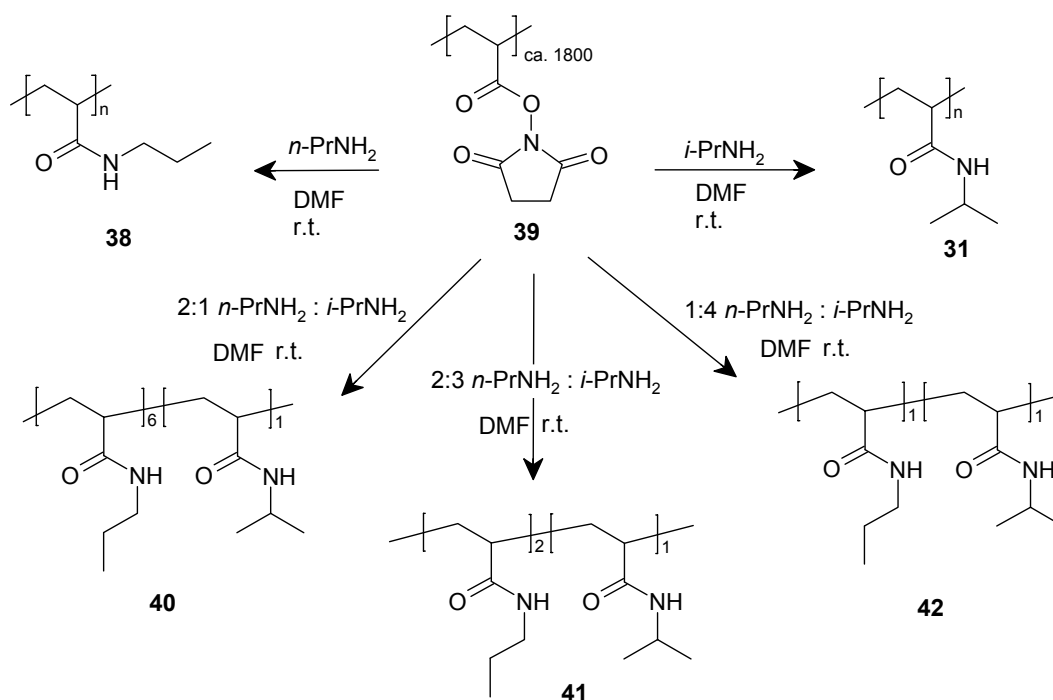
Polymer Synthesis and Characterization

The poly(*N*-alkylacrylamide)s used in this study were prepared either by polymerization of the monomers (eq. 6) or by derivatizing a polymer containing an activated ester (eq 7). Homopolymers of poly(*N*-*n*-propylacrylamide) (PNNPAM) and poly(*N*-isopropylacrylamide) (PNIPAM) were prepared by both routes. Copolymers of poly(*N*-*n*-propylacrylamide) and poly(*N*-isopropylacrylamide) (PNNPAM-*c*-PNIPAM) were all prepared by aminolysis of the active ester polymer poly(*N*-acryloxysuccinimide) (PNASI) (eq. 7). The steric bulk of isopropylamine diminished its rate of substitution for the active ester by a factor of 3 relative to that of the straight-chain *n*-propylamine; therefore, the ratio of amines incorporated into the polymer was not the same as the ratio of amines added. This did not pose a problem since the ratio of amides on the copolymers could be determined easily by ¹H NMR spectroscopy.





The advantage of using reaction 7 is shown in the synthesis in Scheme 6 where a library of structurally isomeric copolymers was prepared that differ only in their mole fraction of $-\text{CH}_2\text{CH}_2\text{CH}_3$ vs $-\text{CH}(\text{CH}_3)_2$ groups.



Scheme 6. Synthesis of an isomeric library of poly(*N*-propylacrylamide)s containing *N*-*n*-propyl, *N*-isopropyl or mixtures of *N*-*n*-propyl and *N*-isopropyl pendant alkyl groups.

In terms of the present work, the use of the common starting active ester polymer **39** has significant advantages and some possible disadvantages. The major advantages are that polymers derived from **39** using mixtures of isomeric amines have the same molecular weight, degree of polymerization, and polydispersity. Whereas homo and copolymers derived from free radical polymerization of the respective monomer/monomer mixtures will have properties that are batch dependant. Each synthesis will produce a polymer with a different degree of polymerization and polydispersity. The effects that these variables have on the polymers LCST could skew or distort the subtle changes in LCST caused by polymer microstructure that we are trying to measure. Copolymer synthesis via polymerization of monomer mixtures can result in even more complications.

Differences in the reactivity ratios of comonomers could result in non-uniform distribution of each monomer throughout the polymer backbone. Blocks of homopolymer or alternating copolymer could be incorporated unevenly throughout each polymer chain. The resulting microdomains could alter the LCST of the polymer. Non-uniform composition between polymer chains would result in bulk properties that are dependant on complex mixtures of different polymers. Our split-pool synthesis of copolymers should also result in a completely random distribution of each alkyl group along the polymer backbone and throughout the polymer chains since the presence of one alkyl group should not influence the incorporation of others. The fact that the product copolymers had an LCST that was linearly dependent on the mole fraction of the different amide alkyl groups (*vide infra*) provides evidence (although does not prove)

that these products are random copolymers. This synthesis also offers advantages in that more structurally diverse libraries are also potentially available. There are, however, some potential problems with using **39** as a common precursor. Specifically, since we can measure the LCST with significant precision, variations of polymer composition from run to run due to adventitious hydrolysis of < 1% of the active ester groups or due to incorporation of trace amounts of other groups from impurities in the amines can occur. The presence of < 1% of an impurity cannot be detected by NMR spectroscopy and could lead to superficially similar samples with small differences in LCST values. For example, in one sample where only a small excess of $\text{CH}_3\text{CH}_2\text{CH}_2\text{NH}_2$ relative to **39** was used, the PNNPAM product had a much higher LCST, an effect we attributed to the presence of some $-\text{CO}_2\text{H}$ groups (from hydrolysis of the NASI groups upon workup).^{138,}
¹³⁹ However, in our experience the differences seen for LCST values of the “same” poly(*N*-alkylacrylamide) derived from different samples of **39** using excess amine are no greater than the differences in LCST values for different samples of **31** prepared in separate conventional polymerizations.

The molecular weights of the PNIPAM samples used in this study and in our earlier work were determined by viscosimetric analysis using literature values of $K = 9.59 \times 10^{-3}$ and $\alpha = 0.65$.¹⁴⁰ Recently, we found another report listing these values as a range of $K = (2.2-15) \times 10^{-3}$ (mean value being 5.8×10^{-3}) and $\alpha = 0.78 \pm 0.09$.¹⁴¹ Different exponents of the Mark-Houwink-Sakurai equation in these two reports produce very disparate molecular weights. This has led us to analyze the PNASI derived PNIPAM polymers molecular weight by static light scattering. Two independent

preparations of PNIPAM made by substitution of the active esters of PNASI with isopropylamine were analyzed, and M_w values of 320,000 and 350,000 Da were obtained. These light scattering reports confirm that the PNASI derived materials are indeed high molecular weight materials and that the M_w values of these polymers are comparable to the M_w values we originally measured by viscometry using the literature K and α values reported by Winnik.¹⁴⁰

High-Throughput Temperature Gradient Measurements

Until now LCST measurements have been made consecutively as a function of *time* using a temperature ramp on macroscopic samples. The Cremer group adapted the linear temperature gradient apparatus, shown in Figure 25, for combinatorial temperature measurements for use in LCST studies as a high-throughput alternative to these existing procedures.^{136, 142, 143} The use of a temperature gradient allows data to be collected as a function of *position* instead and makes it possible to obtain multiple temperature measurements for multiple samples in a single experiment.

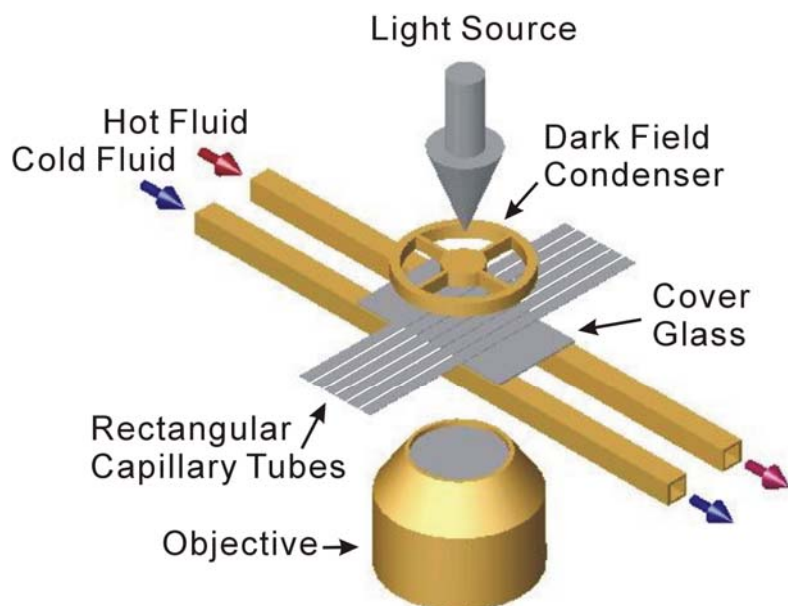


Figure 25. Schematic drawing of a temperature gradient device. Up to 10 rectangular borosilicate capillary tubes were put on the temperature gradient device without noticeable temperature discrepancy across the tubes. Each CCD image fits six capillary tubes simultaneously under a 2× objective.

The fact that this procedure only requires minute amounts of sample means that the effects of many variables on a material's LCST can be studied more economically with libraries of similar substrates. These high-throughput techniques also provide us with the ability to make very precise relative measurements of the LCST and, hence, facilitate studies of subtle effects of polymer microstructure and environment on a substance's LCST.

In the actual apparatus (Figure 25), dark field microscopy was used to image the scattering intensity of the folded and aggregated polymers as a function of position. Six rectangularly shaped borosilicate capillary tubes ($100\ \mu\text{m} \times 1\ \text{mm} \times 2\ \text{cm}$) were placed

under a $\times 2$ objective parallel to the temperature gradient. The temperature values along the tubes were determined by measuring the lengthwise position in a CCD camera image. As a demonstration, the tubes were filled with aqueous solutions containing 10 mg/mL of PNIPAM in a series with varying NaCl concentrations. The amount of polymer required in each experiment was only 2 mg, and the 200 μL of solution prepared with this amount of polymer was sufficient to fill dozens of the capillaries described above whose volume was 2 μL each. The phase transition temperature was determined by the onset point of the clouding curve (Figure 26 and inset). As shown in Figure 26, all six positions can be samples of interest. However, in most other experiments we found it useful to place two polymer solutions with known LCSTs at positions 1 and 6. Such solutions served as internal standards and allowed the slope of the temperature gradient to be determined each time an assay was performed and facilitated more precise measurements of the LCST temperature.

The small volumes utilized in this device allow very efficient, almost instantaneous heat flow into the sample. This not only has the advantage of providing quick measurements but also allows this device to be used to study the kinetics of LCST phenomena.¹⁴⁴ The scale of this method also avoids the issue of hysteresis. The sample tubes can be flipped to invert the hot and cold sides and within seconds the same LCST can be measured again. This is in contrast to traditional methods requiring slow temperature ramps in order to minimize the effects of hysteresis.^{132, 133}

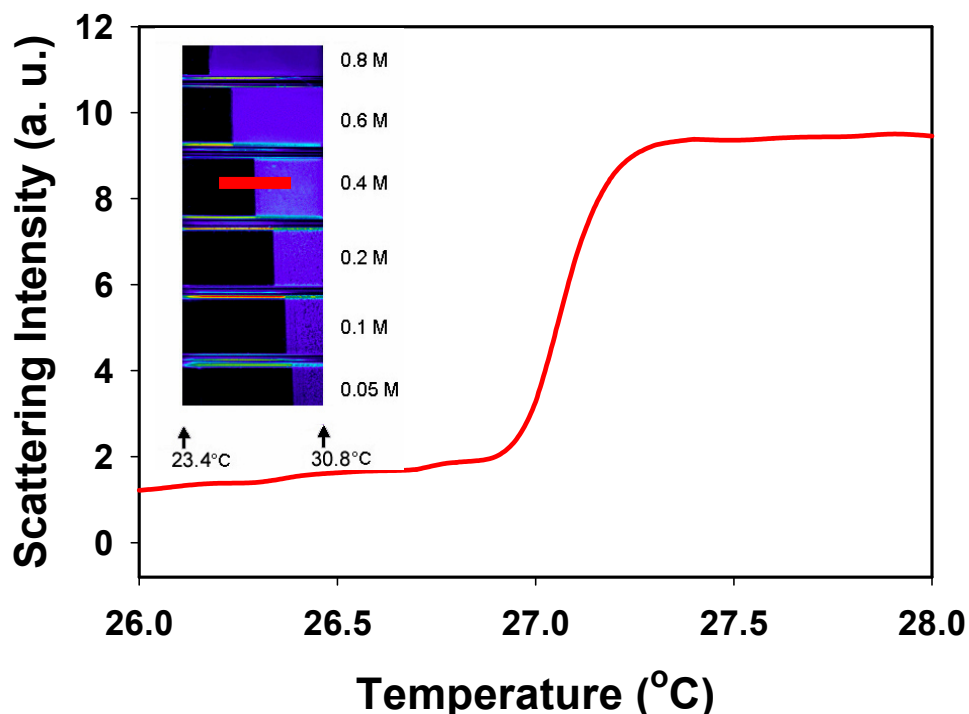


Figure 26. A typical clouding curve for PNIPAM 10 mg/mL in 0.4 M aqueous NaCl. The hot and cold extremes were calibrated with two standard polymer solutions and were 30.8 and 23.4°C. This curve derives from the red portion of one sample in the inset. Inset: A CCD image of six samples inside square capillary tubes. Solutions of PNIPAM (10mg/mL) were prepared using NaCl concentrations that ranged from 0.05 M to 0.8 M. The precipitant was pseudo-colored blue for clarity.

Hofmeister Effect

In 1887 S. Lew with a student of Franz Hofmeister at the University of Prague described the efficacy of certain ions in their ability to precipitate proteins from blood serum from aqueous solutions.¹⁴⁵ In 1888 Hofmeister published a more detailed study of the regularities in the protein precipitating ability of different salts. This original “Hofmeister series” rank ordered the ability of both cations ($\text{Mg}^{2+} > \text{Li}^+ > \text{Na}^+ \approx \text{K}^+ >$

NH_4^+) and anions (citrate³⁻ > SO_4^{2-} \approx tartrate²⁻ > HPO_4^{2-} > CrO_4^{2-} > acetate⁻ > HCrO_3^- > Cl^- > ClO_3^-) to precipitate hen egg white proteins from aqueous solutions. Hofmeister found that this series was the same for both hen egg white and blood serum proteins. He hypothesized that the protein precipitation was caused by the salts ability to absorb solvent from the macromolecule, and that the absorbing strength of water for each salt is what caused this repeated trend. He reasoned that this trend should also hold for other colloidal substances, and further studies on more diverse colloidal materials like ferric oxide and sodium oleate showed that the precipitation power of different salts on aqueous solutions of these substances also followed this same general trend. Later these specific ion or “Hofmeister” effects would appear in other areas such as attenuation of enzymatic activity, membrane transport, and bubble-bubble fusion.¹⁴⁶⁻¹⁴⁹ It is quite remarkable that all of the specific ion effects follow nearly identical trends, providing evidence that there should be some common theory that describes all of these effects. In 1985 Collins and Washabaugh proposed a molecular theory to describe this phenomenon based on water stabilization effects.¹⁴⁹ Previously they had discovered that anions will elute in the same rank order as the Hofmeister series (SO_4^{2-} \approx HPO_4^{2-} > F^- > Cl^- > Br^- > I^- (\approx ClO_4^-) > SCN^-) when separated by aqueous chromatography on a Sephadex G-10 epichlorohydrin cross-linked dextran column.^{149, 150} They described species that eluted before Cl^- as polar kosmotropes (water-structure makers) and those that eluted after Cl^- as chaotropes (water-structure breakers). Solutes that destabilized native protein structures (kosmotropes) would adsorb to the column and increase the hydrodynamic radii of test solutes chromatographed in their presence, while solutes that stabilize native

protein structures (chaotropes) do not absorb to the column and decrease the hydrodynamic radii of test solutes chromatographed in their presence. Chaotropes should interact with the first layer of immediately adjacent water molecules less strongly than bulk water, while kosmotropes should interact with this first hydration layer more strongly than bulk water. The ions that bind water less tightly will dehydrate easier and be retained more by the column. When ions are absorbed to the column polar kosmotropes compete more effectively for nearby water molecules than bulk water. Chaotropes compete less effectively for nearby water molecules when compared to bulk water. This water structure perturbation by ions is similar to Hofmeister's original theory of water attracting ions with hydration shells. This water-structure theory can be used to explain why all of the specific ion effects follow the same trends.

We decided to investigate the specific ion effects on the precipitation temperature of PNIPAM for a series of halide and alkali metal ion solution components. We reasoned that our ability to measure the LCST of a polymer solution quickly with a great deal of precision coupled with our ability to produce designer polymers should allow us to gain some insight into the underlying theory behind the specific ion effect. Using the methods described above, LCST measurements of a series of PNIPAM solutions in water were made as a function of ion type and concentration. For each salt, eight solutions with different ion concentrations were prepared. The effects of these solution components on the LCSTs of PNIPAM are plotted as a function of both the particular halide anion (Figure 27) as well as the alkali cation (Figure 28).

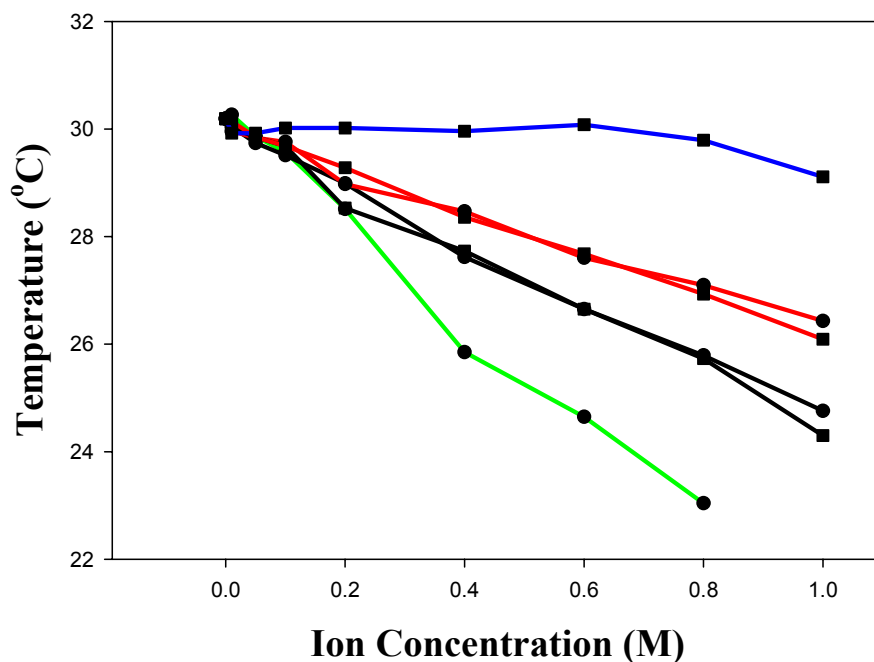


Figure 27. The effect of various sodium and potassium halide solutions on the LCST of PNIPAM. The LCSTs of PNIPAM were measured at eight different concentrations for each sodium or potassium halide (0.01-1.0 M of metal halide in water). The lines were drawn as guides to the eye. Potassium (●) and sodium (■) salts of fluoride (green), chloride (blue), bromide (red), and iodide (black).

As can be seen from Figure 27, the ability of a given halide to lower the LCST decreased with its size. Since fluoride has the strongest tendency to form hydrogen bonds with water molecules, less water was available to solvate the macromolecules. According to traditional Hofmeister analysis, this should effectively decrease the number of solvent molecules available to solvate the polymer, thereby making it easier for molecules to aggregate or salt-out of solution.

On the other hand, the low charge density of the iodide ion should provide the least competition for hydration waters with PNIPAM. Hence the unfolded state of PNIPAM was stable to a higher temperature at a given halide anion concentration when iodide was present in place of fluoride. While some of these "water organization" effects have recently been called into question and the exact mechanism of action may be controversial,^{128, 151} the important point is that the effects observed in our microscopic high-throughput technique are the same as have been seen previously both for PNIPAM solutions and for protein solutions.

The observed effects were more complex for the alkali metal cations as expected (Figure 28). The propensity of cations to lower the LCST increased from lithium to sodium and then decreased from potassium to cesium ($\text{Li} < \text{Cs} < \text{Rb} < \text{K} < \text{Na}$). Again, the series obtained here agrees well with the known ability of these ions to salt out proteins and nonelectrolyte solutes like PNIPAM.¹⁵²⁻¹⁵⁴

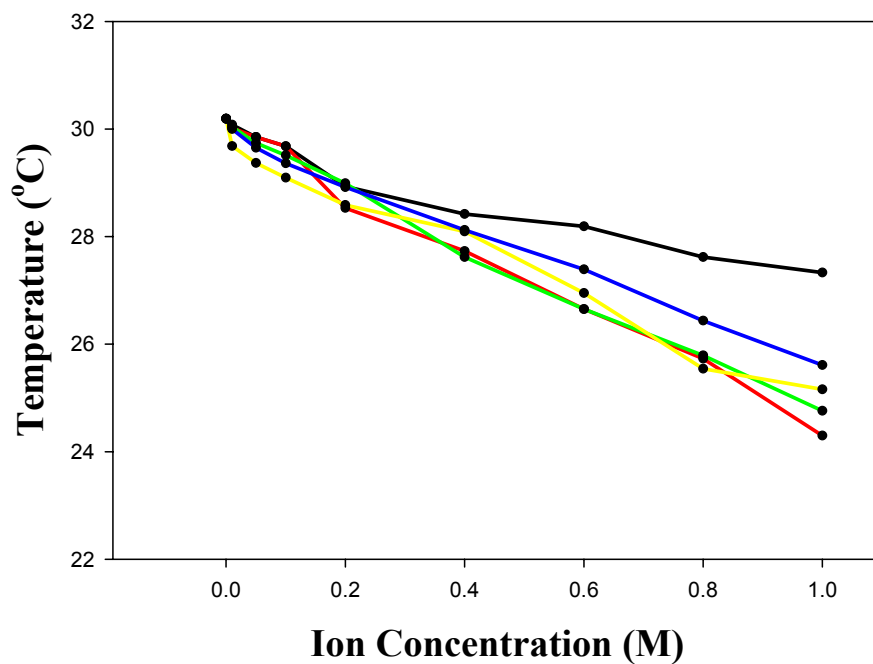


Figure 28. The effect of alkali metal ion variation on the LCST of PNIPAM. The LCSTs of PNIPAM were measured with various alkali metal cations at eight different concentrations (0.01-1.0 M) using chloride as a common anion: Lithium (black), sodium (red), potassium (green), rubidium (yellow), and caesium (blue).

Solvent Isotope Effects

The precision in our measurements of the LCST for polymers like PNIPAM should allow us to measure effects that are much more subtle than the effects of solution ion components. First we decided to see how the changes in solvent isotope from H₂O to D₂O would affect the LCST of PNIPAM. The effects of hydrogen bonding with solvent water were studied on solutions of PNIPAM using varying molar ratios of D₂O and H₂O (Figure 29).

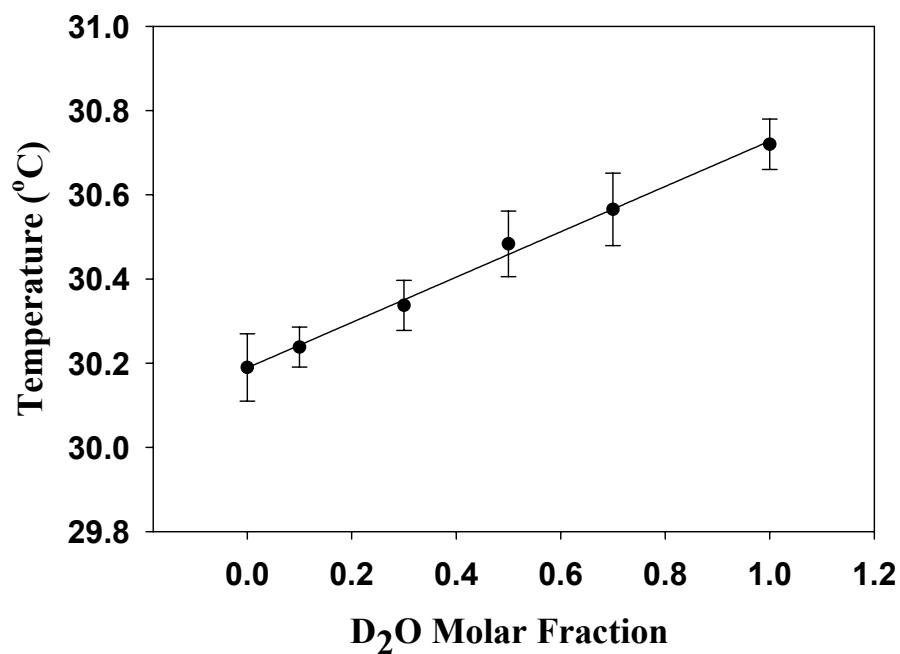


Figure 29. Solvent isotope effects on the LCST of PNIPAM measured using PNIPAM concentrations of 10 mg/mL in a series of solutions with various mole fractions of D₂O contents. The LCST range was from 30.2 to 30.6°C.

As can be seen from the data, the LCST is higher in heavy water than light water.

Similar effects have been reported in previous light scattering¹⁵⁵ and pressure perturbation calorimetry¹³⁷ measurements using PNIPAM. While the change is relatively small in these experiments, the LCST has a roughly linear relationship with the mole fraction of D₂O. The underlying reasons for this increase in the LCST with D₂O are not precisely known; however, it has been observed that polymer chains in D₂O solutions take on more extended conformations than with H₂O.¹⁵⁵ Furthermore, the

amide bonds of the PNIPAM should be relatively well exposed to water below the LCST. Since hydrogen bonding is approximately 5% stronger in D₂O than in H₂O,¹⁵⁶ it is expected that breaking the bonds to the amide moieties would be more enthalpically costly in the former case. This would explain the nearly linear change in LCST with heavy water content. On the other hand, if species such as HOD had more complex interactions with the polymer, one might have expected nonlinear changes instead. We have also made the isotope measurements with poly(*N-n*-propylacrylamide) and found roughly the same behavior. In this case, a ΔT of approximately 0.4 °C was found between pure H₂O and pure D₂O; however, the error bars on the measurements were larger because the scattering cross section of poly(*N-n*-propylacrylamide) is roughly half of that for poly(*N*-isopropylacrylamide) at the same concentration.

The effects of solution components on the LCST of poly(*N*-isopropylacrylamide) in H₂O and D₂O were also investigated. The specific ion effect for three different salts (NaClO₄, NaI, and NaSCN) were investigated in normal and heavy water. The even spacing between H₂O and D₂O data points throughout each plot in Figures 30-32 indicates that the perturbation effect of heavy water and the ionic components are additive and that there are no synergistic effects.

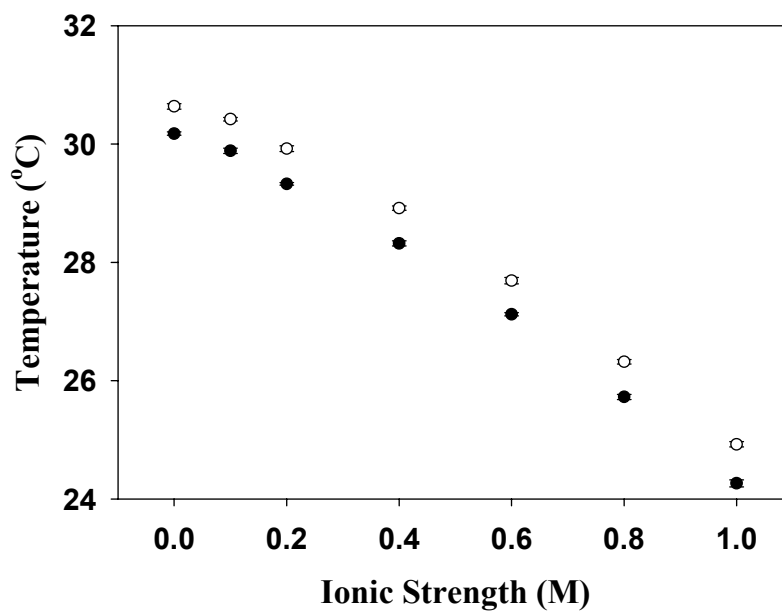


Figure 30. The effect of NaClO_4 at varying ionic strength on the LCST of PNIPAM in H_2O (●) and D_2O (○).

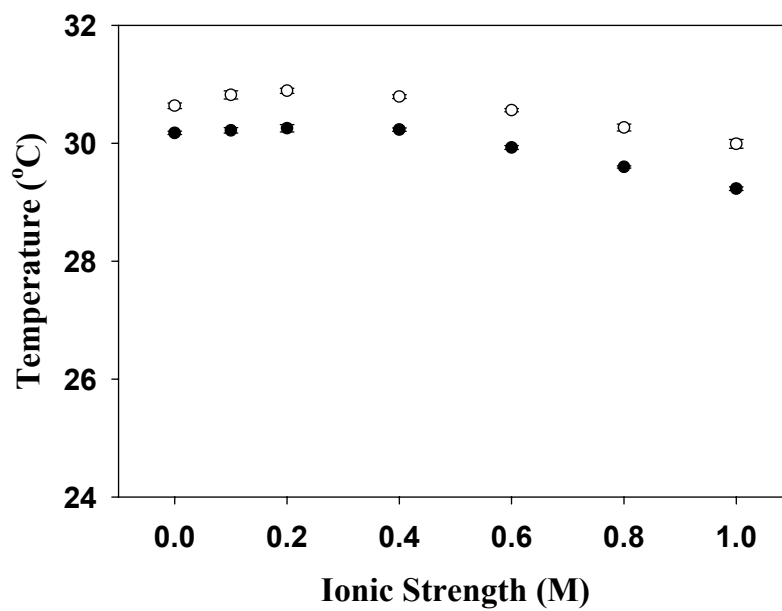


Figure 31. The effect of NaI at varying ionic strength on the LCST of PNIPAM in H_2O (●) and D_2O (○).

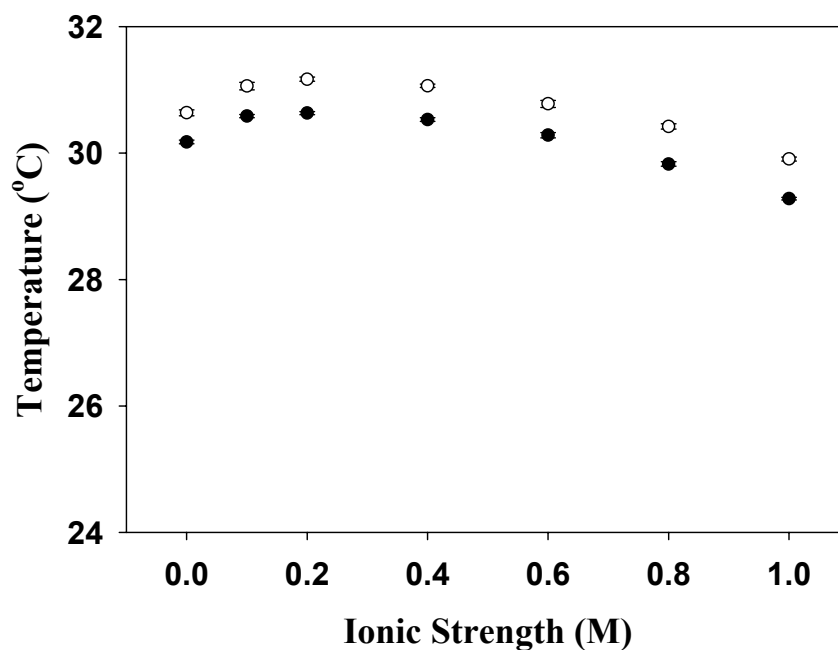


Figure 32. The effect of NaSCN at varying ionic strength on the LCST of PNIPAM in H₂O (●) and D₂O (○).

Effects of Polymer Microstructure

To test the utility of our apparatus for studies of the effects of molecular structure on PNIPAM-like systems, we elected to investigate structurally isomeric polymers by substituting varying amounts of *n*-propyl groups for isopropyl groups on the side chains of PNIPAM (polymers **38**, **31**, **40**, **41** and **42** in Scheme 6). As noted above, these syntheses were designed so that the homo- and copolymers all had the same degree of polymerization, polydispersity and molecular weight by preparing all the polymers from the same polymeric intermediate **39** (Scheme 6). LCSTs were measured for each system

and the results are shown as a function of the ratio of the *N*-isopropyl to *N*-*n*-propyl substituents (Figure 33).

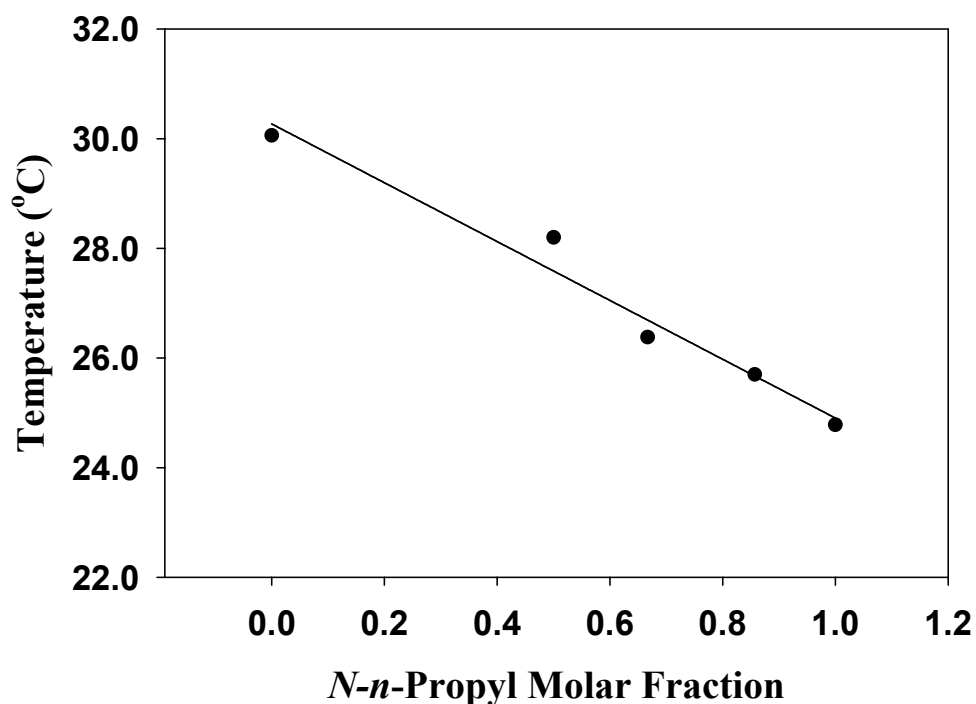


Figure 33. The effect of the identity of the *N*-alkyl substituent on the LCSTs for isomeric poly(*N*-alkylacrylamide)s containing varying ratios of isopropyl/*n*-propyl *N*-alkyl groups. The concentration of the poly(*N*-alkylacrylamide) **38, 31, 40, 41, or 42** was 10 mg/mL in deionized water.

The difference in LCST between PNIPAM and poly(*N*-*n*-propylacrylamide) (PNNPAM) was approximately 5.4 °C, and a monotonic trend can be clearly seen as the ratio of *N*-isopropyl to *N*-*n*-propyl groups was increased. Since the two side chains are very

similar, the slightly lower LCST for the *n*-propyl group may reflect a slightly reduced solvent accessible area for the linear molecule vs the branched chain.

Reproducibility of the Measurements

We examined the reproducibility of our measurements of LCST values using both multiple measurements of the same sample and multiple measurements of separately prepared but otherwise identical samples. The values are given in Table 7 and indicate precision on the order of $\pm 0.2^\circ\text{C}$ as well as accuracy on the order of $\pm 0.2^\circ\text{C}$ for five different trials each of four different samples. Each sample represented a separate synthesis, and the polymers were the product of polymerizations in two different solvents, MeOH and *tert*-BuOH. Syntheses were done in duplicate. A trial was defined as taking a given sample and placing it across the brass tubes. Subsequent trials required repeatedly removing the sample and replacing it across the temperature gradient and remeasuring the LCST. The mean, standard deviation, and standard error for all 20 data points are 24.9, 0.28, and 0.062 $^\circ\text{C}$, respectively. The LCST temperature values measured with this technique are within experimental error of those measured by other techniques.

Table 7. Repeated LCST measurements on two different samples of poly(*N-n*-propylacrylamide) (PNNPAM) prepared in two different solvents showing the precision of the LCST temperature analyses that use darkfield microscopy and the linear gradient temperature apparatus described here to measure LCSTs.

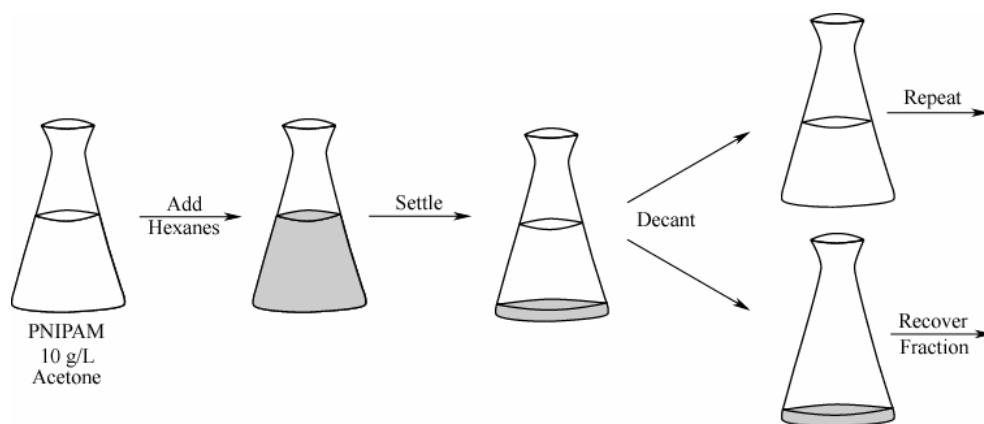
| | | LCST ^a (°C) | LCST ^b (°C) |
|----------|------------------------|------------------------|------------------------|
| Sample 1 | Trial 1 | 25.0 | 25.1 |
| | Trial 2 | 24.9 | 25.1 |
| | Trial 3 | 25.1 | 25.3 |
| | Trial 4 | 25.1 | 25.1 |
| | Trial 5 | 24.9 | 25.0 |
| Sample 2 | Trial 1 | 24.5 | 25.1 |
| | Trial 2 | 24.6 | 25.0 |
| | Trial 3 | 24.4 | 24.4 |
| | Trial 4 | 24.5 | 24.7 |
| | Trial 5 | 24.6 | 24.7 |
| | Mean ^c | 24.8 | 25.0 |
| | Std. Dev. ^c | 0.26 | 0.27 |
| | Std. Err. ^c | 0.084 | 0.085 |

^aThe polymer was prepared via free radical polymerization of *N-n*-propylacrylamide in *t*-BuOH. ^bThe polymer was prepared via free radical polymerization of *N-n*-propylacrylamide in MeOH. ^cThe statistical parameters listed are derived from the 10 data points obtained for two different samples of the same polymer preparation. The mean, standard deviation and standard error for all 20 data points are 24.9, 0.28, and 0.062 °C, respectively.

Effects of PNIPAM Molecular Weight

Several previous studies on the effects of molecular weight on the LCST of PNIPAM have produced inconsistent results. Work by Fujishige et al.¹⁵⁷, Ptitsyn et al.¹²⁶, Okano et al.¹⁵⁸, and Hoffman et al.¹⁵⁹ all report no appreciable change in LCST with changes in the molecular weight of PNIPAM. Where work by Tong et al.¹²² as well as Heskins and Guillet¹⁶⁰ report increasing LCST with increasing molecular weight. Finally Freitag et al.¹⁶¹ as well as Schild and Tirell¹⁶² report decreasing LCST with increasing molecular weight. We thought that our experience in molecular weight determination for PNIPAM combined with our ability to measure these very subtle differences in LCST with a great deal of precision would enable us to provide more definitive results as to how changes in molecular weight of PNIPAM effects it's LCST.

This work was carried out by initially preparing 15 g of PNIPAM *via* free radical polymerization of *N*-isopropylacrylamide in methanol. Then, 10 g of this material was fractionated into several samples with different molecular weights as shown in Scheme 7.^{163, 164}



Scheme 7. Fractionation of PNIPAM *via* selective precipitation.

The fractionation involved the selective precipitation of higher molecular weight PNIPAM molecules from solution. This process is similar to the standard solvent precipitation method mentioned in chapter I involving the use of “good” and “bad” solvents for the polymer, however in this case the bad solvent is gradually added much like the “bad” solvent in a normal two solvent recrystallization. A dilute solution of PNIPAM (10 g/L) in a good solvent, in this case acetone, was prepared. Then a second “bad” solvent for the polymer but miscible with the first solvent, in this case hexanes, was added slowly until the solution became turbid. The solution was then allowed to settle for approximately 18 hours. The resulting higher molecular weight polymer-gel phase was then separated from the supernatant lower molecular weight solution phase. The fraction was isolated and the precipitation process repeated with the supernatant.

The data in Table 8 lists the weight average molecular weight and LCST data for the starting polymer and the fractionated samples 1-4.

Table 8. LCST and M_w data for unfractionated (starting polymer) and fractionated PNIPAM samples.

| | M_w (g/mol) | LCST (°C) |
|------------------|--------------------|-----------|
| Starting Polymer | 2.13×10^5 | 30.22 |
| Fraction 1 | 4.75×10^5 | 30.18 |
| Fraction 2 | 1.70×10^5 | 30.21 |
| Fraction 3 | 5.58×10^4 | 30.40 |
| Fraction 4 | 1.78×10^4 | 30.83 |

It is important to note that the weighted average (based on the mass of each fraction recovered) of the M_w for fractions 1-4 is the same as the M_w for the starting polymer (eq. 8).

$$\frac{2.5 \text{ g (1)} + 4.2 \text{ g (2)} + 1.8 \text{ g (3)} + 1.1 \text{ g (4)}}{10 \text{ g}} = 2 \times 10^5 \text{ g/mol} \quad (8)$$

The observation that the weighted average for the M_w of samples 1-4 is the same as the M_w for the unfractionated sample provides evidence that our measurements of M_w are at least reproducible and self consistent.

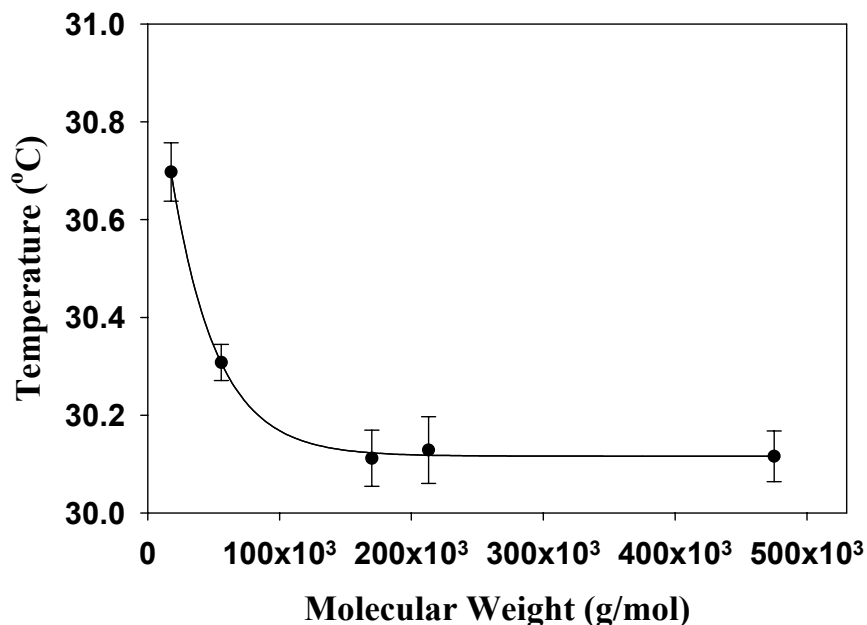


Figure 34. The variation of LCST with M_w of PNIPAM.

From the plot in Figure 34 we can see that the change in LCST with M_w of PNIPAM is more pronounced for lower molecular weight samples. The LCST decreases as the M_w of the PNIPAM samples increase until a threshold of about 2.0×10^5 g/mol above which the effect begins to level off. Zhu et al. obtained a similar curve when evaluating the effect of M_n on the LCST of poly(*N,N*-diethylacrylamide) in water.¹⁶⁵ The inverse relationship between molecular weight and LCST has been explained by Patterson using Flory-Huggins theory.¹⁶⁶

$$\chi_c = 1/2(1 + r^{-1/2})^2$$

Where χ_c is the critical value of the Flory-Huggins polymer-solvent interaction parameter. Therefore r , the ratio of molar volumes of polymer over solvent, will decrease as the degree of polymerization decreases causing χ_c to increase. This increase will shift the polymers phase diagram resulting in a higher LCST for polymers with lower molecular weight.

We were concerned about the ability of the fractionation process to concentrate impurities like small amounts of residual monomer into the lower molecular weight samples. In order to ascertain whether or not the effects of increasing amounts of monomer could account for the changes in LCST we evaluated the effect the addition of monomer had on the LCST of PNIPAM. The plot in Figure 35 shows the effect that added *N*-isopropylacrylamide has on the LCST of two different molecular weight fractions of PNIPAM. From the plot we can see that the effect of increasing concentrations of monomer actually lowers the polymers LCST and therefore could not account for the increase we observe in Figure 34.

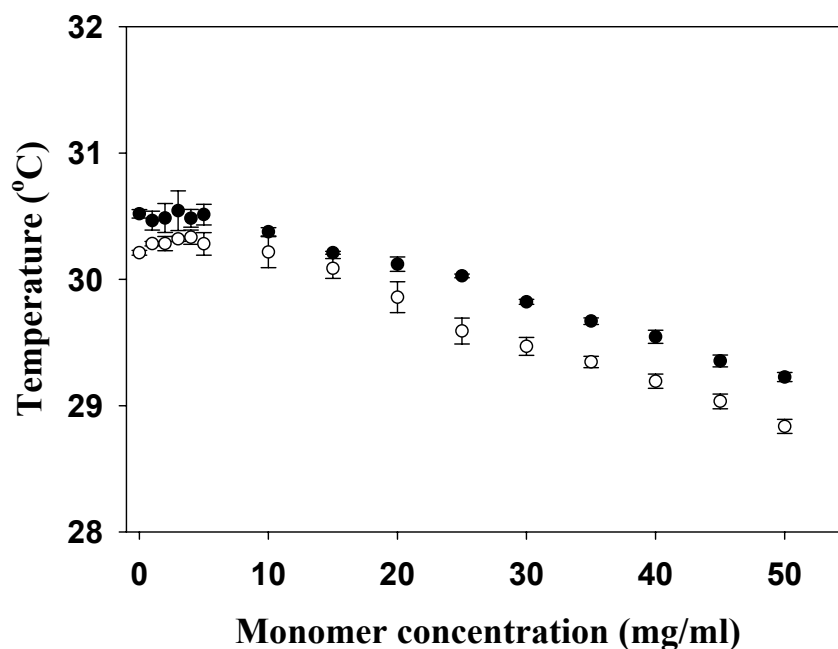


Figure 35. The effect of added monomer (*N*-isopropylacrylamide) on the LCST of PNIPAM ($M_w = 55,800$ (●) and $475,000$ (○)).

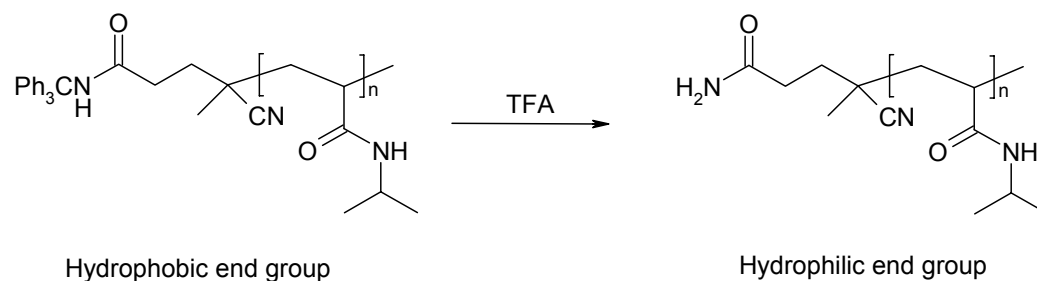
The plot in Figure 34 also raised concerns that we could be observing polymer end group effects rather than changes in the LCST resulting purely from differences in molecular weight. The influence of end groups would explain the sudden increase in the perturbation of LCST as the polymer chains get shorter and shorter.

Freitag et al.¹⁶¹ and Hoffman et al.¹⁵⁹ prepared carboxyl-terminated PNIPAM oligomers with molecular weights ranging from 2 to 50×10^3 g/mol and did not see any changes in LCST. Okano et al.¹⁵⁸ prepared the same carboxyl-terminated PNIPAM derivatives but noted that while there was no observable effect on the LCST for solutions of about 1 wt%, solutions consisting of about 500 wt% resulted in higher LCSTs for the hydrophilic terminated PNIPAM derivatives. The group also prepared

amine and hydroxyl-terminated PNIPAM oligomers of $M_w = 7300$ g/mol and found that the hydroxyl group has a pronounced effect on the polymers LCST.¹⁶⁷ Some of the most interesting results were obtained when Okano's group decided to look at the effects of adding hydrophobic end groups on to PNIPAM. They found that the position of the hydrophobic groups on the polymer chain played a crucial role in the effect the ability of the group to alter the polymers LCST. They prepared PNIPAM oligomers of similar molecular weight that were terminated with $C_{18}H_{37}$ chains as well as random copolymers containing $C_{18}H_{37}$ pendant groups and found that the PNIPAM oligomers with hydrophobic end groups had a significant impact on reduction of the LCST. The hydrophobic contribution for a single $C_{18}H_{37}$ end group was dramatic when compared to similar polymers with $C_{18}H_{37}$ groups random incorporated along the copolymer chain.¹⁶⁷ They also went on to compare the ability of different carbon chain lengths to alter the LCST on terminally modified PNIPAM oligomers.¹⁶⁸ They prepared PNIPAM oligomers ($M_w = 7,300$ g/mol) with terminal propyl, hexyl, octyl, dodecyl, and octadecyl chains. They found that the effects of terminal hydrophobic groups were more complex. The propyl, hexyl, and octyl groups of terminally functionalized PNIPAM oligomers progressively lowered the LCST with increasing alkyl chain length, but the trend reversed and the LCST increased for the dodecyl and octadecyl chains.

Our concerns about the significance of the data in Figure 34 combined with the pronounced end group effects seen in literature precedents resulted in our investigating the significance of end group hydrophobicity on the LCST of PNIPAM. In order to eliminate as many variables as possible we decided that the ideal solution would be to

measure the same polymer with hydrophilic and hydrophobic end groups and compare the variation, if any, in LCST as the M_w changes. This was accomplished by preparing a PNIPAM derivative that contained end groups that could be quantitatively converted from hydrophobic to hydrophilic. The strategy of using a triphenylmethyl protecting group to change the hydrophobicity of PNIPAM end groups is outlined in Scheme 8.¹⁶⁹



Scheme 8. Cleavage of terminal tritylamide from PNIPAM converting hydrophobic end group to hydrophilic end group.

This chemistry was first tested on a low molecular weight model compound. The model *N*-triphenylmethylhexaneamide (**43**) was prepared *via* condensation between hexanoyl chloride and triphenylmethylamine in dichloromethane as shown in Figure 36.

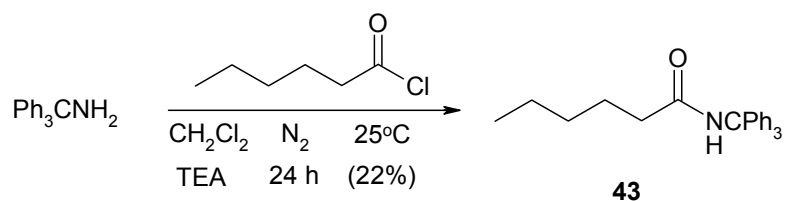


Figure 36. Synthesis of *N*-triphenylmethylhexaneamide.

The triphenylmethyl group was then quantitatively removed in neat TFA (Figure 37).

The primary amide could be detected by ^1H and ^{13}C NMR spectroscopy as well as TLC.

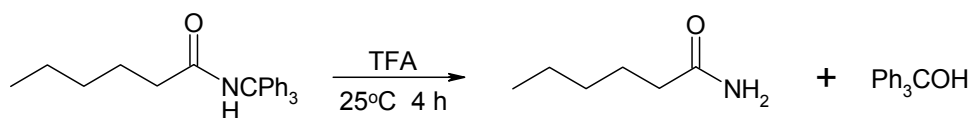


Figure 37. Cleavage of triphenylmethyl group from *N*-triphenylmethylhexaneamide.

The functionalized initiator, 4,4'-Azobis(*N*-triphenylmethyl-4-cyanovaleramide) (**45**) was synthesized in order to prepare a trityl terminated PNIPAM derivative. This was accomplished by converting the commercially available 4,4'-azobis(4-cyanovaleric acid) to the moisture, heat, and light sensitive 4,4'-azobis(4-cyanovaleroyl chloride) (**44**) followed by condensation with triphenylmethylamine as shown in Figure 38.

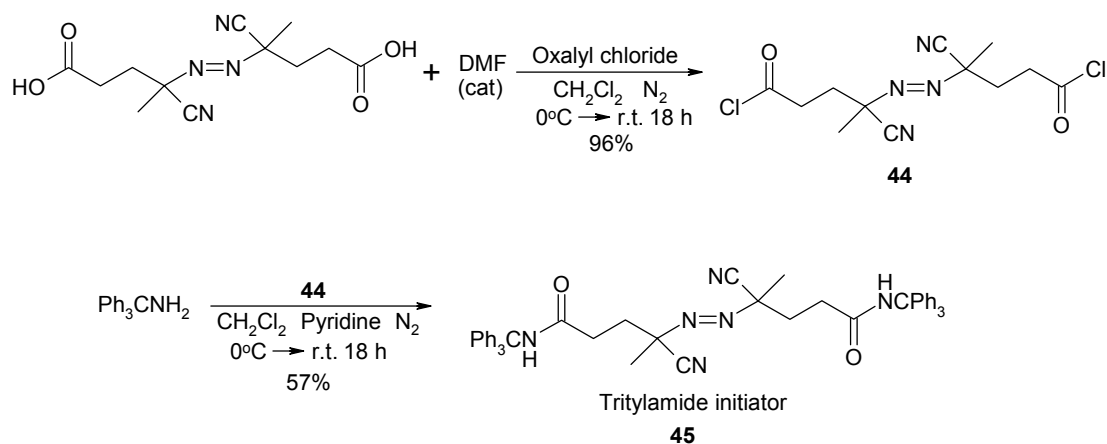


Figure 38. Synthesis of 4,4'-azobis(*N*-triphenylmethyl-4-cyanovaleramide).

Polymerization of *N*-isopropylacrylamide was initiated with **45** resulting in the triphenylmethyl terminated poly(*N*-isopropylacrylamide) (PNIPAM-CONH-Tr) derivative. The resulting polymer was then fractionated in the same manner as mentioned above (Figure 39).

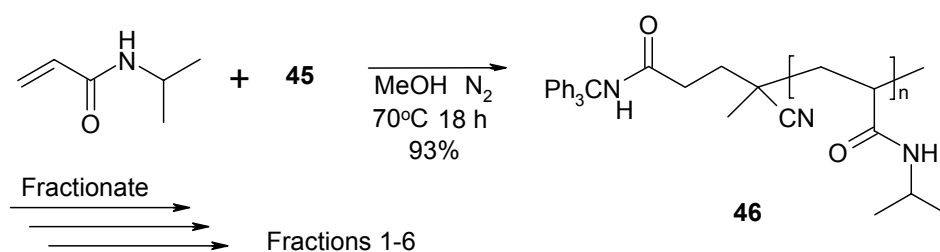


Figure 39. Synthesis of PNIPAM-CONH-Tr.

The data in Table 9 lists the weight average molecular weight and LCST data for the starting polymer and the fractionated samples 1-6.

Table 9. LCST and M_w data for unfractionated (starting polymer) and fractionated PNIPAM-CONH-Tr samples.

| | M_w (g/mol) | LCST (°C) |
|------------------|--------------------|-----------|
| Starting Polymer | 2.02×10^5 | 30.19 |
| Fraction 1 | 3.84×10^5 | 30.27 |
| Fraction 2 | 1.95×10^5 | 30.21 |
| Fraction 3 | 1.70×10^5 | 30.18 |
| Fraction 4 | 1.44×10^5 | 29.95 |
| Fraction 5 | 9.32×10^4 | 29.94 |
| Fraction 6 | 4.58×10^4 | 29.74 |

From the plot in Figure 40 we can see that the change in LCST with M_w of PNIPAM containing the hydrophobically modified end groups is more pronounced as the molecular weight decreases. This more pronounced effect for the lower M_w samples is similar to that seen in Figure 34. However in this case the LCST of the polymer *increases* as the molecular weight of the samples increases due to the higher loading of hydrophobic groups at shorter chain lengths.

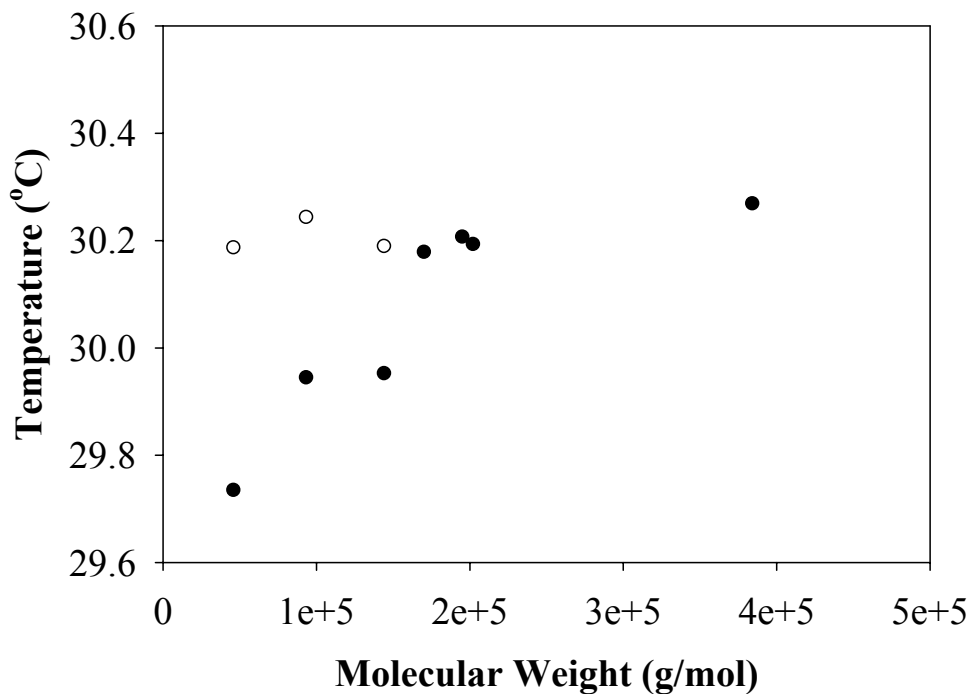


Figure 40. The variation of LCST with the M_w of PNIPAM-CONH-Tr (●) and PNIPAM-CONH₂ (○).

This data clearly shows the importance of the end groups hydrophobicity as the polymer chains become increasingly shorter.

In order to further verify the effects of end group hydrophobicity/hydrophilicity, the hydrophobic end groups of PNIPAM-CONH-Tr (**46**) were converted to the more hydrophilic end groups of PNIPAM-CONH₂ (**47**) (Figure 41). The results obtained from this experiment should provide less ambiguous data since we are comparing the difference between end groups on the same polymer sample.

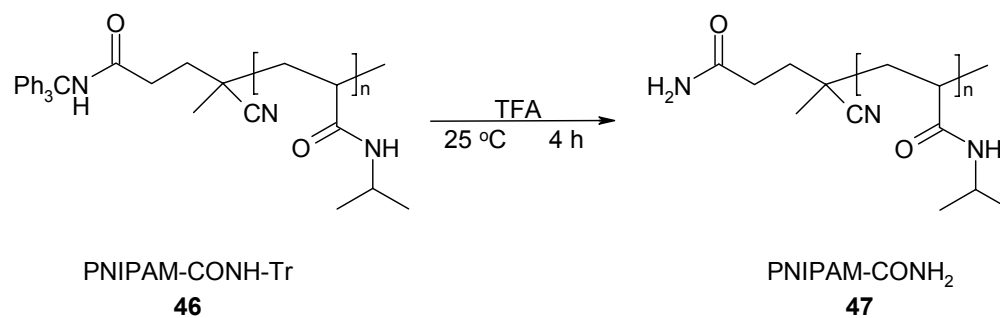


Figure 41. Conversion of PNIPAM-CONH-Tr to PNIPAM-CONH₂.

The higher LCST (open circle points in Figure 40) observed for **47** when compared to **46** combined with the data from Figure 35 proves that the changes seen in the LCST of a polymer as the chain length decreases is due to the hydrophobicity/hydrophilicity of the polymer's end groups.

Effects of Polymer Stereochemistry

The stereoregularity of a polymer can have profoundly effect the polymers solubility. Typically more stereoregular chains pack more efficiently resulting in a more stable solid structure and therefore less soluble polymer. *N*-Isopropylacrylamide was polymerized in the presence of a dithioester chain-transfer agent to control molecular weight and $Y(OTf)_3$ to yield a highly stereoregular polymer (Figure 42).¹⁷⁰

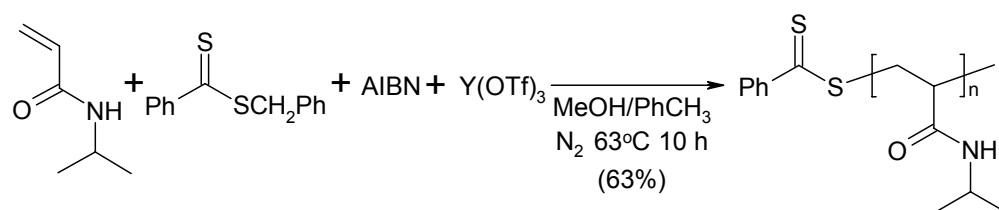


Figure 42. Synthesis of 80% isotactic PNIPAM.

The tacticity of the polymer can be determined by ¹H NMR spectroscopy of a polymer solution in DMSO-*d*₆ at 130 °C (Figure 43).

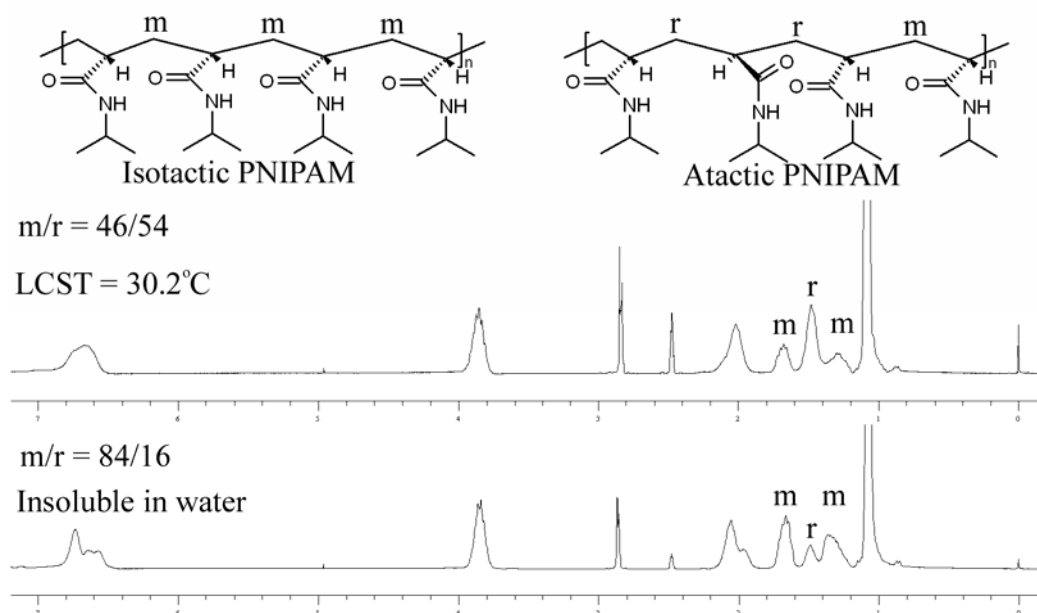


Figure 43. Determination of PNIPAM tacticity by ^1H NMR (DMSO- d_6 , 130 °C) analysis.

At 130 °C the peaks corresponding to the tactic dyads for the meso (m) and racemic (r) configurations are well resolved. The fact that 80% isotactic PNIPAM is not even soluble in cold water while the atactic polymer has an LCST of 30.2 °C clearly illustrates the significant impact a polymer's stereoregularity can have on its LCST. The stereoregularity of different LCST polymers used in this study were evaluated. This was done to verify that the differences in LCST that were measured were not due to differences in stereoregularity caused by different polymerization or post modification procedures. The tacticity data for several polymers is given in table 10.

Table 10. Tacticity data for LCST polymers.

| Polymer | Remarks | m/r |
|--------------------------|--|------------|
| PNIPAM | AIBN/ <i>t</i> BuOH | 45/55 |
| PNNPAM | AIBN/ <i>t</i> BuOH | 53/47 |
| PNNPAM | AIBN/MeOH | 59/41 |
| PNIPAM | PNASI | 48/52 |
| PNIPAM | AIBN/DTE ^a /PhH | 47/53 |
| PNIPAM | AIBN/DTE ^a /Y(OTf) ₃ /MeOH:PhCH ₃ 1:1 v:v | 82/18 |
| PNIPAM-CONH-Tr | Unfractionated | 48/52 |
| PNIPAM-CONH-Tr | Fraction 1 | 47/53 |
| PNIPAM-CONH-Tr | Fraction 6 | 48/52 |
| PNIPAM-CONH ₂ | Fraction 6 | 47/53 |

^a Dithioester (DTE) benzyl dithiobenzoate

Conclusions

The linear temperature gradient apparatus for combinatorial temperature measurements described here coupled with a split-pool synthesis of poly(*N*-alkylacrylamide)s is a simple, precise, and high-throughput way to study the effects of polymer microstructure and solution composition of the LCST of thermoresponsive polymers. With polymers like poly(*N*-isopropylacrylamide), effects that produce differences for a polymer's LCST of <0.5 °C can be studied using only a microgram of the polymer in a few microliters of solvent.

CHAPTER V

EXPERIMENTAL

Materials and General Methods. All reagents and solvents were obtained from commercial sources and used without further purification unless specified. ^1H NMR spectra were obtained on Varian Inova 300, Mercury 300, or Inova 500 spectrometers at 300 or 500 MHz. ^{13}C NMR spectra were obtained on Varian Inova 300, Mercury 300, or Inova 500 spectrometers at 75 or 125 MHz. ^1H and ^{13}C NMR spectroscopy chemical shifts are reported in ppm referenced to tetramethylsilane, or residual solvent peaks respectively. Gas chromatography was performed on a Shimadzu GC-14A gas chromatograph equipped with a flame ionization detector using a SUPELCO 30 m long, 0.53 mm ID fused silica capillary column with a 3.0 μm thick film bonded poly(5% diphenyl/95% dimethylsiloxane) stationary phase. UV-Vis spectroscopic measurements were performed on a Cary 100 UV-Visible spectrophotometer. Fluorescence spectroscopic analyses were carried out using Fluorolog-3 or SLM-Aminco spectrofluorometers. LC-MS experiments were conducted on a Waters XTerra MS using a 2.0-mm \times 150-mm C18 column, eluting fractions with a 60:40 water:methanol gradient. Total ion count (area under the curve) was determined after atmospheric pressure chemical ionization using a Thermofinnigan LC Q Deca mass spectrometer and was compared to a calibration curve. Elemental analysis was carried out on a Perkin Elmer DRCII ICP-MS. Light scattering experiments were carried out using a Brookhaven Instruments BI-200SM goniometer, BI-9000AT digital correlator, and a

Melles Griot HeNe laser. M_w analysis of light scattering data was performed using Brookhaven Instruments Zimm Plot Software. Microwave reactions were carried out using a CEM Discover™ or Personal Chemistry Emrys™ Creator model microwave reactors.

Synthesis of MeOPEG₃₅₀-OMs. Triethylamine (62 mL, 0.46 mol) was added to a solution of poly(ethylene glycol) monomethyl ether $M_w \approx 350$ g/mol (100 mL, 0.31 mol) in 500 mL of CH₂Cl₂. This solution was cooled to 0 °C and methanesulfonyl chloride (36 mL, 0.46 mol) was slowly added to the reaction mixture. The thick yellow slurry so formed was then stirred at room temperature for 24 h. The slurry was allowed to settle for several minutes and the resulting clear brown solution was separated from the less dense, white, crystalline solid by decantation. This organic phase was washed with 3 M HCl (3 x 125 mL), saturated NaHCO₃ (2 x 125 mL), and brine (1 x 125 mL) and then dried over MgSO₄. The solvent was removed under reduced pressure and the thick brown oil isolated was dried under vacuum yielding 127.3 g (96%) of the pure product. ¹H NMR (CDCl₃) δ 3.09 (3H, s), 3.38 (3H, s), 3.55-3.78 (26H, PEG), 4.38 (2H, t, ³J_{HH} = 4.5 Hz); ¹³C NMR (CDCl₃) δ 37.49, 52.56, 53.59, 58.81, 68.82-71.73 (PEG).

Synthesis of MeOPEG₃₅₀SCOCH₃ (19). A mixture of MeOPEG₃₅₀-OMs (20.0 g, 47 mmol) and potassium thioacetate (10.0 g, 87 mmol) in 500 mL of DMF was mechanically stirred at 75 °C for 24 h. The thick, dark-red suspension that formed was filtered hot and the supernatant was allowed to cool to room temperature. This solution

was filtered again and most of the solvent (~75 mL) remaining was removed with gentle heat *in vacuo*. The resulting thin, dark-red oil was then taken up into 800 mL of water and this aqueous phase was extracted with CH₂Cl₂ (4 x 100 mL). A small amount of brine was added to break up any emulsion. The organic phase was in turn washed with water (5 x 100 mL), brine (2 x 100 mL) and then dried over MgSO₄. The solvent was removed under reduced pressure to yield a reddish-brown oil that was further dried under vacuum to yield 16.85 g (84%) of **19**. ¹H NMR (CDCl₃) δ 2.31 (3H, s), 3.09 (2H, t, ³J_{HH} = 6.5 Hz), 3.38 (3H, s), 3.55-3.78 (26H, PEG); ¹³C NMR (CDCl₃) δ 29.06, 30.80, 59.27, 69.97-72.16 (PEG), 195.73.

Synthesis of 1,3-Bis(MeOPEG₃₅₀thiomethyl)benzene (20). Clean, dry sodium metal (563 mg, 25 mmol) was dissolved in 150 mL of dry MeOH. Once all of the sodium had dissolved the flask was sealed and N₂ was bubbled through the system. During this time α,α'-dichloro-*m*-xylene (1.07 g, 6 mmol) and **19** (5.00 g, 12 mmol) were added to a 250 mL two-necked, round-bottomed flask equipped with a condenser and the system was flushed with N₂ for 2 h. The base solution was transferred by forced siphon to this reaction flask and the resulting reaction mixture was protected from light while it was stirred at 60 °C under N₂ for 12 h. Then the reaction solution was allowed to cool to room temperature under N₂ and was acidified to a pH≈7 (pH paper) with 1 M H₂SO₄. The majority of the solvent was removed under reduced pressure and the resulting oil was taken up into 450 mL of water. The aqueous solution that formed was extracted with CH₂Cl₂ (5 x 100 mL). A small amount of brine was added to break up any emulsion. The organic phase was washed with brine (2 x 100 mL) and then dried

over MgSO₄. The solvent was removed under reduced pressure and the resulting oil was dried under vacuum to yield 4.6 g (92%) of **20**. ¹H NMR (CDCl₃) δ 2.61 (4H, t, ³J_{HH} = 6.7 Hz), 3.38 (6H, s), 3.55-3.70 (52H, PEG), 3.75 (4H, s), 7.2 (4H, m); ¹³C NMR (CDCl₃) δ 30.99, 36.75, 59.15, 70.49-72.14 (PEG), 127.80, 128.75, 129.59, 138.93.

Synthesis of 1,3-Bis(MeOPEG₃₅₀thiomethyl)benzene Palladium

Chloride(21). A solution of **20** (1.40 g, 1.7 mmol) in 100 mL of CH₃CN was added to a solution of Pd(PhCN)₂Cl₂ (644 mg, 1.7 mmol) in 100 mL of CH₃CN. The clear solution so formed was stirred at room temperature for 12 h and then refluxed for 24 h. The solvent was removed under reduced pressure and the resulting brown oil was taken up into 300 mL of water. The aqueous solution was washed with Et₂O (4 x 50 mL), and the product was extracted into CH₂Cl₂ (4 x 100 mL). Brine was added as needed to enhance separation of layers. The organic phase was dried over MgSO₄ and the solvent was removed under reduced pressure. The resulting oil was dried under vacuo to yield 1.13 g (76%) of the product **21**. ¹H NMR (CDCl₃) δ 2.61 (4H, t, ³J_{HH} = 4.9 Hz), 3.38 (6H, s), 3.55-3.70 (52H, PEG), 4.00 (4H, bs), 4.45 (4H, bs), 6.85 (3H, m); ¹³C NMR (CDCl₃) δ 38.55, 48.22, 59.06, 70.46-71.97 (PEG), 122.17, 124.82, 149.42.

General Procedure for Use of **21** in Homogeneous Heck Reactions in DMA.

An aryl halide (0.5 mmol), an alkene acceptor (1.0 mmol), and either TEA (2.0 mmol), K₂CO₃ (1.5 mmol with halobenzoic acids) or K₂CO₃ (0.5 mmol with acrylamide) as a base were added to 2.5 mL of DMA in a 10 mL microwave vial. Then either 42 μL of a 12 mM (5 x 10⁻⁷ mol, 0.1 mol%) solution of **21** in DMA or 42 μL of a 1.2 mM (5 x 10⁻⁸ mol, 0.01 mol%) solution of **21** in DMA were added. A *t* = 0 sample was taken and the

vial was sealed with a Teflon septum using an aluminum crimp. The reaction solution was then either placed in a silicone oil bath at 150 °C or irradiated at 30W using a microwave reactor (with the maximum temperature set to 150 °C). In kinetic studies of the conventional oil bath heated reaction, a sample was removed every 10 min using a syringe. In the microwave reactor samples were also taken every 10 minutes. However, in this case the microwave tube was quickly cooled using the cooling gas (N₂) feature on the microwave and then a sample was removed using a syringe. The remaining reaction solution was simply placed back into the reactor and further irradiated. All samples were analyzed by gas chromatography following disappearance of the PhX starting material and appearance of cinnamate product (*n*-C₁₂H₂₆ was used as an internal standard). When the reaction was complete, the product was isolated by pouring the reaction mixture into 20 mL of water and either collecting the precipitate or extracting the product from the aqueous phase several times with diethyl ether. The structures of the isolated products were confirmed by ¹H and ¹³C NMR spectroscopy.

General Procedure for Recycling **21 in Homogeneous Heck Reactions Under Thermomorphic Conditions.** A 9.7 mM (104 μL, 1 x 10⁻⁶ mol, 0.2 mol%) solution of **21** in DMA was added to 1 mL of 10% aqueous DMA in a 10 mL microwave vial. The aryl iodide (0.50 mmol), the alkene acceptor (0.60 mmol), and TEA (0.75 mmol) were dissolved in 2 mL of heptane. This heptane solution was added to the catalyst solution and the vessel was sealed and microwaved at 150 °C for 20 minutes. The mixture was allowed to cool and the heptane phase was removed. Fresh reactants in heptane were then added to the catalyst solution for each additional cycle. Each cycle proceeded to

greater than 96% conversion by GC analysis. The products were isolated by taking the heptane phase after each cycle and removing the solvent under reduced pressure.

The isolated products' structures were confirmed by ^1H and ^{13}C NMR spectroscopy.

General Procedure for Using **21 in Homogeneous Heck Reactions in D_2O .** A halobenzoic acid (0.5 mmol), acrylic acid or *N,N*-dimethylacrylamide (1.0 mmol), and K_2CO_3 (1.5 mmol for acrylic acid or 0.5 mmol for dimethylacrylamide) were added to 2.5 mL of D_2O in a 10 mL microwave vial. Then 60 μL of a 8.4 mM (5×10^{-7} mol, 0.1 mol%) solution of **21** in D_2O were added. A ^1H NMR spectrum was obtained for $t = 0$. Then the NMR spectroscopy sample was poured back into the reaction mixture and the vial was sealed with a Teflon septum using an aluminum crimp. The sample was then irradiated at 30W with the maximum temperature set to 150 $^\circ\text{C}$. After 10 min, the sample was quickly cooled using the cooling gas (N_2) feature on the microwave. The percent conversion was determined by ^1H NMR spectroscopy of reaction mixture monitoring disappearance of ArX and appearance of product peaks. When the reaction was complete, the solution was neutralized with 6 M H_2SO_4 and the precipitate was collected and washed with water. The product was then dried under vacuum and the structures of the isolated products were confirmed by ^1H and ^{13}C NMR spectroscopy.

NMR Spectra Data for Heck Coupling Products

***tert*-Butyl cinnamate (22):** ^1H NMR (CDCl_3) δ 1.55 (9H, s), 6.39 (1H, d, $^3J_{\text{HH}} = 16$ Hz), 7.38 (3H, m), 7.50 (2H, m), 7.59 (1H, d, $^3J_{\text{HH}} = 16$ Hz); ^{13}C NMR (CDCl_3) δ 28.41, 80.67, 120.40, 128.15, 129.02, 130.15, 134.87, 143.75, 166.51.

Methyl cinnamate (23): ^1H NMR (CDCl_3) δ 3.60 (3H, s), 6.45 (1H, d, $^3J_{\text{HH}} = 16$ Hz), 7.39 (3H, m), 7.52 (2H, m), 7.70 (1H, d, $^3J_{\text{HH}} = 16$ Hz); ^{13}C NMR (CDCl_3) δ 51.96, 118.02, 128.32, 129.13, 130.55, 134.60, 145.12, 167.68.

Stilbene (24): ^1H NMR (CDCl_3) δ 7.12 (2H, s), 7.25 (2H, m), 7.35 (4H, m), 7.52 (4H, m); ^{13}C NMR (CDCl_3) δ 126.77, 127.88, 128.94, 137.57.

4-Stilbazole (25): ^1H NMR (CDCl_3) δ 7.00 (1H, d, $^3J_{\text{HH}} = 16$ Hz), 7.31 (1H, d, $^3J_{\text{HH}} = 16$ Hz), 7.38 (5H, m), 7.55 (2H, m), 8.59 (2H, m); ^{13}C NMR (CDCl_3) δ 121.09, 126.23, 127.25, 129.00, 129.09, 133.38, 136.37, 144.81, 150.47.

***tert*-Butyl β -(1-Naphthyl)acrylate (26):** ^1H NMR (CDCl_3) δ 1.49 (9H, s), 6.42 (1H, d, $^3J_{\text{HH}} = 16$ Hz), 7.50 (3H, m), 7.72 (1H, d, $^3J_{\text{HH}} = 7$ Hz), 7.85 (2H, $^3J_{\text{HH}} = 8.5$), 8.19 (1H, d, $^3J_{\text{HH}} = 8.5$ Hz), 8.41 (1H, d, $^3J_{\text{HH}} = 16$ Hz); ^{13}C NMR (CDCl_3) δ 28.51, 88.88, 123.07, 123.70, 125.14, 125.71, 126.40, 126.99, 128.93, 130.46, 131.66, 132.26, 133.90, 140.83, 166.50.

Methyl β -(1-Naphthyl)acrylate (27): ^1H NMR (CDCl_3) δ 3.82 (3H, s), 6.51 (1H, d, $^3J_{\text{HH}} = 16$ Hz), 7.50 (3H, m), 7.72 (1H, d, $^3J_{\text{HH}} = 7.08$ Hz), 7.85 (2H, t, $^3J_{\text{HH}} = 7.9$ Hz), 8.19 (1H, d, $^3J_{\text{HH}} = 7.8$ Hz), 8.51 (1H, d, $^3J_{\text{HH}} = 16$ Hz); ^{13}C NMR (CDCl_3) δ 52.06, 120.66, 123.61, 125.23, 125.71, 126.49, 127.14, 128.99, 130.81, 131.65, 131.95, 133.91, 142.13, 167.58.

***m*-Carboxycinnamic acid (28):** ^1H NMR ($\text{DMSO-}d_6$) δ 6.60 (1H, d, $^3J_{\text{HH}} = 16$ Hz), 7.58 (1H, t, $^3J_{\text{HH}} = 7.7$ Hz), 7.65 (1H, d, $^3J_{\text{HH}} = 16$ Hz), 7.98 (2H, d, $^3J_{\text{HH}} = 7.7$ Hz),

8.19 (1H, s), 12.82 (1H, bs); ^{13}C NMR (DMSO- d_6) δ 121.12, 129.66, 129.92, 131.42, 132.21, 132.66, 135.34, 143.61, 167.57, 168.03.

2-Methyl-5-carboxycinnamic acid (29): ^1H NMR (DMSO- d_6) δ 2.22 (3H, s), 6.41 (1H, d, $^3J_{\text{HH}} = 16$ Hz), 7.41 (1H, d, $^3J_{\text{HH}} = 8$ Hz), 7.83 (1H, d, $^3J_{\text{HH}} = 16$ Hz), 7.86 (1H, dd, $^3J_{\text{HH}} = 8$ Hz, $^4J_{\text{HH}} = 2$ Hz), 8.17 (1H, d, $^4J_{\text{HH}} = 2$ Hz), 12.82 (1H, bs); ^{13}C NMR (DMSO- d_6) δ 20.17, 122.10, 127.85, 129.78, 131.03, 131.78, 133.98, 141.18, 142.96, 167.61, 167.93.

***N,N*-Dimethyl-3-carboxycinnamamide (30):** ^1H NMR (DMSO- d_6) δ 2.95 (3H, s), 3.19 (3H, s), 7.29 (1H, d, $^3J_{\text{HH}} = 16$ Hz), 7.51 (1H, d, $^3J_{\text{HH}} = 16$ Hz), 7.54 (1H, t, $^3J_{\text{HH}} = 7.7$ Hz), 7.93 (1H, d, $^3J_{\text{HH}} = 7.7$ Hz), 7.97 (1H, d, $^3J_{\text{HH}} = 7.7$ Hz), 8.21 (1H, s); ^{13}C NMR (DMSO- d_6) δ 35.35, 36.90, 119.90, 128.48, 129.09, 130.04, 131.44, 132.15, 135.61, 139.89, 165.34, 167.06.

Synthesis of Poly(*N*-isopropylacrylamide)(31). A solution of *N*-isopropylacrylamide (10.00 g, 89 mmol) in 200 mL of *tert*-butylalcohol was degassed and heated to 70 °C under positive pressure of N_2 . Then a degassed solution of 2,2'-azobisisobutylnitrile (50 mg, 0.3 mmol) in 15 mL of *tert*-butylalcohol was added to the reaction flask *via* forced siphon. After 18 h the *tert*-butylalcohol was removed under reduced pressure and the polymer was dried under vacuum. The crude product was then reprecipitated from 100 mL THF into 1 L of hexanes 3 times, yielding 9.82 g (98%) of the pure product **31**. ^1H NMR (CDCl_3) δ 1.18 (bs, 6H), 2.25-1.40 (bm, 3H), 4.00 (bs, 1H), 6.40 (bs, 1H).

Synthesis of Poly(*N*-isopropylacrylamide-*c*-*N*-(aminomethyl)piperidinylacrylamide) 20:1 (32). A solution of **37** (5.00 g, 2 mmol) was added to 100 mL of TFA, and the resulting mixture was stirred at 25 °C for 18 h. The solvent was removed under reduced pressure, and the polymer product was dissolved in 100 mL of ice-cold deionized water. Saturated aqueous Na₂CO₃ was added until the polymer solution was basic (pH~9 by pH paper). The polymer precipitate that formed was separated from the supernatant solution using centrifugation at 50 °C (1,500 rpm) for 1 h followed by decantation of the supernatant. The solid polymer product was dissolved in 100 mL of ice-cold deionized water, and separated again as a solid after a second centrifugation at 50 °C (1,500 rpm) for 1h. On some occasions the centrifugation produced a milky suspension. In those cases, brine was added. This facilitated formation of a separable solid after centrifugation. After centrifugation, the supernatant was separated from the solid polymer product by decantation. This process was repeated a total of 3 times. The white solid polymer product was dried under vacuum. The polymer was added to 75 mL of THF and stirred for 1 h. The resulting THF solution contained a small amount of solid that was separated by centrifugation. Then the polymer product was recovered as a precipitate by slowly adding this THF solution to 800 mL of hexanes. The polymer powder **32** obtained in this way was dried to yield 4.32 g (90%) of product. ¹H NMR (CDCl₃) δ 1.18 (120H, bs), 1.50-2.60 (56H, bm), 4.00 (20H, bs), 6.30 (21H, bs); $M_w = 3.8 \times 10^5$ g/mol (light scattering in MeOH using literature value for the parent polymer, PNIPAM, of 0.201 mL/g for dn/dc, change in refractive index with concentration).¹⁷¹

Synthesis of Atrazine (33). This material was prepared according to a literature procedure.¹⁷²

Synthesis of *p*-Methyl Red. To a solution of *p*-aminobenzoic acid (8.00 g, 58.3 mmol) dissolved in a mixture of H₂O (50 mL) and concentrated HCl (10 mL) at 0 °C a solution of NaNO₂ (4.21 g, 60.9 mmol) in H₂O (50 mL) was added in several small portions. The resulting solution was allowed to stir at 0 °C for 30 min. After this time, this solution of freshly formed diazonium salt was added dropwise over a period of 30 min to a solution of *N,N*-dimethylaniline (6.01 mL, 61.0 mmol) in 10% aqueous acetic acid at 0 °C. After the addition was complete, the dark red reaction mixture was allowed to stir for 1 h, warming to room temperature and resulting in the formation of a deep red suspension. The precipitated red solid material was isolated by filtration, washed with H₂O (5 X 50 mL) and 10% aqueous acetic acid (2 X 50 mL) and then air-dried the red crude product. The red solid product was then recrystallized from MeOH (100 mL), isolated by filtration, and then dried under vacuum to yield 7.97 g (51%) of product. ¹H NMR (DMSO-*d*₆) δ 3.10 (s, 6H), 6.85 (d, 2H), 7.85 (m, 4H), 8.05 (d, 2H); ¹³C NMR (DMSO-*d*₆) δ 111.59, 121.74, 125.28, 130.51, 130.88, 142.07, 152.99, 155.07, 166.92.

Synthesis of Amine-Terminated Methyl Red Label. A solution of *p*-methyl red (1.75 g, 6.6 mmol) and 1,1'-carbonyldiimidazole (1.07 g, 6.6 mmol) in 100 mL of CH₂Cl₂ was stirred at 25 °C under N₂ for 5 h. The solution was then transferred to an addition funnel, and added dropwise to a solution of 2-{2-[2-(2-aminoethoxy)ethoxy]ethoxy}-ethylamine (JEFFAMINE[®] EDR-192 (Texaco)) (8.82 g, 46 mmol) in 250 mL of CH₂Cl₂ under N₂. Once all of the activated acid solution was

added, the mixture was stirred for 8 h under N₂. The solution was then washed with water (4 x 125 mL), and brine (4 x 125 mL), and then dried over MgSO₄. The solvent was removed under reduced pressure and the resulting red oil was dried under vacuum to yield 2.61 g (90%) of the product. ¹H NMR CDCl₃ δ 2.83 (2H, bs), 3.10 (6H, s), 3.47 (2H, t, *J* = 5.3 Hz), 3.56-3.76 (14H, m), 6.76 (2H, d, *J* = 8.5 Hz), 7.59 (1H, bs), 7.86 (2H, d, *J* = 8.5 Hz), 7.89 (2H, d, *J* = 8.5 Hz), 7.97 (2H, d, *J* = 8.5 Hz); ¹³C NMR (CDCl₃) δ 39.83, 40.24, 41.41, 53.40, 69.96, 69.99, 70.14, 70.38, 70.47, 72.75, 111.39, 122.00, 125.29, 128.09, 134.74, 143.56, 152.69, 154.84, 167.14. MS (ESI): calcd for C₃₃H₃₃N₅O₄: 443.25; found 444.22 (M+H)⁺, 222.60 (M+2H)²⁺.

Synthesis of Methyl Red-Atrazine (34). A solution of the amine-terminated methyl red label (100 mg 0.226 mmol) in 40 mL of THF was added to an ice-cold solution of cyanuric chloride (40 mg, 0.217 mmol) and *N,N*-diisopropylethylamine (0.2 mL, 1.4 mmol) in 10 mL of THF. The reaction mixture was stirred for 4 h at 0 °C, and then warmed to 25 °C. 2-(2-Aminoethoxy)ethanol (0.15 mL 1.4 mmol) was then added to the reaction flask, and the mixture was stirred at 25 °C for 8 h. The solvent was removed under reduced pressure, and the crude product was dissolved in 150 mL of CH₂Cl₂. The organic solution was washed with 0.1 M aqueous acetic acid (2 x 100 mL), saturated aqueous NaHCO₃ (3 x 100 mL), and brine (2 x 100 mL). The organic solvent was removed under reduced pressure, and the crude product was purified by column chromatography (19:1 CH₂Cl₂:MeOH, with 0.5 % NH₄OH). The solvent was removed under reduced pressure, and the resulting red crystals were dried under vacuum to yield 90 mg (60%) of the product **34**. ¹H NMR (CDCl₃) δ 3.19 (6H, s), 3.39-3.82 (24H, m),

5.91 (1H, bs), 6.05 (1H, bs), 6.74 (2H, d, $J = 8.8$ Hz), 7.07 (1H, bs), 7.88 (2H, d, $J = 8.8$ Hz), 7.92 (2H, d, $J = 8.8$ Hz); ^{13}C NMR (CDCl_3) δ 30.23, 39.73, 40.20, 40.53, 61.46, 69.22, 69.66, 70.05, 70.22, 70.38, 72.28, 111.34, 121.98, 125.27, 127.88, 127.93, 134.45, 134.62, 143.46, 152.67, 154.78, 165.20, 165.46, 167.15, 168.27. MS (ESI): calcd for $\text{C}_{30}\text{H}_{42}\text{N}_9\text{O}_6\text{Cl}$: 659.29; found 660.29 ($\text{M}+\text{H}$) $^+$, 330.65 ($\text{M}+2\text{H}$) $^{2+}$. A standard solution of 8.0 ppm of **34** was prepared by dissolving 8.0 mg of **34** in 1.0 mL of DMSO. This solution was diluted to 1 L by the addition of distilled water in a volumetric flask. Further dilutions using serological pipettes and volumetric flasks were carried out to prepare solutions of 0.08, 0.80, 1.60, 4.00, 5.60 ppm. The concentrations of **34** in water were determined by measuring the absorbance at $\lambda_{\text{max}} = 474$ nm. UV-visible analysis of a series of aqueous solutions of **34** showed that the extinction coefficient of **34** was 29,960.

Synthesis of Dansyl-Atrazine (35). 5-Dimethylaminonaphthalene-1-sulfonic acid (2-aminoethyl)amide (dansylamine) (50 mg, 0.17 mmol) was added to an ice-cold solution of cyanuric chloride (30 mg, 0.16 mmol) and *N,N*-diisopropylethylamine (0.2 mL, 1.4 mmol) in 10 mL of THF. The reaction mixture was stirred for 1 h at 0 °C and then warmed to 25 °C. 2-(2-Aminoethoxy)ethanol (0.15 mL 1.4 mmol) was then added to the reaction flask and the mixture was stirred at 25 °C for 8 hours. The solvent was removed under reduced pressure and the crude product was purified by column chromatography (19:1 CH_2Cl_2 :MeOH, with 0.5 % NH_4OH). The solvent was removed under reduced pressure and the resulting product was dried under vacuum to yield 70 mg (80%) of the product **35**. ^1H NMR (CDCl_3) δ 2.83 (6H, s), 2.93 (2H, m), 3.21 (2H, m),

7.25 (1H, d, $J = 8$ Hz), 7.60 (3H, m), 7.70 (1H, t, $J = 6$ Hz), 7.81 (1H, t, $J = 6$ Hz), 8.10 (1H, m), 8.25 (1H, m), 8.45 (1H, d, $J = 8$ Hz); ^{13}C NMR (CDCl_3) δ 45.06, 60.17, 68.38, 72.05, 72.17, 115.10, 118.95, 123.52, 127.83, 128.15, 129.04, 129.44, 135.88, 151.34, 165.21, 165.45, 167.55, 168.06. MS (ESI): calcd for $\text{C}_{21}\text{H}_{28}\text{N}_7\text{O}_4\text{ClS}$: 509.16; found 510.18 ($\text{M}+\text{H}$) $^+$. A standard solution of 10.0 ppm of **35** was prepared by dissolving 10 mg of **35** in 1.0 mL of DMSO. This solution was diluted to 1 L by the addition of distilled water in a volumetric flask. Concentrations of **35** were determined by fluorescence spectroscopy with λ_{Ex} at 357 nm and λ_{Em} at 548 nm.

Synthesis of 1-(tertbutoxycarbonyl)-4-(aminomethyl)piperidine. This material was prepared according to a literature procedure.¹⁷³

Synthesis of 1-(tertbutoxycarbonyl)-4-(aminomethyl)piperidinylacrylamide (36). A solution of acryloyl chloride (3 g, 33 mmol) in 100 mL of THF was added dropwise to a solution of 1-(tertbutoxycarbonyl)-4-(aminomethyl)piperidine (5 g, 23 mmol) and triethylamine (2.5 mL, 19 mmol) in 100 mL of THF over 6 h. The reaction was stirred at 25 °C for an additional 6 h. The solvent was removed under reduced pressure, and the resulting oil was dissolved in 200 mL of CH_2Cl_2 . The solution was washed with aqueous acidic acid 0.1 M (3 x 100 mL), saturated aqueous NaHCO_3 (3 x 100 mL), brine (3 x 100 mL), and was then dried over MgSO_4 overnight. Following filtration, the solvent was removed under reduced pressure, and the resulting oil was dried under reduced pressure, yielding 5.56 g (90%) of the product **36**. ^1H NMR (CDCl_3) δ 6.28 (1H, dd), 6.11 (1H, dd), 5.64 (1H, dd), 4.07 (2H, bs), 3.12 (2H, bs), 2.66 (2H, bs), 1.67 (3H, m), 1.43 (9H, s), 1.11 (2H, m); ^{13}C NMR (CDCl_3) δ 165.96, 155.03,

130.98, 126.75, 79.66, 45.16, 36.63, 30.00, 28.66. MS (ESI): calcd for C₁₄H₂₄N₂O₃: 268.18; found 269.17 (M+H)⁺, 291.15 (M+Na)⁺.

Synthesis of Poly(*N*-isopropylacrylamide-*c*-BOC-4-(aminomethyl)piperidinylacrylamide)20:1 (37). A solution of *N*-isopropylacrylamide (10.95 g, 97.00 mmol) and **36** (1.3 g, 4.80 mmol) in 200 mL of *tert*-butylalcohol was degassed and heated to 70 °C under positive pressure of N₂. Then, a degassed solution of 2,2'-azobisisobutylnitrile (30 mg, 0.18 mmol) in 15 mL of *tert*-butylalcohol was added to the reaction flask via forced siphon. After 18 h of heating, the solvent was removed under reduced pressure, and the polymer product was dried under vacuum. The crude product was dissolved in 150 mL of THF and purified by precipitation using 2 L of hexanes to yield 11.03 g (90%) of the product. ¹H NMR (CDCl₃) δ 6.30 (21H, bs), 4.00 (20H, bs), 2.60-1.50 (56H, bm), 1.45 (9H, s), 1.18 (120H, bs).

Polymer Solutions. Stock solutions of polymers **31** and **32** (50 mg/mL) in water were prepared by adding 2 g of polymer **31** or **32** to flasks equipped with magnetic stirring bars containing 40 mL of distilled water. The flasks were then placed in an ice bath and stirred for 2 h until the polymers dissolved.

Solutions of 33 for LC-MS Analysis. Two stock solutions of **33** were prepared. For the fast precipitation protocol, a solution of 12.0 ppm of **33** was prepared by dissolving 12.0 mg of **33** in 1 mL of DMSO and diluting it to 1 L in a volumetric flask by the addition of distilled water. The solution was diluted to a concentration of 120 ppb, by taking 10.0 mL of this 12.0 ppm solution and diluting it to 1 L in a volumetric flask with distilled water. Further dilutions using serological pipettes and 100-ml

volumetric flasks were carried out to prepare solutions with 1.2, 9.6, 12.0, 24.0, 48.0, 60.0, and 96.0 ppb concentrations of **33**. These solutions were used to make the calibration curve. For the slow precipitation protocol, a solution of 10 ppm of **33** was prepared.

Fast Precipitation Protocol. An 8 mL solution of analytes **33-35** were placed in a 40 mL centrifuge tube. A previously prepared solution of either polymer **31** or **32** was added (2 mL, 100 mg of polymer) to the desired analyte solution. Within 5 min of mixing, the solution was heated in an oil bath for 15 min at 40 °C for solutions containing polymer **31**, and 60 °C for 15 min for solutions containing polymer **32**. A 100 mg portion of NaCl was added, and the polymer that precipitated (**31** or **32**) was separated from the supernatant by centrifugation at 55 °C (463 g, 20 min). The supernatant was then decanted and analyzed by liquid chromatography mass spectrometry, UV-Vis spectroscopy, or fluorescence, spectroscopy for analytes **33-35** respectively.

Slow Precipitation Protocol. A 10 mL solution of analytes **33-35**, were placed in a 40 mL centrifuge tube. Either polymer **31** or **32** was added (100 mg) as a solid to the analyte solution. The polymer was dissolved by placing the flask in an ice bath. The process of dissolving the polymer took between 1 to 1.5 h. The resulting solution was then heated in an oil bath for 8 h at 40 °C for solutions containing polymer **1**, and at 60 °C for 8 h for solutions containing polymer **32**. A 100 mg portion of NaCl was added, and the polymer precipitate (**31** or **32**) was separated from the supernatant by centrifugation at 55 °C (463 g, 1 h). The supernatant was then decanted and analyzed by

liquid chromatography mass spectrometry, UV-Vis spectroscopy, or fluorescence, spectroscopy for analytes **33-35** respectively.

Fabrication of temperature gradient device. Fabrication of the temperature gradient device has been previously described.^{136, 142, 143} Briefly, two 1/8th inch wide hollow square brass tubes (K&S Engineering, Chicago, IL) were laid in parallel and separated by 3 mm spacers made of glass slides. The two brass tubes were then fixed into position using clamps and placed under a darkfield condenser in an inverted microscope (Nikon, Eclipse TE 2000-U). To establish the temperature gradient, hot and cold antifreeze solutions were circulated through individual brass tubes using standard waterbath circulators (Fisher Scientific, Pittsburgh, PA). A coverglass was laid on top of two brass tubes by applying vacuum grease and the linear temperature gradient was confirmed by taking temperature measurements at various points perpendicular to the copper tubes with a type E thermocouple.

LCST measurement of thermoresponsive polymers. To measure the LCSTs of thermoresponsive polymers, rectangularly shaped borosilicate capillary tubes (Vitrocom, Mountain Lakes, NJ) with a high aspect ratio (100 $\mu\text{m} \times 1 \text{ mm} \times 2 \text{ cm}$) were used as sample containers. Polymer solutions were introduced into the tubes through capillary action and were subsequently sealed with vacuum grease before being laid parallel to the temperature gradient. Polymer clouding was imaged through a darkfield condenser using a CCD camera. Two standard polymer solutions, PNIPAM 10mg/mL in water (LCST 30.2 °C) and PNIPAM 10mg/mL in 0.7 M KCl (LCST 26.0 °C), were

used as internal temperature standards to determine the temperature gradient for every experiment. Clouding curves of polymers were plotted from linescans of scattering intensity drawn along the temperature gradient where pixel positions were converted to temperatures according to the gradient obtained in the reference samples. The LCST was defined as the onset point of in the clouding curve.

Synthesis of *N-n*-propylacrylamide. A solution of *n*-propylamine (65.3 g, 1.1 mol) in 50 mL of CH₂Cl₂ was added dropwise to a solution of acryloyl chloride (50.0 g, 0.55 mol) in 300 mL of CH₂Cl₂ at 0 °C. After all of the amine solution had been added the mixture was stirred at room temperature for 1 h. The white precipitate was removed and the supernatant was concentrated under reduced pressure. The resulting oil was dissolved in 500 mL of CH₂Cl₂ and washed with 3 X 100 mL portions of deionized water, 10% HCl solution, saturated NaHCO₃, and brine. The organic phase was dried over MgSO₄, the solvent was removed under reduced pressure, and the resulting oil was dried under vacuum, yielding 42.28 g (68%) of the product. ¹H NMR (CDCl₃) δ 0.95 (t, 3H), 1.58 (m, 2H), 3.25 (q, 2H), 5.60 (d, 1H), 6.15 (dd, 1H), 6.25 (d, 1H), 6.35 (bs, 1H); ¹³C NMR (CDCl₃) δ 11.60, 22.98, 41.51, 126.11, 131.35, 165.97.

Synthesis of Poly(*N-n*-propylacrylamide)(38) from *N-n*-propylacrylamide (tBuOH). A solution of *N-n*-propylacrylamide (5.00 g, 44 mmol) in 100 mL of *tert*-butylalcohol was degassed and heated to 70 °C under positive pressure of N₂. Then a degassed solution of 2,2'-azobisisobutylnitrile (15 mg, 91 μmol) in 20 mL of *tert*-butylalcohol was added to the reaction flask *via* forced siphon. After 18 h the *tert*-butylalcohol was removed under reduced pressure and the polymer was dried under

vacuum. The crude product was then reprecipitated from 50 mL THF into 500 mL of hexanes 3 times, yielding 4.09 g (82%) of the pure product **38**. $^1\text{H NMR}$ (CDCl_3) δ 0.90 (bs, 3H), 1.40-2.60 (bm, 5H), 3.15 (bs, 2H), 6.40 (bs, 1H).

Synthesis of Poly(*N-n*-propylacrylamide)(38**) from *N-n*-propylacrylamide (**MeOH**).** A solution of *N-n*-propylacrylamide (5.00 g, 44 mmol) in 100 mL of methanol was degassed and heated to 70 °C under positive pressure of N_2 . Then a degassed solution of 2,2'-azobisisobutylnitrile (15 mg, 91 μmol) in 20 mL of methanol was added to the reaction flask via forced siphon. After 18 h the methanol was removed under reduced pressure and the polymer was dried under vacuum. The crude product was then reprecipitated from 50 mL THF into 500 mL of hexanes 3 times, yielding 4.13 g (83%) of the pure product **38**. $^1\text{H NMR}$ (CDCl_3) δ 0.90 (bs, 3H), 1.40-2.60 (bm, 5H), 3.15 (bs, 2H), 6.40 (bs, 1H).

Synthesis of *N*-Acryloxysuccinimide. This compound was prepared following a literature procedure.¹⁷⁴

Synthesis of Poly(*N*-Acryloxysuccinimide) (39**).** This polymer was prepared following a literature procedure.¹⁷⁵ A solution of *N*-acryloxysuccinimide (15.00 g, 89 mmol) in 600 mL of dry benzene was degassed and heated to 60 °C under positive pressure of N_2 . A degassed solution of 2,2'-azobisisobutylnitrile (90 mg, 0.55 mmol) in 20 mL of dry benzene was then added to the monomer solution *via* forced siphon. After stirring for 36 h the heat was removed and the mixture was allowed to cool to room temperature under a positive pressure of N_2 . The white precipitate was filtered and washed with fresh dry benzene, freshly distilled THF, and finally anhydrous ether. The

material was then dried for 18 h under vacuum. The dry white powder so obtained was then triturated under N₂ with 400 mL of freshly distilled THF for 3 days. The fine white powder was then filtered, washed with anhydrous ether, and dried under vacuum to yield 14.17 g (95%) of the pure polymer. ¹H NMR (CDCl₃) δ 2.10 (bs, 2H), 2.80 (bs, 4H), 3.15 (bs, 1H).

Synthesis of homo- and co-polymers of *N*-alkylacrylamides from poly(*N*-acryloxysuccinimide). Homopolymers were prepared using a single amine (in these cases either 1-aminopropane or 2-aminopropane) using a 5-fold excess of the amine during aminolysis of the active ester PNASI. In the case of copolymers, the similar 5-fold molar excess of amines was used but the molar ratio of the two amines was varied. Due to the differences in nucleophilicity of the primary versus secondary amine (NH₂CH₂CH₂CH₃ versus CH₃CH(NH₂)CH₃), the ratio of *N*-*n*-propyl/*N*-isopropyl groups incorporated into the product copolymer was not the same as the ratio of the amines added. In the specific case of copolymers 2-4, an initial 2:1 mole: mole ratio of [*n*-PrNH₂]₀/[*i*-PrNH₂]₀ produced a 6:1 ratio of *n*-Pr/*i*-Pr groups in the PNNPAM-*c*-PNIPAM product; a 1:1.5 mole: mole ratio of [*n*-PrNH₂]₀/[*i*-PrNH₂]₀ produced a 2:1 ratio of *n*-Pr/*i*-Pr groups in the PNNPAM-*c*-PNIPAM product; and a 1:4 mole:mole ratio of [*n*-PrNH₂]₀/[*i*-PrNH₂]₀ produced a 1:1 ratio of *n*-Pr/*i*-Pr groups in the PNNPAM-*c*-PNIPAM product. This result is consistent with the idea that the secondary amine is less nucleophilic than the primary amine.

Synthesis of Poly(*N*-isopropylacrylamide)(31) from Poly(*N*-Acryloxysuccinimide). A solution of isopropylamine (1.3 mL, 15 mmol) in 5 mL of

dry DMF was added to a solution of **39** (500 mg, 3 meq NASI) in 10 mL of dry DMF. Within 10 seconds a large amount of precipitate formed and the slurry was stoppered and stirred for 18 h. The mixture was filtered and the supernatant was precipitated into 700 mL of ether. After stirring for a few minutes, the fine white precipitate, which initially forms aggregates, evolved to large particles. After allowing this suspension to settle for 10 minutes, the solution was decanted and 500 mL of fresh ether were added. After stirring the resulting suspension for 10 minutes, the crude product was isolated by filtration and dried. The crude product was then redissolved in 10 mL of THF and reprecipitated using 125 mL of hexanes. This process was repeated 3 times, yielding 200 mg (60%) of the pure polymer **31**. $^1\text{H NMR}$ (CDCl_3) δ 1.18 (bs, 6H), 1.40-2.25 (bm, 3H), 4.00 (bs, 1H), 6.40 (bs, 1H); $M_w = 320,000$ g/mol (light scattering in MeOH using literature value of 0.201 mL/g for dn/dc).¹⁷¹

Synthesis of Poly(*N*-*n*-propylacrylamide)(38**) from Poly(*N*-Acryloxysuccinimide).** A solution of *n*-propylamine (1.2 mL, 15 mmol) in 5 mL of dry DMF was added to a solution of **39** (500 mg, 3 meq NASI) in 10 mL of dry DMF. Within 10 seconds a large amount of precipitate formed and the slurry was stoppered and stirred for 18 h. The mixture was filtered and the supernatant was precipitated into 700 mL of ether. After stirring for a few minutes, the fine white precipitate, which initially forms aggregates, evolved to large particles. After allowing this suspension to settle for 10 minutes, the solution was decanted and 500 mL of fresh ether were added. After stirring the resulting suspension for 10 minutes, the crude product was isolated by filtration and dried. The crude product was then redissolved in 10 mL of THF and

reprecipitated using 125 mL of hexanes. This process was repeated 3 times, yielding 240 mg (72%) of the pure polymer **38**. $^1\text{H NMR}$ (CDCl_3) δ 0.90 (bs, 3H), 1.40-2.60 (bm, 5H), 3.15 (bs, 2H), 6.40 (bs, 1H).

Synthesis of Poly(*N-n*-propylacrylamide-*c-N*-isopropylacrylamide) 6:1 (40).

A solution of isopropylamine (0.4 mL, 5 mmol) and *n*-propylamine (0.8 mL, 10 mmol) in 5 mL of dry DMF was added to a solution of **39** (500 mg, 3 meq NASI) in 10 mL of dry DMF. Within 10 seconds a large amount of precipitate formed and the slurry was stoppered and stirred for 18 h. The mixture was filtered and the supernatant was precipitated into 700 mL of ether. After stirring for a few minutes, the fine white precipitate, which initially forms aggregates, evolved to large particles. After allowing this suspension to settle for 10 minutes, the solution was decanted and 500 mL of fresh ether were added. After stirring the resulting suspension for 10 minutes, the crude product was isolated by filtration and dried. The crude product was then redissolved in 10 mL of THF and reprecipitated using 125 mL of hexanes. This process was repeated 3 times, yielding 220 mg (66%) of the pure polymer **40**. $^1\text{H NMR}$ (CDCl_3) δ 0.90 (bs, 18H), 1.18 (bs, 6H), 1.25-2.60 (bm, 37H), 3.15 (bs, 12H), 4.00 (bs, 1H), 6.80 (bs, 7H).

Synthesis of Poly(*N-n*-propylacrylamide-*c-N*-isopropylacrylamide) 2:1 (41).

A solution of isopropylamine (0.8 mL, 9 mmol) and *n*-propylamine (0.5 mL, 6 mmol) in 5 mL of dry DMF was added to a solution of **39** (500 mg, 3 meq NASI) in 10 mL of dry DMF. Within 10 seconds a large amount of precipitate formed and the slurry was stoppered and stirred for 18 h. The mixture was filtered and the supernatant was precipitated into 700 mL of ether. After stirring for a few minutes, the fine white

precipitate, which initially forms aggregates, evolved to large particles. After allowing this suspension to settle for 10 minutes, the solution was decanted and 500 mL of fresh ether were added. After stirring the resulting suspension for 10 minutes, the crude product was isolated by filtration and dried. The crude product was then redissolved in 10 mL of THF and reprecipitated using 125 mL of hexanes. This process was repeated 3 times, yielding 220 mg (66%) of the pure polymer **41**. $^1\text{H NMR}$ (CDCl_3) δ 0.90 (bs, 6H), 1.18 (bs, 6H), 1.30-2.60 (bm, 16H), 3.15 (bs, 4H), 4.00 (bs, 1H), 6.80 (bs, 3H).

Synthesis of Poly(*N-n*-propylacrylamide-*c-N*-isopropylacrylamide) 1:1 (42**).**

A solution of isopropylamine (1.0 mL, 12 mmol) and *n*-propylamine (0.3 mL, 3 mmol) in 5 mL of dry DMF was added to a solution of **39** (500 mg, 3 meq NASI) in 10 mL of dry DMF. Within 10 seconds a large amount of precipitate formed and the slurry was stoppered and stirred for 18 h. The mixture was filtered and the supernatant was precipitated into 700 mL of ether. After stirring for a few minutes, the fine white precipitate, which initially forms aggregates, evolved to large particles. After allowing this suspension to settle for 10 minutes, the solution was decanted and 500 mL of fresh ether were added. After stirring the resulting suspension for 10 minutes, the crude product was isolated by filtration and dried. The crude product was then redissolved in 10 mL of THF and reprecipitated using 125 mL of hexanes. This process was repeated 3 times, yielding 220 mg (66%) of the pure polymer **42**. $^1\text{H NMR}$ (CDCl_3) δ 0.90 (bs, 3H), 1.18 (bs, 6H), 1.30-2.60 (bm, 9H), 3.15 (bs, 1H), 4.00 (bs, 1H), 6.80 (bs, 2H).

Fractional Precipitation of Poly(*N*-isopropylacrylamide). Poly(*N*-isopropylacrylamide) was fractionated using a literature procedure.¹⁶³

Synthesis of *N*-Triphenylmethylhexaneamide (43). A solution of hexanoyl chloride (507 mg, 3.8 mmol) in 10 mL of dry CH₂Cl₂ was slowly added to a solution of tritylamine (963 mg, 3.7 mmol) and TEA (0.8 mL, 6.0 mmol) in 20 mL of dry CH₂Cl₂. The system was flushed with N₂ and then allowed to stir at 25 °C under positive pressure of N₂ for 21 hours. The clear solution was washed with deionized water (3 X 20 mL) and brine (1 X 20 mL) and then dried over MgSO₄. The solvent was removed under reduced pressure and the resulting yellow solid was dried under vacuum. The crude product was purified *via* column chromatography (silica, hexanes:EtOAc 10:90) to yield 290 mg (22%) of the pure product *N*-triphenylmethylhexaneamide. ¹H NMR (CDCl₃) δ 0.90 (t, 3H), 1.30 (m, 4H), 1.61 (q, 2H), 2.25 (t, 2H), 6.55 (s, 1H), 7.18-7.35 (m, 15H); ¹³C NMR (CDCl₃) δ 13.94, 22.39, 25.30, 31.43, 37.76, 126.95, 127.90, 128.66, 144.80, 171.90; IR (KBr) 3257, 3060, 3034, 2955, 2929, 2857, 1649, 1535, 1489, 1443, 1391, 697 cm⁻¹.

Removal of Triphenylmethyl Group From *N*-Triphenylmethylhexaneamide .

N-triphenylmethylhexaneamide (50 mg, 140 μmol) was dissolved in 10 mL of trifluoroacetic acid (the solution immediately turned bright yellow) and was allowed to stir at 25 °C for 4 h. The yellow solution was then added to 100 mL of anhydrous ethanol and the solvent was then removed under reduced pressure. Fresh ethanol (100 mL) was then added and this process was repeated three more times to remove all of the trifluoroacetic acid. The oil was then dried under vacuum to yield 0.1 g (>100%) of the primary amide. The product was not separated from the triphenylcarbinol by-product. The efficiency of the cleavage was determined by the shift in the ¹H NMR (CDCl₃)

spectrum for the $-\text{CH}_2-$ group adjacent to the carbonyl from δ 2.25 to 2.23 ppm for the secondary to the primary amide respectively. The cleavage was also evaluated by TLC on Silica with fluorescent indicator (ethyl acetate:hexanes 1:4). *N*-triphenylmethylhexaneamide had an R_f of 0.45 and was visible only under shortwave (λ_{254}) UV light whereas the product and triphenylcarbinol had the same R_f of 0.61 and were visible under both shortwave and longwave (λ_{365}) UV light.

Synthesis of 4,4'-Azobis(4-cyanovaleroyl chloride) (44). All glassware was flame dried before synthesis. Three drops of DMF were added to a suspension of 4,4'-azobis(4-cyanovaleric acid) (1.00 g, 3.6 mmol) in 20 mL of dry CH_2Cl_2 . The system was fitted with an air condenser, sealed with septa, and flushed with N_2 for 5 minutes. The suspension was then cooled to 0 °C and oxalyl chloride (1.0 mL, 11.6 mmol) was added *via* syringe and the reaction mixture was protected from light and allowed to stir at 25 °C under a slow stream of N_2 for 3 hours. The solid dissolved as the reaction proceeded. The solvent was removed under reduced pressure keeping the flask below 30 °C at all times. The resulting yellow oil was then dried under vacuum in the dark yielding 1.09 g (96%) of the yellow solid **44**. ^1H NMR (CDCl_3) δ 170 (s, 3H), 1.75 (s, 3H), 2.41-2.65 (m, 4H), 2.90-3.21 (m, 4H)

Synthesis of 4,4'-Azobis(*N*-triphenylmethyl-4-cyanovaleramide) (45).

Triethylamine (1.64 g, 6.3 mmol) and pyridine (549 mg, 6.9 mmol) were dissolved in 20 mL of dry CH_2Cl_2 . The system was flushed with N_2 and then cooled to 0 °C. Then **44** (1.00 g, 3.15 mmol) was dissolved in 10 mL of dry CH_2Cl_2 and flushed with N_2 . The acid chloride solution was transferred *via* forced siphon to the amine solution and the

reaction mixture was allowed to stir at 25 °C under a positive pressure of N₂ for 24 hours. The resulting precipitate was filtered and the clear, orange supernatant was washed with deionized water (5 X 20 mL) and brine (1 X 20 mL) and was then dried over MgSO₄. The solvent was removed under reduced pressure and the crude product was dried *in vacuo*. The resulting solid was then triturated with 50 mL of diethyl ether, filtered, and then dried under vacuum yielding 1.36 g (57%) of the pure product **45**. ¹H NMR (CDCl₃) δ 1.61 (s, 3H), 1.62 (s, 3H), 2.50-2.55 (m, 8H), 6.60 (s, 1H), 6.61 (s, 1H), 7.10-7.40 (m, 30H); ¹³C NMR (CDCl₃) δ 23.60, 23.84, 31.68, 33.42, 70.73, 71.79, 117.93, 127.10, 128.01, 128.61, 144.37, 168.99; IR (KBr) 1692, 1489, 1450, 1384, 697 cm⁻¹.

Synthesis of PNIPAM-CONH-Tr (46). A solution of *N*-isopropylacrylamide (15.01 g, 133 mmol) and **45** (127 mg, 0.166 mmol) in 200 mL of MeOH was degassed and heated to 70°C under positive pressure of N₂. After 17 h the MeOH was removed under reduced pressure and the polymer was dried under vacuum. The crude product was then reprecipitated from 100 mL THF into 750 mL of hexanes 3 times, yielding 14.00 g (93%) of the pure product **46**. ¹H NMR (CDCl₃) δ 1.18 (bs, 6H), 2.25-1.40 (bm, 3H), 4.00 (bs, 1H), 6.40 (bs, 1H).

Fractional Precipitation of PNIPAM-CONH-Tr. The trityl-terminated poly(*N*-isopropylacrylamide) derivative was fractionated using a literature procedure.¹⁶³ The lowest molecular weight sample ($M_w=4.58 \times 10^4$ g/mol) had an extra peak (corresponding to the triphenylmethyl end groups) at δ 7.20 ppm in the ¹H NMR spectrum (CDCl₃).

Synthesis of PNIPAM-CONH₂ (47). The cleavage of the lowest M_w sample ($M_w=4.58 \times 10^4$ g/mol) is representative of the procedure used to cleave each sample. PNIPAM-CONH-Tr (500 mg) was dissolved in 10 mL of trifluoroacetic acid (the solution immediately turned bright yellow) and was allowed to stir at 25 °C for 4 h. The yellow solution was then added to 100 mL of anhydrous ethanol and the solvent was then removed under reduced pressure. Fresh ethanol (100 mL) was then added and this process was repeated three more times to remove all of the trifluoroacetic acid. The oil was then dried under vacuum. The product was dissolved in 10 mL of THF and precipitated into 75 mL hexanes. The white powder was filtered and dried and then dissolved in 10 mL THF and precipitated into 75 mL of anhydrous diethyl ether. The fine white precipitate was separated *via* centrifuge at 25° C and the white solid was dried under vacuum yielding 370 mg (73%) of the pure product.

¹H NMR spectroscopy (D₂O) was used to observe the removal of the triphenylmethyl group from the lowest molecular weight sample only. PNIPAM-CONH-Tr and PNIPAM-CONH₂ had identical ¹H NMR spectra in D₂O except for one peak at δ 7.38 ppm (corresponding to the triphenylmethyl end groups) that only appeared in the PNIPAM-CONH-Tr spectra.

Synthesis of Benzyl Dithiobenzoate. This compound was prepared using a literature procedure.¹⁷⁶

Synthesis of 80% Isotactic PNIPAM. Followed literature procedure using benzyl dithiobenzoate as the chain transfer agent.¹⁷⁰

REFERENCES

1. Love, L., *Science* **1973**, 182, 343-352.
2. Siyam, T., *Des. Monomers Polym.* **2001**, 4, 107-168.
3. Giddings, J. C., *Unified Separation Science*. Wiley-Interscience: New York, 1991.
4. Melnechuk, T., *Int. Sci. Technol.* **1963**, 26-37.
5. Stewart, G., *J. Chromatogr. Sci.* **1976**, 14, 69-70.
6. Curran, D., *Angew. Chem., Int. Ed. Engl.* **1998**, 37, 1175-1196.
7. *Waste Minimisation: A Chemist's Approach*. The Royal Society of Chemistry: Cambridge, 1994.
8. Laird, T., *Chem. Br.* **1996**, 32, 43-45.
9. Mercier, C.; Chabardes, P., *Pure Appl. Chem.* **1994**, 66, 1509-1518.
10. Ito, S.; Aihara, K.; Matsumoto, M., *Tetrahedron Lett.* **1983**, 24, 5249-5252.
11. Wender, P.; Handy, S.; Wright, D., *Chem. Ind. (London)* **1997**, 19, 765-769.
12. Dandapani, S.; Curran, D.; Ley, S.; Massi, A.; Rodriguez, F.; Harwell, D.; Lewthwaite, R.; Pritchard, M.; Reid, A.; Zhang, S.-Q.; Fukase, K.; Izumi, M.; Fukase, Y.; Kusumoto, S.; Bosanac, T.; Yang, J.; Wilcox, C., *Chemtracts* **2001**, 14, 635-641.
13. Bergbreiter, D., *Chem. Rev.* **2002**, 102, 3345-3383.
14. Merrifield, R., *Angew. Chem., Int. Ed. Engl.* **1985**, 24, 799-810.
15. Pollak, A.; Whitesides, G., *J. Am. Chem. Soc.* **1976**, 98, 289-291.

16. Bergbreiter, D.; Hughes, R.; Besinaiz, J.; Li, C.; Osburn, P., *J. Am. Chem. Soc.* **2003**, 125, 8244-8249.
17. Bergbreiter, D.; Sung, S.; Li, J.; Ortiz, D.; Hamilton, P., *Org. Process Res. Dev.* **2004**, 8, 461-468.
18. Whitesides, G., *Angew. Chem., Int. Ed. Engl.* **1990**, 29, 1209-1218.
19. Merrifield, R., *J. Am. Chem. Soc.* **1963**, 85, 2149-2154.
20. Greig, J.; Sherrington, D., *Polymer* **1978**, 19, 163-172.
21. Collman, J.; Kosydar, K.; Bressan, M.; Lamanna, W.; Garrett, T., *J. Am. Chem. Soc.* **1984**, 106, 2569-2579.
22. Keifer, P.; Baltusis, L.; Rice, D.; Tymiak, A.; Shoolery, J., *J. Magn. Reson., Ser. A* **1996**, 119, 65-75.
23. Bailar, J., *Catal. Rev.-Sci. Eng.* **1974**, 10, 17-36.
24. Herrmann, W.; Cornils, B., *Angew. Chem., Int. Ed. Engl.* **1997**, 36, 1049-1067.
25. Michalska, Z.; Webster, D., *Platinum Met. Rev.* **1974**, 18, 65-73.
26. Chauvin, Y.; Commereuc, D.; Dawans, F., *Prog. Polym. Sci.* **1977**, 5, 95-226.
27. *Catalysis from A to Z*. Wiley-VCH: Weinheim, Germany, 2000.
28. Bergbreiter, D., *Catal. Today* **1998**, 42, 389-397.
29. Osburn, P.; Bergbreiter, D., *Prog. Polym. Sci.* **2001**, 26, 2015-2081.
30. Bergbreiter, D., *J. Polym. Sci., Part A: Polym. Chem.* **2001**, 39, 2351-2363.
31. *Aqueous-Phase Organometallic Catalysis*. 2 ed.; Wiley-VCH: Weinheim, Germany, 2004.
32. Bergbreiter, D.; Osburn, P.; Liu, Y., *J. Am. Chem. Soc.* **1999**, 121, 9531-9538.

33. Bergbreiter, D.; Liu, Y., *Tetrahedron Lett.* **1997**, 38, 3703-3706.
34. Bergbreiter, D., *Med. Res. Rev.* **1999**, 19, 439-450.
35. Bergbreiter, D.; Weatherford, D., *J. Org. Chem.* **1989**, 54, 2726-2730.
36. Bergbreiter, D.; Chandran, R., *J. Am. Chem. Soc.* **1987**, 109, 174-179.
37. Bergbreiter, D.; Chandran, R., *J. Org. Chem.* **1986**, 51, 4754-4760.
38. Bergbreiter, D.; Liu, Y., *Tetrahedron Lett.* **1997**, 38, 7843-7846.
39. Herrmann, W.; Kohlpaintner, C., *Angew. Chem., Int. Ed. Engl.* **1993**, 32, 1524-1544.
40. Cornils, B.; Kuntz, E., *J. Organomet. Chem.* **1995**, 502, 177-186.
41. Wachsen, O.; Himmler, K.; Cornils, B., *Catal. Today* **1998**, 42, 373-379.
42. Cornils, B., *Angew. Chem., Int. Ed. Engl.* **1995**, 34, 1575-1577.
43. Horvath, I.; Rabai, J., *Science* **1994**, 266, 72-75.
44. Horvath, I., *Acc. Chem. Res.* **1998**, 31, 641-650.
45. Cornils, B., *Angew. Chem., Int. Ed. Engl.* **1997**, 36, 2057-2059.
46. Bergbreiter, D.; Franchina, J., *Chem. Commun.* **1997**, 1531-1532.
47. Bergbreiter, D.; Franchina, J.; Case, B.; Williams, L.; Frels, J.; Koshti, N., *Comb. Chem. High Throughput Screening* **2000**, 3, 153-164.
48. Bergbreiter, D.; Franchina, J.; Case, B., *Org. Lett.* **2000**, 2, 393-395.
49. Klement, I.; Lutjens, H.; Knochel, P., *Angew. Chem., Int. Ed. Engl.* **1997**, 36, 1454-1456.
50. Bergbreiter, D.; Liu, Y.; Osburn, P., *J. Am. Chem. Soc.* **1998**, 120, 4250-4251.

51. Bergbreiter, D. E.; Osburn, P. L.; Wilson, A.; Sink, E. M., *J. Am. Chem. Soc.* **2000**, 122, 9058-9064.
52. Bergbreiter, D.; Osburn, P.; Frels, J., *J. Am. Chem. Soc.* **2001**, 123, 11105-11106.
53. Anastas, P.; LWarner, J., *Green Chemistry: Theory and Practice*. Oxford University Press: New York, 1998.
54. Anastas, P.; Kirchhoff, M., *Acc. Chem. Res.* **2002**, 35, 686-694.
55. Anastas, P.; Kirchhoff, M.; Williamson, T., *Appl. Catal., A* **2001**, 221, 3-13.
56. Bergbreiter, D.; Osburn, P.; Wilson, A.; Sink, E., *J. Am. Chem. Soc.* **2000**, 122, 9058-9064.
57. Bergbreiter, D.; Liu, Y.; Furyk, S.; Case, B., *Tetrahedron Lett.* **1998**, 39, 8799-8802.
58. Ohff, M.; Ohff, A.; vanderBoom, M. E.; Milstein, D., *J. Am. Chem. Soc.* **1997**, 119, 11687-11688.
59. Errington, J.; McDonald, W. S.; Shaw, B. L., *J. Chem. Soc., Dalton Trans.* **1980**, 2312-2314.
60. Gruber, A. S.; Zim, D.; Ebeling, G.; Monteiro, A. L.; Dupont, J., *Org. Lett.* **2000**, 2, 1287-1290.
61. Zim, D.; Gruber, A. S.; Ebeling, G.; Dupont, J.; Monteiro, A. L., *Org. Lett.* **2000**, 2, 2881-2884.
62. Silveira, P. B.; Lando, V. R.; Dupont, J.; Monteiro, A. L., *Tetrahedron Lett.* **2002**, 43, 2327-2329.

63. Recent unpublished work suggests that while the SCS-Pd(II) complexes are thermally stable, that they may not be molecular catalysts but rather precursors to an unidentified but much more active catalyst, Frels, J. D. Soluble polymer supports as ligands for metal sequestration and catalysis. P.h.D. Dissertation, Texas A&M University, College Station, TX, 2002.
64. Dickerson, T. J.; Reed, N. N.; Janda, K. D., *Chem. Rev.* **2002**, 102, 3325-3343.
65. Gravert, D. J.; Janda, K. D., *Chem. Rev.* **1997**, 97, 489-509.
66. Smyth, H. F. J.; Carpenter, C. P.; Weil, C. S., *J. Am. Pharm. Assoc.* **1950**, 39, 349-354.
67. Braun, D. B.; DeLong, D. J., Polyethers. Ethylene Oxide Polymers. In *Kirk-Othmer Encyclopedia of Chemical Technology*, 3 ed.; Wiley: New York, 1982; Vol. 18, pp 616-632.
68. Reed, N.; Janda, K. D., *Org. Lett.* **2000**, 2, 1311-1313.
69. Reed, N. N.; Janda, K. D., *Org. Lett.* **2000**, 2, 1311-1313.
70. Wang, Y. H.; Wu, X. W.; Cheng, F.; Jin, Z. L., *J. Mol. Catal. A: Chem.* **2003**, 195, 133-137.
71. Li, J.; Kao, W. J., *Biomacromolecules* **2003**, 4, 1055-1067.
72. Conover, C. D.; Zhao, H.; Longley, C. B.; Shum, K. L.; Greenwald, R. B., *Bioconjugate Chem.* **2003**, 14, 661-666.
73. Larhed, M.; Moberg, C.; Hallberg, A., *Acc. Chem. Res.* **2002**, 35, 717-727.
74. Larhed, M.; Hallberg, A., *J. Org. Chem.* **1996**, 61, 9582-9584.
75. Namboodiri, V. V.; Varma, R. S., *Green Chem.* **2001**, 3, 146-148.

76. Blettner, C. G.; Konig, W. A.; Stenzel, W.; Schotten, T., *J. Org. Chem.* **1999**, 64, 3885-3890.
77. Bergbreiter, D. E.; Osburn, P. L.; Liu, Y. S., *J. Am. Chem. Soc.* **1999**, 121, 9531-9538.
78. Pollino, J. M.; Weck, M., *Synthesis* **2002**, 1277-1285.
79. Dupont, J.; Beydoun, N.; Pfeffer, M., *J. Chem. Soc., Dalton Trans.* **1989**, 9, 1715-1720.
80. Gimenez, R.; Swager, T. M., *J. Mol. Catal. A: Chem.* **2001**, 166, 265-273.
81. de Vries, A. H. M.; Mulders, J.; Mommers, J. H. M.; Henderickx, H. J. W.; de Vries, J. G., *Org. Lett.* **2003**, 5, 3285-3288.
82. Distinguishing between homogeneous and heterogeneous catalysis or catalysis via 'nanoclusters' remains a general problem, cf. "Is It Homogeneous or Heterogeneous Catalysis? Identification of Bulk Ruthenium Metal as the True Catalyst in Benzene Hydrogenations Starting with the Monometallic Precursor, Ru(II)(η^6 -C₆Me₆)(OAc)₂, Plus Kinetic Characterization of the Heterogeneous Nucleation, Then Autocatalytic Surface-Growth Mechanism of Metal Film Formation", Widegren, J. A.; Bennett, M. A.; Finke, R. G., *J. Am. Chem. Soc.* **2003**, 125, 10301.
83. Yu, K.; Sommer, W.; Weck, M.; Jones, C., *J. Catal.* **2004**, 226, 101-110.
84. Rocaboy, C.; GLADYSZ, J., *New J. Chem.* **2003**, 27, 39-49.
85. Consorti, C.; Zanini, M.; Leal, S.; Ebeling, G.; Dupont, J., *Org. Lett.* **2003**, 5, 983-986.
86. Perreux, L.; Loupy, A., *Tetrahedron* **2001**, 57, 9199-9223.

87. Leadbeater, N.; Marco, M., *J. Org. Chem.* **2003**, 68, 888-892.
88. Botella, L.; Najera, C., *Tetrahedron* **2004**, 60, 5563-5570.
89. Curran, D.; Fischer, K.; Moura-Letts, G., *Synlett* **2004**, 8, 1379-1382.
90. Kuhnert, N., *Angew. Chem., Int. Ed. Engl.* **2002**, 41, 1863-1866.
91. Strauss, C., *Angew. Chem., Int. Ed. Engl.* **2002**, 41, 3589-3590.
92. Datta, G.; Vallin, K.; Larhed, M., *Molecular Diversity* **2003**, 7, 107-114.
93. Svennebring, A.; Nilsson, P.; Larhed, M., *J. Org. Chem.* **2004**, 69, 3345-3349.
94. Li, C. J.; Chan, T. H., *Organic Reactions in Aqueous Media*. 1 ed.; John Wiley & Sons: New York, 1997; p 199.
95. Genet, J. P.; Savignac, M., *J. Organomet. Chem.* **1999**, 576, 305-317.
96. Bumagin, N. A.; More, P. G.; Beletskaya, I. P., *J. Organomet. Chem.* **1989**, 371, 397-401.
97. Bumagin, N. A.; Bykov, V. V.; Sukhomlinova, L. I.; Tolstaya, T. P.; Beletskaya, I. P., *J. Organomet. Chem.* **1995**, 486, 259-262.
98. Reed, D.; Tasker, I.; Cunnane, J.; Vandergrift, G. Environmental Restoration and Separation Science, In *Environmental Remediation: Removing Organic and Metal Ion Pollutants*, Vandergrift, G.; Reed, D.; Tasker, I., Eds.; ACS Symposium Series 509; American Chemical Society: Washington DC, 1992; 1-19.
99. Wood, P., Remediation Methods for Contaminated Sites. In *Contaminated Land and Its Reclamation*, Hester, R.; Harrison, R., Eds. The Royal Society of Chemistry: Cambridge, United Kingdom, 1997; pp 47-71.
100. Alexandratos, S.; Crick, D., *Ind. Eng. Chem. Res.* **1996**, 35, 635-644.

101. Beauvais, R.; Alexandratos, S., *React. Funct. Polym.* **1998**, 36, 113-123.
102. Alexandratos, S.; Natesan, S., *Eur. Polym. J.* **1998**, 35, 431-436.
103. Geckeler, K.; Volchek, K., *Environ. Sci. Technol.* **1996**, 30, 725-734.
104. Geckeler, K., *Pure Appl. Chem.* **2001**, 73, 129-136.
105. Bergbreiter, D. E.; Frels, J. D.; Li, C. M., *Macromol. Symp.* **2003**, 204, 113-140.
106. Cole, C.; Shreiner, S.; Priest, J.; Monji, N.; Hoffman, A. *N*-Isopropylacrylamide and *N*-acryloxysuccinimide copolymer: a thermally reversible, water-soluble, activated polymer for protein conjugation, In *Reversible Polymeric Gels and Related Systems*, Russo, P., Ed. ACS Symposium Series 350; American Chemical Society: Washington DC, 1987; 245-254.
107. Bolharnordenkamp, H., *Z. Naturforsch., C: Biosci.* **1979**, 34, 923-925.
108. Bouzaher, A.; Lakshminarayan, P.; Cabe, R.; Carriquiry, A.; Gassman, P.; Shogren, J., *Water Resour. Res.* **1993**, 29, 1579-1587.
109. Goolsby, D.; Battaglin, W.; Fallon, J.; Aga, D.; Koplun, D.; Thurman, E. *Persistence of herbicides in selected reservoirs in the midwestern United States; some preliminary results*; U.S. Geological Survey: Denver, CO; 1993.
110. Low, G. K.; McEvoy, S. R.; Matthews, R. W., *Environ. Sci. Technol.* **1991**, 25, 460-467.
111. Koeber, R.; Fleischer, C.; Lanza, F.; Boos, K. S.; Sellergren, B.; Barcelo, D., *Analytical Chemistry* **2001**, 73, 2437-2444.
112. Schild, H. G., *Prog. Polym. Sci.* **1992**, 17, 163-249.

113. Bergbreiter, D.; Case, B.; Liu, Y.; Caraway, J., *Macromolecules* **1998**, 31, 6053-6062.
114. Pan, Y. V.; Wesley, R. A.; Luginbuhl, R.; Denton, D. D.; Ratner, B. D., *Biomacromolecules* **2001**, 2, 32-36.
115. Yamashita, K.; Nishimura, T.; Nango, M., *Polym. Adv. Technol.* **2003**, 14, 189.
116. Kim, B. Y.; Kang, H. S.; Kim, J. D., *J. Microencapsulation* **2002**, 19, 661.
117. Zhu, X. X.; Avoce, D.; Liu, H. Y.; Benrebouh, A., *Macromol Symp* **2004**, 207, 187-191.
118. Mao, H. B.; Li, C. M.; Zhang, Y. J.; Furyk, S.; Cremer, P. S.; Bergbreiter, D. E., *Macromolecules* **2004**, 37, 1031-1036.
119. Steffensen, M.; Simanek, E., *Org. Lett.* **2003**, 5, 2359-2361.
120. Acosta, E. J.; Gonzalez, S.; Simanek, E., *Abstr. Pap.-Am. Chem. Soc.* **2003**, 226.
121. Acosta, E. J.; Steffensen, M. B.; Tichy, S. E.; Simanek, E. E., *J. Agric. Food Chem.* **2004**, 52, 545-549.
122. Tong, Z.; Zeng, F.; Zheng, X.; Sato, T., *Macromolecules* **1999**, 32, 4488-4490.
123. Acosta, E.; Deng, Y.; White, G.; Dixon, J.; McInnes, K.; Senseman, S.; Frantzen, A.; Simanek, E., *Chem. Mater.* 15, 2903-2909.
124. Bell, S.; McLean, M.; Oh, S.; Tichy, S.; Zhang, W.; Corn, R.; Crooks, R.; Simanek, E., *Bioconjugate Chem.* **2003**, 14, 488-493.
125. Galaev, I. Y.; Mattiason, B., *Smart Polymers for Bioseparation and Bioprocessing*. Taylor & Francis: London, 2002.

126. Tiktopulo, E. I.; Uversky, V. N.; Lushchik, V. B.; Klenin, S. I.; Bychkova, V. E.; Ptitsyn, O. B., *Macromolecules* **1995**, *28*, 7519-7524.
127. Bruscolini, P.; Buzano, C.; Pelizzola, A.; Pretti, M., *Macromol. Symp.* **2002**, *181*, 261-273.
128. Omta, A. W.; Kropman, M. F.; Woutersen, S.; Bakker, H. J., *Science* **2003**, *301*, 347-349.
129. Hribar, B.; Southall, N. T.; Vlachy, V.; Dill, K. A., *J. Am. Chem. Soc.* **2002**, *124*, 12302-12311.
130. Qiu, X.; Li, M.; Kwan, C. M. S.; Wu, C., *J. Polym. Sci., Part B: Polym. Phys.* **1998**, *36*, 1501-1506.
131. Maeda, Y.; Higuchi, T.; Ikeda, I., *Langmuir* **2001**, *17*, 7535-7539.
132. Boutris, C.; Chatzi, E. G.; Kiparissides, C., *Polymer* **1997**, *38*, 2567-2570.
133. Idziak, I.; Avoce, D.; Lessard, D.; Gravel, D.; Zhu, X. X., *Macromolecules* **1999**, *32*, 1260-1263.
134. Percot, A.; Zhu, X. X.; Lafleur, M., *J. Polym. Sci., Part B: Polym. Phys.* **2000**, *38*, 907-915.
135. Wu, C.; Zhou, S., *Macromolecules* **1995**, *28*, 8381-8387.
136. Mao, H.; Li, C.; Zhang, Y.; Bergbreiter, D. E.; Cremer, P. S., *J. Am. Chem. Soc.* **2003**, *125*, 2850-2851.
137. Kujawa, P.; Winnik, F. M., *Macromolecules* **2001**, *34*, 4130-4135.
138. Impurities in a polymer due to side reactions as hypothesized in derivation of PNASI in this case or to trace quantities of impurities even in highly purified monomers

are recognized as a general source of changes in a product polymer's properties, cf.

Bielawski, C. W.; Benitez, D.; Grubbs, R. H. *J. Am. Chem. Soc.* **2003**, 125, 8424-8425.

139. Bergbreiter, D. E.; Case, B. L.; Liu, Y. S.; Caraway, J. W., *Macromolecules* **1998**, 31, 6053-6062.

140. Ringsdorf, H.; Venzmer, J.; Winnik, F. M., *Macromolecules* **1991**, 24, 1678-1686.

141. Ganachaud, F.; Monteiro, M. J.; Gilbert, R. G.; Dourges, M.; Thang, S. H.; Rizzardo, E., *Macromolecules* **2000**, 33, 6738-6745.

142. Mao, H.; Holden, M. A.; You, M.; Cremer, P. S., *Analytical Chemistry* **2002**, 74, 5071-5075.

143. Mao, H.; Yang, T.; Cremer, P. S., *J. Am. Chem. Soc.* **2002**, 124, 4432-4435.

144. Zhang, Y.; Mao, H.; Cramer, P., *J. Am. Chem. Soc.* **2003**, 125, 15630-15635.

145. Kunz, W.; Henle, J.; Ninham, B. W., *Curr. Opin. Colloid Interface Sci.* **2004**, 9, 19-37.

146. Kunz, W.; Nostro, P. L.; Ninham, B., *Curr. Opin. Colloid Interface Sci.* **2004**, 9, 1-18.

147. Nostro, P. L.; Fratoni, L.; Ninham, B. W.; Baglioni, P., *Biomacromolecules* **2002**, 3, 1217-1224.

148. Cacace, M.; Landau, E.; Ramsden, J., *Q. Rev. Biophys.* **1997**, 30, 241-277.

149. Collins, K.; Washabaugh, M., *Q. Rev. Biophys.* **1985**, 18, 323-422.

150. Washabaugh, M.; Collins, K., *J. Biol. Chem.* **1986**, 261, 12477-12485.

151. Gurau, M.; Lim, S.; Castellana, E.; Falbertorio, F.; Kataoka, S.; Cremer, P. S., *J. Am. Chem. Soc.* **2004**, 126, 10522-10523.
152. von Hippel, P. H.; Schleich, T., *Acc. Chem. Res.* **1969**, 2, 257-265.
153. Janado, M.; Yano, Y.; Doi, Y.; Sakamoto, H., *J. Solution Chem.* **1983**, 12, 741-754.
154. Freitag, R.; Garret-Flaudy, F., *Langmuir* **2002**, 18, 3434-3440.
155. Wang, X.; Wu, C., *Macromolecules* **1999**, 32, 4299-4301.
156. Nemethy, G.; Scheraga, H. A., *J. Chem. Phys.* **1964**, 41, 680-689.
157. Fujishige, S.; Kubota, K.; Ando, I., *J. Phys. Chem.* **1989**, 93, 3311-3313.
158. Takei, Y.; Aoki, T.; Sanui, K.; Ogata, N.; Okano, T.; Sakurai, Y., *Bioconjugate Chem.* **1993**, 4, 42-46.
159. Ding, Z.; Chen, G.; Hoffman, A., *Bioconjugate Chem.* **1996**, 7, 121-125.
160. Heskins, M.; Guillet, J., *Journal of Macromolecular Science, Chemistry* **1968**, A2, 1441-1455.
161. Baltes, T.; Garret-Flaudy, F.; Freitag, R., *J. Polym. Sci., Part A: Polym. Chem.* **1999**, 37, 2977-2989.
162. Schild, H. G.; Tirell, D. A., *J. Phys. Chem.* **1990**, 94, 4352-4356.
163. Fujishige, S., *Polym. J. (Tokyo)* **1987**, 19, 297-300.
164. Xie, X.; Zeng, F.; Tong, Z., *J. South China Univ. Technol., Nat. Sci. Ed.* **1998**, 26, 64-67.
165. Lessard, D.; Ousalem, M.; Zhu, X., *Can. J. Chem.* **2001**, 79, 1870-1874.
166. Patterson, D., *Macromolecules* **1969**, 2, 672-677.

167. Chung, J.; Yokoyama, M.; Aoyagi, T.; Sakurai, Y.; Okano, T., *J. Controlled Release* **1998**, 53, 119-130.
168. Chung, J.; Yokoyama, M.; Suzuki, K.; Aoyagi, T.; Sakurai, Y.; Okano, T., *Colloids Surf., B* **1997**, 9, 37-48.
169. Hoshikawa, N.; Hotta, Y.; Okamoto, Y., *J. Am. Chem. Soc.* **2003**, 125, 12380-12381.
170. Ray, B.; Isobe, Y.; Morioka, K.; Habaue, S.; Okamoto, Y.; Kamigaito, M.; Sawamoto, M., *Macromolecules* **2003**, 36, 543-545.
171. Chiantore, O.; Guaita, M.; Trossarelli, L., *Makromolekulare Chemie-Macromolecular Chemistry and Physics* **1979**, 180, 969-973.
172. Barton, B.; Gouws, S.; Schaefer, M.; Zeelie, B., *Org. Process Res. Dev.* **2003**, 7, 1071-1076.
173. Carceller, E.; Merlos, M.; Giral, M.; Balsa, D.; GarciaRafanell, J.; Forn, J., *J. Med. Chem.* **1996**, 39, 487-493.
174. Pollak, A.; Blumenfeld, H.; Wax, M.; Baughn, R.; Whitesides, G., *J. Am. Chem. Soc.* **1980**, 102, 6324-6336.
175. Mammen, M.; Dahmann, G.; Whitesides, G. M., *J. Med. Chem.* **1995**, 38, 4179-4190.
176. Chong, Y.; Krstina, J.; Le, T.; Moad, G.; Postma, A.; Rizzardo, E.; Thang, S., *Macromolecules* **2003**, 36, 2256-2272.

VITA

Steven M Furyk graduated from Rider University in May 1999 with a B.S. in Chemistry. In August 1999, he entered Texas A&M University under the advisement of Professor David E. Bergbreiter. He received his Ph.D. in May 2005. His permanent address is 117 Princeton Ave, Trenton, NJ, 08619.